Contents

Chapter 1

Introduction

1.1 Outline

1.2 The Foreign Exchange (FX) Market

1.3 Project Objective

1.4 Thesis Overview

Part I

Black-Scholes and the Smile Problem

Chapter 2

Black-Scholes Model

2.1 Outline

This chapter discusses the basics of option theory. Section 2.2 starts with some option terminology and presents the derivation of the Black-Scholes option pricing model. Section 2.3 explains the put-call parity. Section 2.4 explains the idea of risk neutral valuation. Section 2.5 discusses the sensitivities of the option price for the values of the parameters in the model, which are known as the greeks. Next, section 2.6 handles on exotic options. While there are many different kinds of exotic options, we will only discuss the options which are important for this project: the compound option, the forward start option and the barrier option. Finally, section 2.7 discusses incomplete markets.

2.2 Derivation of the Black-Scholes Model

An option is a contract that gives the buyer of the contract (the *holder* of the option) the right, but *not* the obligation, to buy (in case of a *call option*) or sell (in case of a *put option*) an asset (the *underlying*) for a specified price (the *strike price*) at a specified time in the future (the *expiry date* or the *maturity date*). The holder of a call option expects the asset price to rise. If this happens indeed, then at maturity he can buy the asset, paying the fixed strike K, and then immediately sel the option in the market to receive the value S of the asset, yielding a profit $S - K$. For the holder of a put option the opposite holds true; he expects the asset price to fall. Let $C(S(t), t)$ and $P(S(t), t)$ denote the value of the call and put option respectively, when the asset price at time t is equal to $S(t)$. The *payoff* is the value of the option at maturity. It follows that the payoff for the call and put option are given by

$$\begin{aligned} C(S(T), T) &= \max(S(T) - K, 0) \\ P(S(T), T) &= \max(K - S(T), 0), \end{aligned}$$

respectively. These are examples of *European* options, where there is only one possible time to exercise the option. By contrast, *American* options can be exercised at any time before expiry.

Because an option gives the holder the *right*, but not the *obligation*, to buy the underlying, there has to be paid a certain price for this contract, called the *premium*. Now the question arises: what premium should be paid for the option? In other words, what is the value $V(S,t)$ of the option at $t = 0$?

Black and Scholes [7] showed that the value of an option can be determined by a *no-arbitrage* argument. No-arbitrage means that it is not possible to make a riskless profit that is greater than the risk-free interest rate earned when putting the amount of money on a bank account. They derive the option value by constructing a portfolio based on the underlying and on the option itself. Then the weights in this portfolio are chosen in such a way that the portfolio becomes riskless at maturity, so that the value of the portfolio at maturity is known. Then the price of the option follows from the no-arbitrage argument.

We will now give a derivation of the Black-Scholes model for the value of an option, following Björk[5]. The Black-Scholes model corresponds to a financial market consisting of two assets. The first one is a risk free asset with price process B with dynamics given by

$$dB(t) = rB(t)dt,$$

where r is the short rate of interest, which is assumed to be a deterministic constant. B can be considered to be the bank account. The second asset is a stock with price process S; its dynamics are given by

$$dS(t) = \alpha S(t)dt + \sigma S(t)d\overline{W}(t),$$

where $\overline{W}$ is a Wiener process and α and σ are given deterministic constants, α is the local mean rate of return of S and σ is the volatility of S. We denote Wiener process using a bar ($\overline{W}$) to indicate that this are the dynamics in the real world. Later we will encounter the so-called 'risk-neutral dynamics' of the stock, then we will use a Wiener process denoted by W.

Now we start by making a number of assumptions. The most important assumption is the following:

- There are no arbitrage opportunities.

a key role in the pricing of an option, as we will see in this section. The other assumptions are:

- The risk free rate of interest r is known and constant.
- There are no dividend payments.
- There are no transaction costs or taxes for buying and/or selling stocks.
- Short selling is allowed.

- Security trading is continuous.
- Stocks are infinitely divisible.

Consider a simple contingent claim of the form $\chi = \phi(S(T))$ and assume that this claim can be traded on a market. Assume that χ has price process $\Pi(t) = F(t, S(t))$, for some smooth function F. Note that we assume that the price $\Pi(t)$ depends only on the stock price $S(t)$ and time t, and not on the price history up to time t. This assumption is justified by the Markov property of the price process $S(t)$ given by equation (2.1). We can determine what the function F should look like for a market without arbitrage opportunities.

Application of Itô's formula to $F(t, S(t))$ results in

$$dF(t, S(t)) = (F_t + \alpha S(t)F_s + \frac{1}{2}\sigma^2 S^2(t)F_{ss})dt + \sigma S(t)F_s d\overline{W}(t),$$

where F_t and F_s denote the partial derivatives of F with respect to t and s, respectively. We can write this as

$$d\Pi(t) = \alpha_\pi(t)\Pi(t)dt + \sigma_\pi(t)\Pi(t)d\overline{W}(t),$$

where

$$\begin{aligned} \alpha_\pi(t) &= \frac{F_t + \alpha S(t)F_s + \frac{1}{2}\sigma^2 S^2 F_{ss}}{\Pi(t)}, \\ \sigma_\pi(t) &= \frac{\sigma S(t)F_s}{\Pi(t)}. \end{aligned} \tag{2.1}$$

Construct a portfolio h based on the underlying stock with price process S and on the derivative with price process Π, $h(t) = (h_S(t), h_\pi(t))$, where h_S is the number of shares in the portfolio and h_π is the number of the derivatives in the portfolio. The value V^h of the portfolio is $V^h = h_s S(t) + h_\pi \Pi(t)$. It is convenient to introduce the relative portfolio $u = (u_S, u_\pi)$, with

$$\begin{aligned} u_s(t) &= \frac{h_S(t)S(t)}{V^h(t)}, \\ u_\pi(t) &= \frac{h_\pi(t)\Pi(t)}{V^h(t)}, \end{aligned}$$

where u_S and u_π have to satisfy $u_S + u_\pi = 1$ and where V^h is the value of the portfolio. The dynamics for the value of the portfolio are given by

$$\begin{aligned} dV^h &= h_S(t)dS(t) + h_\pi(t)d\Pi(t) \\ &= V^h(t)[u_S(t)\frac{dS(t)}{S(t)} + u_\pi(t)\frac{d\Pi(t)}{\Pi(t)}] \\ &= V^h u_S[\alpha dt + \sigma d\overline{W}] + u_\pi[\alpha_\pi dt + \sigma_\pi d\overline{W}] \\ &= V^h[u_S\alpha + u_\pi\alpha_\pi]dt + V[u_S\sigma + u_\pi\sigma_\pi]d\overline{W}. \end{aligned}$$

We can make this portfolio riskless by choosing values for u_S and u_π such that the $d\overline{W}$-term cancels:

$$u_S\sigma + u_\pi\sigma_\pi = 0.$$

Combining this with the constraint $u_S + u_\pi = 1$ we find that

$$u_S = \frac{\sigma_\pi}{\sigma_\pi - \sigma} \qquad \text{and} \qquad u_\pi = \frac{-\sigma}{\sigma_\pi - \sigma}.$$

This is in terms of the relative portfolios. We can write it in terms of the original portfolio to obtain a more explicit relation,

$$u_S = \frac{S(t)F_s(t,S(t))}{S(t)F_s(t,S(t)) - F(t,S(t))}, \tag{2.2}$$

$$u_\pi = \frac{-F(t,S(t))}{S(t)F_s(t,S(t)) - F(t,S(t))}, \tag{2.3}$$

where F_s denotes the derivative of F with respect to s. Now in order to meet the no-arbitrage conditions, we must have

$$dV^h(t) = rV^h(t)dt, \tag{2.4}$$

so that

$$u_S\alpha + u_\pi\alpha_\pi = r, \tag{2.5}$$

So we can substitute the expressions for u_S, u_π and α_π from equations (2.1), (2.2), (2.3) respectively, in expression (2.5), to arrive at the *Black-Scholes partial differential equation*

$$F_t(t,s) + rsF_s + \frac{1}{2}s^2\sigma^2(t,s)F_{ss}(t,s) - rF(t,s) = 0,$$

where F has to satisfy the final condition $F(T,s) = \Phi(s)$.

The value of an option can now be obtained by solving the Black-Scholes equation, with the appropriate boundary conditions (determined by the specific contract). For European call and put options this equation can be solved analytically. Here we will not give a derivation of the solution (for example, see Björk [5]). The *Black-Scholes formulae for European call and put options* are given by

$$C(S(t),t) = S(t)\mathcal{N}(d_1) - Ke^{-r(T-t)}\mathcal{N}(d_2) \tag{2.6}$$

$$P(S(t),t) = Ke^{-r(T-t)}\mathcal{N}(-d_2) - S(t)\mathcal{N}(-d_1), \tag{2.7}$$

where $\mathcal{N}$ is the cumulative distribution function of the standard normal distribution, and

$$d_1 = \frac{log(\frac{S_t}{K}) + (r + \frac{1}{2}\sigma^2)(T-t)}{\sigma\sqrt{T-t}}, \tag{2.8}$$

$$d_2 = d_1 - \sigma\sqrt{T-t}.$$

The price of the option at time $t \in [0,T]$ is dependent on: the value of the underlying $S(t)$, the time to maturity $T-t$, the strike K, the interest rate r, and the volatility σ. Note that the drift term in equation (2.1) for the dynamics of the price of the asset, is not present in the Black-Scholes formulae. This is an important aspect and we will return to this later.

2.3 Put-Call Parity

Using arbitrage arguments, we can derive a certain relation that must hold between call and put options with the same strike and the same expiry, the *put-call parity*. When two different portfolios have exactly the same payoff, irrespective of the stock value at expiry, then by the no-arbitrage argument the values of these portfolios must be the same at any time before expiration. If not, one could buy the cheaper portfolios and sell the more expensive portfolio at some time t. Since at expiration the values of the portfolios are the same, a riskless profit would be made at time t.

Consider a call and a put option with the same strike and expiry. Now set up two portfolios: portfolio 1 consisting of a call option and an amount of cash equal to the present value of the strike price, portfolio 2 consisting of a put option and the underlying asset. At expiry, the values of the portfolios are:

- portfolio 1: if the asset value is above the strike, the call is worth $S_T - K$, and the amount of cash equals K. The portfolio has a value of S_T. If the asset value is below the strike, the call is worth zero, and the portfolio value is equal to K.
- portfolio 2: if the asset value is above the strike, the put option is worth zero, and the portfolio is worth S_T. If the asset value at expiry is below the strike, the put option is worth $K - S_T$. The value of the portfolio in this case is equal to K.

So, at expiry the values of the portfolios are equal. By the no-arbitrage argument, we can conclude that the values must be the same at any time before expiry; this is the put-call parity:

$$C(S,t;K,T) + e^{-rT}K = P(S,t;K,T) + S_t,$$

Where the subscript t denotes the time, S_t is the spot value at time t. Given the value of a call (put) option, we can use the above relation to calculate the price of a put (call) option with the same strike and expiry. This relation holds true in general, independent of the model used.

2.4 Risk Neutral Valuation

We have seen that in the Black-Scholes model, the option value should satisfy the Black-Scholes equation. Together with the appropriate boundary conditions (determined by the specific contract), this equation can be solved. Another approach to the pricing of the option is to use *risk neutral valuation*. Note that in the Black-Scholes formulae there is no drift term present. Since the drift term reflects to what extent market participants are risk averse, the price of an option should be independent of this aspect. That is to say, the price of an option can be determined as if market participants are *risk neutral*. When market participants are risk neutral, then there is no risk premium needed for the risk they take, so in this case the drift can be set equal to the riskless interest rate r. Whatever the real world drift is, it is irrelevant when it comes to pricing an option we can use the riskless interest rate.

Now the price of an option can also be obtained by risk neutral valuation. In this case the option price is calculated by discounting the expected value of the payoff. For a claim with payoff $\phi(S(T))$ this results in

$$C(S(t),t) = e^{-r(T-t)}\mathbb{E}^Q[\phi(S(T))],$$

where Q is the so-called risk-neutral measure (under which every traded asset has an expected rate of return equal to the risk free interest rate r), and $\mathbb{E}^Q$ denotes the expectation under this risk neutral measure. For a call option we then have

$$\begin{aligned} C(S(t),t) &= e^{-r(T-t)}\mathbb{E}^Q[\max(S(T)-K,0)] \\ &= e^{-r(T-t)}\int_K^\infty (s-K)f_{S_T}(s)ds, \end{aligned}$$

where f_{S_T} is the density of of the asset at maturity. The risk neutral dynamics of S are given by

$$dS(t) = rS(t)dt + \sigma S(t)dW(t),$$

where W is a Q-Wiener process.

2.5 The Greeks

The option *greeks* are a set of measurements that quantify the risk exposure of an option. Options have a variety of risk exposures that can vary of considerable amount over time, or as markets move. A distinction can be made between two types of sensitivity. First, the sensitivity of the option price with respect to price changes of the underlying asset, which is a measure of risk exposure. Second, the sensitivity of the option value with respect to changes in the model parameters, which is a measure of the sensitivity with respect to misspecifications of the model parameters. In this section we will describe the most important greeks. To this end, let V denote the value of an option.

The delta is the degree to which an option price will move given a small change in the underlying stock price. It is calculated as the derivative of the option value with respect to the spot. For example, an option with a delta of 0.5 will move half a cent for every full cent movement in the underlying stock. Call deltas are positive because the option value is a monotonic increasing function of the spot level. Put deltas are negative, reflecting the fact that the put option price and the underlying stock price are inversely related. The put delta equals the call delta minus one, which can be derived from the put-call parity. A far out-of-the-money call option will have a delta very close to zero; an at-the-money option will have a delta that is close to a half and a far in-the-money call option will have a delta close to one.

Gamma measures how fast the *delta* changes for small changes in the underlying stock price. It is calculated as the second derivative of the option value with respect to the spot. Gamma is an important greek especially in hedging, because gamma reflects how often the portfolio should be changed in order to remain risk neutral (therefore, a low value of gamma is preferred).

Vega is the change in option price given a one percentage change in volatility.

Theta is the the sensitivity of the option price with respect to time. That is, it measures the change in option price given a decrease in time to maturity. It basically it is a measure of the option's sensitivity to time decay.

Rho is the amount the option price will change given a change in the risk-free rate.

Note that when we want to look at one of the greeks, it is under the assumptions that all the other variables are held constant. The greeks are calculated as follows:

$$\begin{aligned} delta &: \frac{\partial V}{\partial S} \\ gamma &: \frac{\partial^2 V}{\partial S^2} \\ theta &: \frac{\partial V}{\partial t} \\ vega &: \frac{\partial V}{\partial \sigma} \\ rho &: \frac{\partial V}{\partial r} \end{aligned}$$

2.6 Hedging

Buying or selling an option implies some exposure to risk. In case of buying an option, one has the right to buy the underlying asset at maturity, but not the obligation. For a call option, this means exercising the option when the price of the underlying at maturity has increased above the strike price. The holder pays the strike price and receives the underlying, and by selling the underlying immediately back in the market a profit is made. However, when the asset price has declined below the strike price, the option is not exercised and expires worthless. When buying an option, one has a chance of making an infinite profit, and the risk is limited to losing the premium (the price that was initially paid for the option contract).

On the other hand, the writer of an option is in the opposite situation. The writer earns the premium, but is exposed to the risk of losing an infinite amount of money in case the option is exercised. The writer of an option can protect himself to this risk. This can be done by taking a position in the underlying asset. *Hedging* is the process of reducing financial risk.

The derivation of the Black-Scholes model is an example of so-called *dynamic delta hedging*. In a dynamic delta hedge a portfolio is constructed so that the sensitivity with respect to spot (delta) of the product one wants to hedge is offset by the sensivity of the hedging instrument. In a similar manner one can also construct a dynamic hedge for other greeks (e.g. gamma). In a dynamic hedge, the corresponding greek of the resulting hedging portfolio is equal to zero.

In the Black-Scholes model, the risk of selling an option is eliminated by constructing a portfolio consisting of the option and a certain amount of the underlying. The number of shares in this portfolio is chosen in such a way that the resulting portfolio is *delta neutral*, which means that the delta of the portfolio is equal to zero. For small changes in the underlying, the value of the portfolio does not change. The no-abitrage principle implies that the option price is equal to the cost of the hedging portfolio. The hedging strategy in this context is called 'dynamic' because it requires continuously rebalancing of the weights in the portfolio in order to keep it riskless. Initially, the weights are chosen so that the portfolio is riskless. The number of shares in the portfolio offsets the risk of option. But as the value of the underlying changes, this balance is the portfolio has to be adjusted to keep it riskless.

To be more concrete, assume that a particular derivative with pricing function $F(t, S)$ has been sold. Our object is to delta hedge this derivative: we want to immunize the portfolio against small changes in the underlying asset. We can hedge this derivative using the underlying asset. The hedging portfolio P is given by $P(t, S) = -F(t, S) + xS$, where x is the number of shares of the underlying asset. In order for the hedging portfolio to be delta neutral, the portfolio should satisfy

$$\Delta_P = \frac{\partial P}{\partial S} = \frac{\partial \left(-F(t, S) + xS\right)}{\partial S} = 0,$$

so that the number of shares x needed is given by

$$x \quad = \quad \Delta_F = \frac{\partial F(t, S)}{\partial S}.$$

In practice, transaction costs make it impossible (or at least infeasible) to continuously rebalance a hedging portfolio. Therefore, a *discrete rebalanced delta hedge* is used. A delta hedge only works for small changes in the underlying, and therefore, for a short period of time. Rebalancing the portfolio often will give a good hedge, but also high transaction costs. A measure of the sensitivity of Δ with respect to spot is gamma: $\frac{\partial^2 P}{\partial S^2}$. A high value of gamma means that the portfolio has to be rebalanced often, whereas a low value of gamma enables it to keep the delta hedge for a longer period of time. For this reason, a portfolio with a low value of gamma is preferred.

2.7 Exotic Options

So far we have considered standard European *vanillas*, i.e., European call and put options. In contrast to these options, where the payoff is only dependent on the value of the underlying at expiry, there are also *exotic options*. An important type of exotic options are path-dependent options, for which the payoff is in some way dependent on the history of the underlying value. There are many kinds of exotic options; here we will shortly discuss three types of exotics (they will be used later in the project).

A *barrier option* is an option in which the payoff depends on whether or not the value of the underlying reaches a certain level (the *barrier* or the *trigger*) at some time during the life of the contract. There are various kinds of barrier options. First, a distinction can be made between *knock-out* options in which the option becomes worthless when the barrier is hit, and *knock-in* options in which the option is worthless, *unless* the barrier level is hit. Second, we distinguish between *up-and-out (up-and-in)* options which in the barrier level is hit from below, and *down-and-out (down-and-in)* options in which the barrier is hit from above. Usually the option is out-of-the-money when the barrier is hit. With a *reverse* barrier option the option is in-the-money when hitting the barrier. The values of barrier option and a reverse barrier option are plotted in figures 2.1 and 2.2.

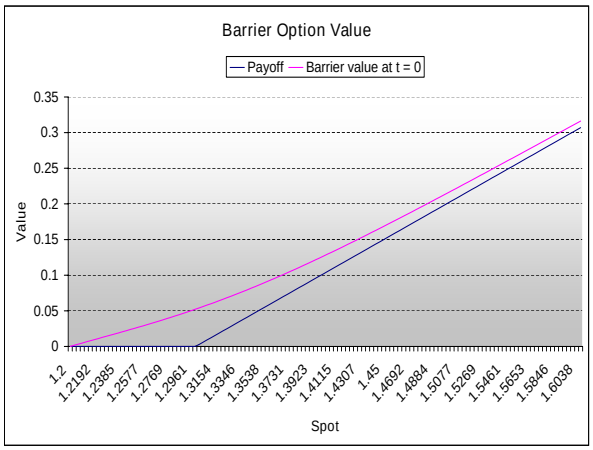

Figure 2.1: Barrier option value.

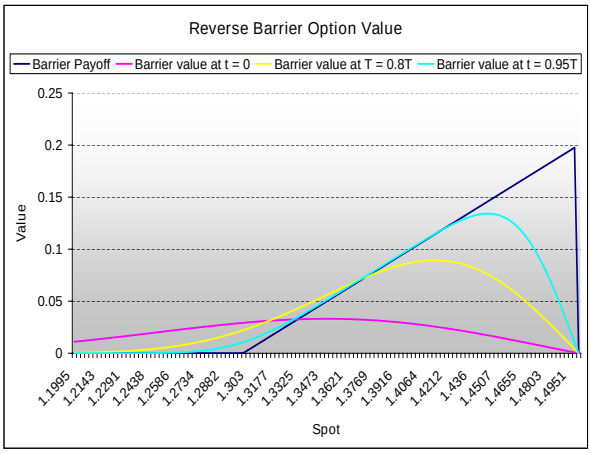

Figure 2.2: Reverse barrier option value.

A *forward start option* is an option which is paid for at time $t = 0$, but the contract only starts at some time $T_1 > 0$ with expiry $T_2 > T_1$; both times are specified in the contract. The strike K is fixed at time T_1, usually this is given by some function of the value of the underlying at time T_1, so $K = K(S_{T_1})$. In the Black-Scholes model, the price FS at $t = 0$ of a forward start option can be calculated by risk neutral valuation,

$$\begin{aligned} FS(S_0, 0) &= e^{-rT_2}\mathbb{E}^Q\left[\max(S_{T_2} - K(S_{T_1}), 0)\right] \\ &= e^{-rT_2}\iint \max(s_2 - K(s_1), 0) f_{S_{T_1}, S_{T_2}}(s_1, s_2) ds_2 ds_1 \\ &= e^{-rT_2}\iint \max(s_2 - K(s_1), 0) f_{S_{T_2}|S_{T_1}}(s_2|s_1) f_{S_{T_1}}(s_1) ds_2 ds_1. \end{aligned}$$

But in fact we do not need to calculate this integral; we can calculate option prices in a simpler way (see also Hakala and Wystup[14]). Note that the asset value at time T_2 can be written in terms of the value at time T_1,

$$\begin{aligned} S_{T_2} &= S_0 e^{\left((r-\frac{1}{2}\sigma^2)T_2 + \sigma W(T_2)\right)} \\ &= S_{T_1} e^{\left((r-\frac{1}{2}\sigma^2)(T_2-T_1) + \sigma(W(T_2)-W(T_1))\right)}. \end{aligned}$$

Let $Y = e^{\left((r-\frac{1}{2}\sigma^2)(T_2-T_1)+\sigma(W(T_2)-W(T_1))\right)}$. Then S_{T_1} and Y are independent. Using this fact, we find that the option value is given by

$$\begin{aligned} FS(S_0,0) &= e^{-rT_2}\mathbb{E}^Q\left[\max(S_{T_2}-K(S_{T_1}),0)\right] \\ &= e^{-rT_2}\mathbb{E}^Q\left[\max(S_{T_1}Y-K(S_{T_1})),0)\right]. \end{aligned}$$

In case the strike is given in relative terms, i.e., $K = \alpha S_{T_1}$, we can reduce this further to

$$\begin{aligned} FS(S_0,0) &= e^{-rT_2}\mathbb{E}^Q\left[\max(S_{T_2}-K(S_{T_1}),0)\right] \\ &= e^{-rT_2}\mathbb{E}^Q\left[\max(S_{T_1}Y-\alpha S_{T_1}),0)\right] \\ &= e^{-rT_2}\mathbb{E}^Q[S_{T_1}]\mathbb{E}^Q\left[\max(Y-\alpha,0)\right] \\ &= S_0 C_{BS}(1,T_1;\alpha,T_2,\sigma,r). \end{aligned}$$

So, in the Black-Scholes model, the price of a relative forward start option with fixing date T_1 and expiry T_2 can be derived from the value of a call option with spot equal to 1, strike equal to α and time to maturity $T_2 - T_1$. The value of a forward start option is plotted in figure 2.3.

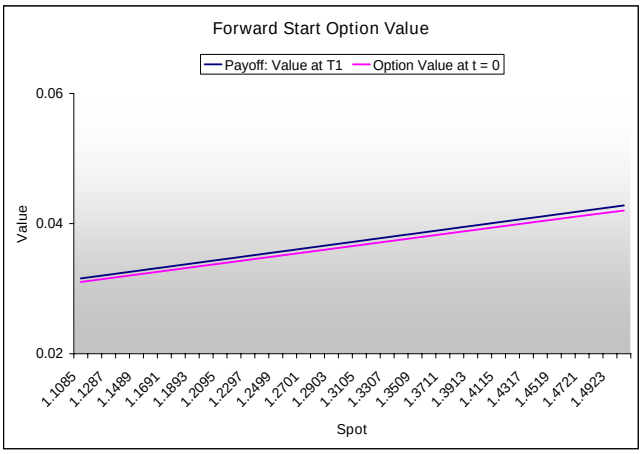

Figure 2.3: Value of a forward start option at $t = T_1$ and at $t = 0$.

Finally, a *compound option* is an option on an option. So this gives four possibilities: a call on a call, a call on a put, a put on a put and a put on a call. The exercise payoff now depends on the value of another option, which is the *underlying option*. Let T_1 be the expiry of the compound option with strike K_1. Let $T_2 > T_1$ be the expiry of the underlying option with strike K_2.

As an example we will consider a call on a call. The cases for the three other combinations are similar. On the first expiration date T_1, the holder has the right to buy a new call (the underlying option) for the strike price K_1. So, the holder will exercise his option only if the value of the underlying option at time T_1 is higher than K_1.

Let $C_{call}(S_t,t;T_1,K_1)$ denote the value of the call on a call at time t with expiry T_1 and strike K_1; let $C(S_t,t;T_2,K_2)$ denote the value of the underlying call at time t with expiry T_2 and strike

K_2. The payoff for this call on a call option at T_1 is given by

$$C_{call}(S_{T_1}, T_1; T_1, K_1) = \max[C(S_{T_1}, T_1; T_2, K_2) - K_1, 0].$$

In the Black-Scholes model we can derive the analytical solution for the compound option. We will show how this can be done using the Girsanov formula,

$$\begin{aligned}
\mathbb{E}\left[e^{\mu+\alpha U}\phi(U)\right] &= \int_{-\infty}^{\infty} e^{\mu+\alpha x}\phi(x)\frac{1}{\sqrt{2\pi}}e^{-\frac{1}{2}x^2}dx \\
&= e^{\mu+\frac{1}{2}\alpha^2}\int_{-\infty}^{\infty}\phi(x)\frac{1}{\sqrt{2\pi}}e^{-\frac{1}{2}(x-\alpha)^2}dx \\
&= e^{\mu+\frac{1}{2}\alpha^2}\mathbb{E}\left[\phi(\alpha+U)\right],
\end{aligned}$$

where U is a standard normal random variable and α and μ are constants.

We can write the value of a compound option as the discounted value of the expectation of its payoff. For $t < T_1$,

$$C_{call}(S_t, t; K_1, T_1, \sigma) = e^{-r(T_1-t)}\mathbb{E}^Q\left[\left(C(S_{T_1}, T_1; K_2, T_2; \sigma) - K_1\right)1_{\{S_{T_1}>S^*\}}\right].$$

The payoff is written in terms of an indicator function. In this expression, S^* is the critical asset value such that the value of the underlying call option at time T_1 is equal to K_1. Since a call option is a monotonic increasing function of spot, there exists a unique critical asset value. We can find the value of S^* through a numerical procedure, for example using the Newton-Raphson method. In the following we consider S^* as known.

The next step is to write the underlying call price also as the discounted value of the expected payoff and then split the compound option value into three terms:

$$\begin{aligned}
C_{call}(S_t, t; K_1, T_1, \sigma_{01}) &= e^{-r(T_1-t)}\mathbb{E}\left[\left\{e^{-r(T_2-T_1)}\mathbb{E}_{T_1}\left[\left(S_{T_2}-K_2\right)1_{\{S_{T_2}>K_2\}}\right] - K_1\right\}1_{\{S_{T_1}>S^*\}}\right] \\
&= e^{-r(T_2-t)}\mathbb{E}\left[S_{T_2}1_{\{S_{T_2}>K_2\}}1_{\{S_{T_2}>S^*\}}\right] \\
&\quad -K_2e^{-r(T_2-t)}\mathbb{E}_t\left[1_{\{S_{T_2}>K_2\}}1_{\{S_{T_2}>S^*\}}\right] \\
&\quad -K_1e^{-r(T_1-t)}\mathbb{E}_t\left[1_{\{S_{T_2}>S^*\}}\right].
\end{aligned}$$

The last two terms on the right hand side are the expectations of indication functions, so they be written directly in terms of a standard normal random variable U. For the first term we apply the Girsanov formula to eliminate the term S_{T_2}. Since

$$S_{T_2} = S_t e^{(r-\frac{1}{2}\sigma^2)(T_2-t)+\sigma\sqrt{T_2-t}U},$$

Comparing with the Girsanov formula, we can see that μ and α in expression (2.9) are given by

$$\begin{aligned}
\mu &= log(S_t) + (r - \frac{1}{2}\sigma^2)(T_2 - t), \\
\alpha &= \sigma\sqrt{T_2 - t}.
\end{aligned}$$

Further, the function $\phi(U)$ is given by

$$\phi(U) = 1_{\left\{U > \frac{log(\frac{K_2}{S_t}) - \left(r - \frac{1}{2}\sigma^2\right)T_2}{\sigma\sqrt{T_2}}\right\}} 1_{\left\{U > \frac{log(\frac{S^*}{S_t}) - \left(r - \frac{1}{2}\sigma^2\right)T_1}{\sigma\sqrt{T_1}}\right\}}.$$

By expressing the expectation of an indicator function as a probability, we arrive at the analytical solution for the value of a call-on-call option:

$$C_{call}(S_t, t) = S_t \mathcal{N}_2(a_+, b_+; \rho) - K_2 e^{-rT_2} \mathcal{N}_2(a_-, b_-; \rho) - K_1 e^{-rT_1} \mathcal{N}(a_-),$$

where $\mathcal{N}$ is the standard normal distribution, $\mathcal{N}_2$ is the bivariate standard normal distribution, ρ is the correlation coefficient. Since $W_{T_2} - W_{T_1}$ is independent of W_{T_1}, this correlation coefficient is given by

$$\begin{aligned} \rho &= \frac{Cov(W_{T_1}, W_{T_2})}{\sqrt{Var(W_{T_1})Var(W_{T_2})}} \\ &= \frac{Var(W_{T_1})}{\sqrt{Var(W_{T_1})Var(W_{T_2})}} = \sqrt{\frac{T_1}{T_2}}. \end{aligned}$$

Further, we have

$$\begin{aligned} a_+ &= \frac{log(\frac{S_t}{S^*}) + \left(r + \frac{1}{2}\sigma^2\right)T_1}{\sigma\sqrt{T_1}} & a_- &= a_+ - \sigma\sqrt{T_1} \\ b_+ &= \frac{log(\frac{S_t}{K_2}) + \left(r + \frac{1}{2}\sigma^2\right)T_2}{\sigma\sqrt{T_2}} & b_- &= b_+ - \sigma\sqrt{T_2}. \end{aligned}$$

The result of applying the Girsanov formula is a change in the drift term, from r to $r + \sigma^2$. In figures 2.4 and 2.5 the value of the underlying option and the compound option is shown.

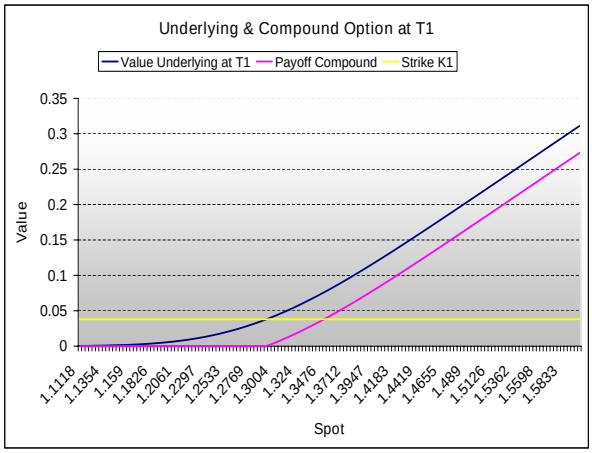

Figure 2.4: Value of the underlying option at T1 and compound option payoff. The compound strike is equal to $K_1 = 0.038$. The critical asset value is equal to $S^* = 1.294$ (it corresponds to the crossing point of the blue and yellow line).

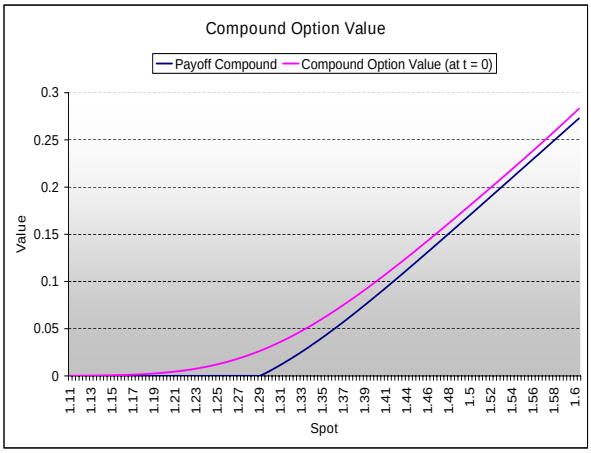

Figure 2.5: Compound option payoff and compound value at t = 0.

2.8 Incomplete Markets

This section is not linked to the rest of the chapter, as it does not assume the Black-Scholes model. As we will need to contents of this section later on, we will discuss it here.

As a rule of thumb, a model is complete if there are as many random sources as there are tradable assets (see Björk[5]). This is the case for the Black-Scholes model, which makes it a complete model. However, there exist many models which are generalizations of the Black-Scholes model. Such generalized models may lead to market incompleteness, in which case there are more random sources than tradable assets. This is for example the case in stochastic volatility models.

In this section we will consider the pricing of derivatives in incomplete markets. The reason to discuss incomplete markets is that we will have to deal with it in the stochastic volatility model discussed in chapter 5. In stochastic volatility models, the volatility is not constant as in de Black-Scholes model, but instead it is assumed to follow a stochastic process itself. In such a model, there is one tradable asset, the underlying stock, and one non-tradable asset, the volatility (after all, you cannot buy or sell volatility). On the other hand, we have two random sources, so we are dealing with an incomplete market.

This section considers the simpler case, a market with no tradable assets, and one non-tradable asset. Let X be this non-tradable asset, and assume that its dynamics under the objective probability measure are given by:

$$dX(t) = \alpha(t, X(t))dt + \sigma(t, X(t))d\overline{W}(t),$$

where $\overline{W}$ is a P-Wiener Process. Also, there is a risk free asset with dynamics given by

$$dB(t) = rB(t)dt,$$

where r is the short rate of interest.

We want to calculate the price of a given contingent claim. Let the T-claim $\mathcal{Y}$ be defined by $\mathcal{Y} = \Phi(X(T))$. We want to price this claim, which is a deterministic function Φ of the underlying (which is a non-tradable process), evaluated at time T. The question arises how we can form a self-financing portfolio. Since X is not tradable, our only possible strategy is to invest all the money in the bank. We cannot include the underlying asset X in a replicating portfolio.

The requirement of an arbitrage free market implies that prices of different derivatives will have to satisfy certain internal consistency relations. To see this, we form a portfolio based on the T-claim $\mathcal{Y}$ and on an extra T-claim $\mathcal{Z}$, which serves as a benchmark:

$$\begin{aligned} \mathcal{Y} &= \Phi(X(T)) \\ \mathcal{Z} &= \Gamma(X(T)) \end{aligned}$$

Assume that the prices of the derivatives are given by $\Pi(t;\mathcal{Y}) = F(t,X(t)))$ and $\Pi(t,\mathcal{Z}) = G(t,X(t))$, and construct a portfolio based on F and G. As in the Black-Scholes case, the idea is to choose the weights of the portfolio so as to make the portfolio riskless. Then the local rate of return of this portfolio is equal to the riskless rate of interest.

Applying Itô to the processes $F(t,X(t))$ and $G(t,X(t))$ we have

$$\begin{aligned} dF &= \alpha_F F dt + \sigma_F F d\overline{W} \\ dG &= \alpha_G G dt + \sigma_G G d\overline{W}, \end{aligned}$$

where α_F and σ_F are given by

$$\alpha_F = \frac{F_t + \alpha F_x + \frac{1}{2}\sigma^2 F_{xx}}{F} \tag{2.9}$$

$$\sigma_F = \frac{\sigma F_x}{F}, \tag{2.10}$$

and similar expressions for α_G and σ_G. F_x denotes the derivative of F with respect to x.

Now construct a self-financing portfolio based on F and G with relative weights u_F and u_G, respectively. The dynamics of the portfolio are given by

$$\begin{aligned} dV &= V[u_F \frac{dF}{F} + u_G \frac{dG}{G}] \\ &= V[(u_F\alpha_F + u_G\alpha_G)dt + (u_F\sigma_F + u_G\sigma_G)d\overline{W}]. \end{aligned}$$

Choose the weights such that $u_F\sigma_F + u_G\sigma_G = 0$, so that the portfolio becomes riskless. Together with the constraint $u_F + u_G = 1$, the weights can be calculated and the result is

$$u_F = \frac{-\sigma_G}{\sigma_F - \sigma_G} \tag{2.11}$$

$$u_G = \frac{\sigma_F}{\sigma_F - \sigma_G}. \tag{2.12}$$

The riskless portfolio should have a rate of return equal to the riskless interest rate r, so

$$u_F\alpha_F + u_G\alpha_G = r,$$

or, by substituting equations (2.11) and (2.12),

$$\frac{\alpha_G\sigma_F - \alpha_F\sigma_G}{\sigma_F - \sigma_G} = r.$$

We can put the terms for F on the left hand side and the terms for G on the right hand side to obtain the equality

$$\frac{\alpha_F - r}{\sigma_F} = \frac{\alpha_F - r}{\sigma_G}$$

Note that the left hand side does not depend on G and the right hand side does not depend on F. This implies that both quotient have to be independent of the choice of F and G; therefore, there exists some function $\lambda(t)$ such that

$$\frac{\alpha_F - r}{\sigma_F} = \frac{\alpha_F - r}{\sigma_G} = \lambda(t). \tag{2.13}$$

In this expression λ is called the *market price of risk*. The left hand side is the risk premium (the local mean excess return of F over the riskless rate r) per unit of volatility.

In order to be free of arbitrage opportunities, all derivatives will have the same market price of risk. To calculate the price of a derivative, we have to know the process of some other derivative in order to obtain the market price of risk. In our case: if we assume that the pricing function G of the ('benchmark') claim $\mathcal{Z}$ is known, then we can calculate the market price of risk by

$$\lambda(t,x) = \frac{\alpha_G(t,x) - r}{\sigma_G(t,x)}.$$

Then we can use this λ to calculate the pricing function F of the claim $\mathcal{Z}$.

Finally, we can substitute the expressions for α_F and σ_F of equations (2.9) and (2.10) respectively into equation (2.13), and this results in the partial differential equation

$$F_t + (\alpha - \lambda\sigma)F_x + \frac{1}{2}\sigma^2 F_{xx} - rF = 0,$$

where λ can be calculated from equation (2.14). We can solve this equation, together with the boundary condition $F(T,x) = \Phi(x)$. Alternatively, the pricing function $F(t,x)$ can be obtained by risk neutral valuation,

$$F(t,x) = e^{-r(T-t)}\mathbb{E}^Q[\Phi(X(T))],$$

where the dynamics of X under Q are given by

$$dX(t) = [\alpha(t,X(t)) - \lambda(t,X(t))\sigma(t,X(t))]\,dt + \sigma(t,X(t))dW(t),$$

where W is a Q-Wiener process.

Chapter 3

Volatility Smile and the Foreign Exchange Market

3.1 Outline

In the previous chapter we have discussed the Black-Scholes model. The Black-Scholes model assumes a constant volatility. However, this assumption contradicts empirical observations: the implied volatility is not constant. In this chapter we will discuss the volatility assumption.

Section 3.2 explains what the implied volatility looks like in practice; section 3.3 explains the relation between the implied volatility and the density of the underlying at maturity.

We will also discuss what happens to the smile when the spot changes; this is referred to as the *smile dynamics*. Section 3.4 presents two well known models for the smile dynamics, at the end of the chapter empirical observations about the smile and its dynamics are presented (section 3.7).

Section 3.5 introduces the foreign exchange market and in section 3.6 explains the foreign exchange market quotes that are used for vanilla options.

3.2 Volatility Smile and Volatility Surface

The Black-Scholes model for a European call or put option results in a formula for the option price. In this formula the option price depends on the value of the underlying, the interest rate, the time to maturity, the strike price and the volatility. The volatility is the only parameter that is not directly observable in the market. One of the assumptions underlying the Black-Scholes model is that the volatility of the underlying stock is constant. For a given market option price we can calculate the corresponding volatility by solving the Black-Scholes formula for the volatility. Since the price of an option is increasing as function of the volatility, the vega of the option - which is the derivative of the option value with respect to the volatility - is positive, and therefore we can find a unique solution. The value obtained is called the *implied volatility*.

If the market were consistent with the assumption of constant volatility, then we would find the same value for the implied volatility for options with different strikes and expiries. However, observed market prices result in implied volatilities that changes with maturity. Further, the implied volatilities also vary with strike; this is called the *volatility smile*, because high and low strike options tend to have higher volatilities than at-the-money options (or, equivalently, far out-of-the-money or far in-the-money options display higher implied volatilities than at-the-money options). From the put-call parity it follows that we have the same implied volatility for a call and a put option with the same strike and maturity. Usually, short-term options have stronger smiles than long-term option. It is also possible that the implied volatility is skewed instead of a smile pattern. Then the implied volatility can be an increasing or a decreasing function of the strike. When the implied volatility is plotted against both maturity and strike we have a so-called *volatility surface*.

3.3 Volatility Smile and Deviation From the Lognormal Density

If the Black-Scholes condition of constant volatility were satisfied, then the underlying process would follow the lognormal distribution. We have seen that the implied volatility displays a smile pattern. In particular, the Black-Scholes model underprices deep in- and out-of-the-money puts and calls. This indicates that stock return distributions are not lognormally distributed, but instead that they are negatively skewed with higher kurtosis compared to the Black-Scholes lognormal distribution. In this section we will give an explanation for this.

We will start by showing that the distribution for the underlying asset is determined by the volatility smile. Or equivalently, we will show that from the prices of call options we can extract an expression for the density of the underlying at maturity.

Let $C(S,t;K,T)$ be the value of a call option at the current time t and current spot S for strike K and maturity T. Assume that these prices are known for all possible strikes and maturities. This is not realistic since call prices are only available for certain strikes and maturities, but it does give us a starting point. The value of a European call option can be calculated by taking the discounted value of the expected payoff,

$$\begin{aligned} C(S,t;K,T) &= e^{-r(T-t)}\mathbb{E}^Q[\max(S_T-K,0)] \\ &= e^{-r(T-t)}\int_0^\infty \max(s-K,0)f_{S_T}(s)ds \\ &= e^{-r(T-t)}\int_K^\infty (s-K)f_{S_T}(s)ds, \end{aligned} \tag{3.1}$$

where f_{S_T} is the density function of S_T. Now we can differentiate the call price twice with respect to K, to obtain an expression for the density of the underlying stock at maturity. The first

derivative is given by

$$\frac{\partial C(S,t;K,T)}{\partial K} = -e^{-r(T-t)} \int_K^\infty f_{S_T}(s)ds = -e^{-r(T-t)} \left(1 - F_{S_T}(K)\right),$$

where $F_{S_t T}$ is the cumulative distribution function of S_T. For the second derivative we have

$$\frac{\partial^2 C(S,t;K,T)}{\partial K^2} = e^{-r(T-t)} f_{S_T}(K).$$

So the density of the underlying at maturity T is given by

$$f_{S_T}(S) = e^{r(T-t)} \frac{\partial^2 C(S_t,t;K,T)}{\partial K^2}|_{K=S}.$$

Now we will proceed by giving an intuitive explanation of how the shape of the volatility smile implies the shape of the density function. See also Hull[17]. We will distinguish between a smile and a skew pattern to show the corresponding deviations from lognormality. Consider first the density corresponding to a smile pattern, see figure 3.1. Here we have a risk reversal equal to $RR = 0$, a strangle equal to $STR = 0.40\%$.

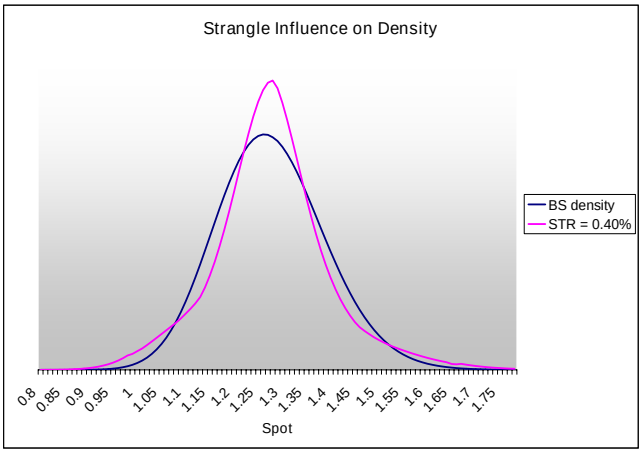

Figure 3.1: Impact of the strangle on the shape of the density (RR = 0). The BS density is the Black-Scholes density with $RR = STR = 0$.

The existence of a smile implies that the probability distributions of the underlying has fatter tails and is more peaked around the mean than the lognormal distribution. This means that both large and small moves in the underlying are more likely than what the lognormal distributions predicts. Consider an out-of-the-money call with high strike K_1 and an out-of-the-money put with low strike K_2 (Considering figures 3.1, take for example $K_1 = 1.6, K_2 = 1.0$.) Then we can see that, compared to the lognormal distribution, the call and put have a higher probability of getting in-the-money. Therefore the volatilities (and price) of these options will be higher than the constant volatility case.

Next, consider the density in figure 3.2 corresponding to right skewed implied volatilities. Consider again the out-of-the-money call and put with strikes K_1 and K_2 respectively. From the density we can see that, compared with the lognormal density, the put has higher probability and the call has lower probability of getting in the money. Therefore, the put has a higher implied volatility and the call a lower implied volatility. For the left skewed density in figure 3.3 a similar argument can be made for the opposite effect.

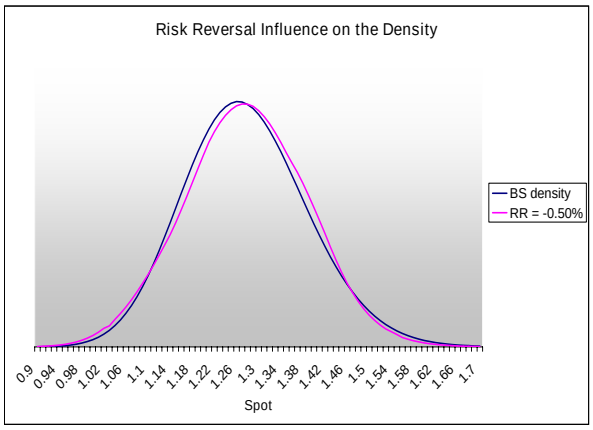

Figure 3.2: Impact of a negative risk reversal on the shape of the density (STR = 0).

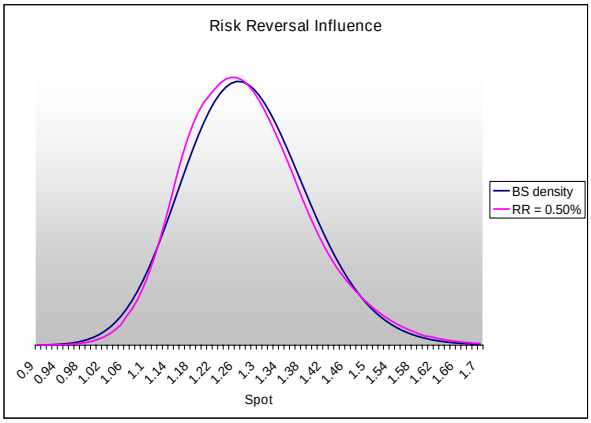

Figure 3.3: Impact of a positive risk reversal on the shape of the density (STR = 0).

Finally, figure 3.4 shows the shape of the density in which a (positve) risk reversal of 0.50% is combined with a strangle of 0.20%.

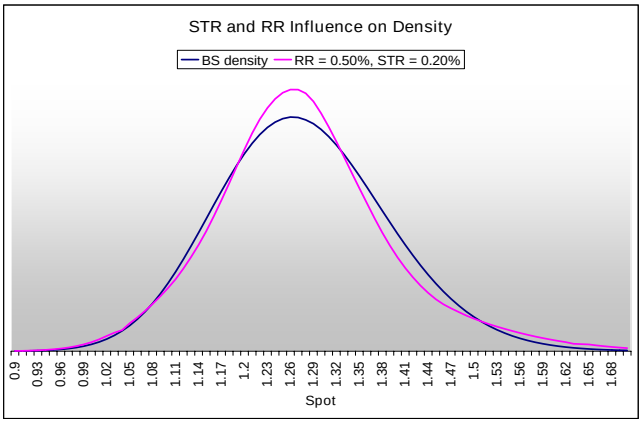

Figure 3.4: Impact of the strangle and risk reversal on the shape of the density.

3.4 Smile dynamics, Sticky Strike and Sticky Delta

From observed market prices for different strikes one can obtain the implied volatility as a function of strike, given today's stock price S_0, by solving the Black-Scholes formula. However, from this

market information we are not able to tell how this function varies when S changes. In practice, it is a known fact that smile patterns do not behave in a random way. Instead, it can be observed that smile movements are linked to spot movements. These observations are discussed in section 3.7. This is referred to as the *smile dynamics*. These smile dynamics have been identified as an important factor in the pricing of path-dependent FX-options, and in the hedging of options.

In this section we will discuss two models of the smile dynamics.

Given the volatility smile, we know that we are not in a 'Black-Scholes world', and the implied volatility is not linked in any simple way to the volatility σ of the process of the underlying stock. Let $C(S,t;T,K;\sigma)$ be the market price of the call option, and let $BS(S,t;K,T;\sigma_{imp}(t,T,S,K))$ be the call price calculated from the Black-Scholes formula. Then we know only that

$$C(S,t;K,T;\sigma) = BS(S,t;K,T;\sigma_{imp}(t,T,S,K)).$$

Fix T and write $\sigma_{imp}(S,K)$ for $\sigma_{imp}(t,T,S,K)$. The smile dynamics refer to the change in the volatility smile for (small) changes in spot. These dynamics are needed in the pricing of exotic options (we will return to this in later chapters), and also in hedging. In chapter 2 we explained that the derivation of the Black-Scholes partial differential equation is based on constructing a dynamic delta hedge, in which the delta of the portfolio is equal to zero. To calculate the value of delta of the call option, we have

$$\begin{aligned}
\Delta &= \frac{dC}{dS}(S,t;K,T;\sigma) \\
&= \frac{dBS}{dS}(S,t;K,T;\sigma_{imp}(S,K)) \\
&= \frac{\partial BS}{\partial S} + \frac{\partial BS(S,t;K,T;\sigma_{imp}(S,k))}{\partial \sigma_{imp}(S,K)} \frac{\partial \sigma_{imp}(S,K)}{\partial S},
\end{aligned} \tag{3.2}$$

where we identify the term $\frac{\partial BS}{\partial \sigma_{imp}}$ is the Black-Scholes vega,

$$\frac{\partial BS(S,t;K,T;\sigma_{imp}(S,K))}{\partial \sigma_{imp}(S,K)} = vega_{BS}(S,t;K,T;\sigma_{imp}(S,K)).$$

So, the delta is equal to the Black-Scholes delta, plus some correction term that accounts for the smile dynamics. In practice it is observed that when spot changes, the smile changes accordingly. Using the Black-Scholes delta can therefore lead to an incorrect value of the 'true' delta. The problem is how to calculate the value of $\frac{\partial \sigma_{imp}}{\partial S}(S,K)$.

In practice, there are two well known models of the smile dynamics, which are exactly opposite to each other (and are the two extreme examples of smile behaviour). The first model of the smile dynamics is the so-called *Sticky Strike Rule*. The sticky strike rule says that the implied volatility is a function of the strike only. This implies that for a fixed strike, the implied volatility does not change when the spot changes. In this case we can see from equation (3.2) that the delta can be calculated using the usual Black-Scholes assumptions because $\frac{\partial \sigma_{imp}}{\partial S} = 0$. So, when spot changes,

the smile remains the same.

The second smile dynamics model is the so-called *Sticky Delta Rule*. The sticky delta rule says that the implied volatility is a function of delta only. This is equivalent to saying that the implied volatility is a function the *moneyness ratio* $\frac{S}{K}$. When the spot level changes (and the delta of an option changes accordingly), this means that the smile curve will move along the strike axis, and a different implied volatility should be used in the Black-Scholes formula. In this case, the greeks of Black-Scholes will no longer apply. For example, consider a skewed implied volatility: suppose that the implied volatility decreases as function of K. This is equivalent with implied volatility increasing as function of $\frac{S}{K}$. Then, under the sticky delta assumption, for a fixed strike the volatility will increase when the asset price increases, so we have $\frac{\partial \sigma_{imp}}{\partial S} > 0$ and the value of delta is higher than computed under the Black-Scholes assumption. For increasing spot, the smile shifts to the right. In figure 3.5 the implied volatility displays a smile shape. In this case, depending on the strike, the delta may either be higher or lower than the Black-Scholes delta (with the crossing point lying around a strike of $K = 1.28$: for $K < 1.28$ we have $\frac{\partial \sigma_{imp}}{\partial S} > 0$, for $K > 1.28$ we have $\frac{\partial \sigma_{imp}}{\partial S} < 0$.

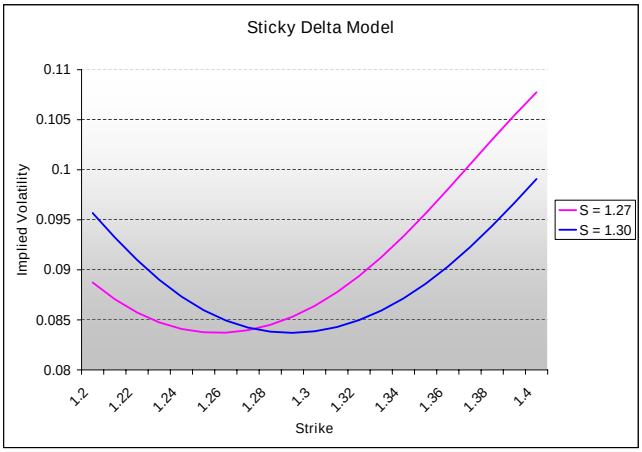

Figure 3.5: Sticky Delta Dynamics: when spot rises, the smile shifts to the right along the strike axis.

When we set up a model, we would like to capture the market behavior. We have seen two opposite smile dynamics models; which of these fits the true smile dynamics that can be observed in the market?

In Baker, Beneder and Zilber[2] and Carr and Wu[8] the empirical smile dynamics that are observed in the foreign exchange market are discussed. In the two following sections we will introduce the foreign exchange market and its conventions, after that we will return to the empirical smile dynamics.

To conclude, we have seen that the volatility smile gives us enough information in order to price

any European option. However, hedging requires the knowledge of the right greeks and therefore we also need to know about the smile dynamics.

Another problem with non-constant volatility arises in the pricing of path-dependent options, when the payoff of the contract depends not only on the final value of the underlying. In this case the smile does not give enough information; we need to know about the smile dynamics as well. We will return to this in more detail later.

3.5 The FX Market

In this section we will give an introduction to the foreign exchange market; we will consider a market for the exchange rate between the domestic currency and a foreign currency. A foreign exchange (FX) option is an option on a foreign currency (so, for a call option this means the right to buy this foreign currency for a fixed price in the domestic currency). Let $S(t)$ denote the spot exchange rate at time t. Then the price of this stock is the price of one unit of some foreign currency. The price of the stock is denoted in the domestic currency. The dynamics of the spot exchange rate (under the objective probability measure) are given by

$$dS = S\alpha_S dt + S\sigma_S d\overline{W},$$

where α_S, σ_S are deterministic constants. We will derive the risk neutral process of S, following Björk[5].

Let r_d be the domestic interest rate, r_f the foreign interest rate (both interest rates are assumed to be constant and deterministic). Then we have two riskless asset prices with dynamics,

$$\begin{aligned} dB_d(t) &= r_d B_d dt \\ dB_f(t) &= r_f B_f dt. \end{aligned}$$

Now consider a T-claim $\mathcal{Z} = \Phi(S(T))$, where Φ is some deterministic function. Then the price $\Pi(t;\mathcal{Z})$ of the claim can be calculated by discounting the expectation of the payoff under the risk neutral measure,

$$\Pi(t;\mathcal{Z}) = e^{-r_d(T-t)}\mathbb{E}^Q[\Phi(S(T))]. \tag{3.3}$$

We need to know the risk neutral dynamics of S. Now one should realize that buying the foreign currency and investing it at the foreign short rate of interest is equivalent to investing in a *domestic* asset with price process $\tilde{B}_f$, where

$$\tilde{B}_f(t) = B_f(t)S(t),$$

We can apply Itô's formula to $\tilde{B}_f$, then the dynamics of $\tilde{B}_f$ are given by

$$d\tilde{B}_f = \tilde{B}_f(\alpha_S + r_f)dt + \tilde{B}_f\sigma_S d\bar{W}.$$

We can conclude that our currency model is equivalent to a model of a domestic market that consists of the assets B_d and $\tilde{B}_f$. The local rate of return of $\tilde{B}_f$ under the risk neutral measure is now equal to the domestic short rate r_d,

$$d\tilde{B}_f = r_d\tilde{B}_f dt + \sigma_S \tilde{B}_f dW,$$

where W is a Q-Wiener process. In the final step we apply Itô to $S(t) = \frac{\tilde{B}_f}{B_f}$ and we obtain the risk neutral process of S:

$$\begin{aligned} dS(t) &= \frac{d\tilde{B}_f}{B_f} - \frac{\tilde{B}_f}{B_f^2} dB_f \\ &= \frac{1}{B_f}\left(r_d\tilde{B}_f dt + \sigma_S\tilde{B}_f dW\right) - \frac{\tilde{B}_f}{B_f^2}\left(r_f B_f dt\right) \\ &= S(r_d - r_f)dt + S\sigma_S dW. \end{aligned} \tag{3.4}$$

So we can calculate the arbitrage free price $\Pi(t;\mathcal{Z})$ in equation (3.3), where the risk neutral dynamics of the exchange rate are given by equation (3.4). By using the Feyman-Kač formula, $\Pi(t;\mathcal{Z}) = F(t,s)$ can also be obtained as a solution to the boundary value problem

$$\begin{aligned} \frac{dF}{dt} + S(r_d - r_f)\frac{dF}{ds} + \frac{1}{2}S^2\sigma^2\frac{d^2F}{ds^2} - r_d F &= 0, \\ F(T,S) &= \Phi(S). \end{aligned}$$

The Black-Scholes formulae for the FX market are now given by

$$C(S(t),t) = S(t)e^{-r_f(T-t)}\mathcal{N}(d_1) - Ke^{-r_d(T-t)}\mathcal{N}(d_2) \tag{3.5}$$

$$P(S(t),t) = Ke^{-r_d(T-t)}\mathcal{N}(-d_2) - S(t)e^{-r_f(T-t)}\mathcal{N}(-d_1), \tag{3.6}$$

where d_1 and d_2 are given by

$$\begin{aligned} d_1 &= \frac{log(\frac{S_t}{K}) + (r_d - r_f + \frac{1}{2}\sigma^2)(T-t)}{\sigma\sqrt{T-t}}, \\ d_2 &= d_1 - \sigma\sqrt{T-t}. \end{aligned} \tag{3.7}$$

3.6 FX Market Quotes

For European vanilla options it is common practice to quote the implied volatility rather than the option price. The implied volatility being known, the price of the option can then be calculated by plugging this value of volatility into the Black-Scholes formulae. The implied volatility varies with expiry and strike, so for options with different strikes and/or different expiries, this results in different prices. However, in the FX market the implied volatility is not quoted in terms of strike and expiry. Instead, the implied volatility is given in terms of *delta* and expiry. By convention the implied volatilities are quoted in terms of the At-The-Money Straddle (ATM), the 25Δ-Risk

Reversal (RR) and the 25Δ-Strangle (STR). In this section we will discuss these three quotes. From these quotes the volatility smile can be constructed; but first we will give an explanation.

The At-The-Money Straddle is a portfolio consisting of long both a call option and a put option, with the same expiry T and with the same strike price. The strike price is chosen in such way that the delta of the portfolio is equal to zero. A payoff diagram is shown in figure 3.6. The delta of a call option is equal to $\mathcal{N}(d_1)$, the delta of a put option is equal to $\mathcal{N}(d_1)-1$ (this follows from the put-call parity). We can find the strike price of this portfolio as follows. The delta of the portfolio is equal to $\Delta_{call}+\Delta_{put}=\mathcal{N}(d_1)+(\mathcal{N}(d_1)-1)$ and since this must be equal to zero, we find that $\mathcal{N}(d_1)=\frac{1}{2}$, which gives a value for d_1 equal to zero. Now we can solve the known expression for d_1 (equation (2.8)) to find the at-the-money strike price K_{ATM}:

$$K_{ATM}=Se^{(r+\frac{1}{2}\sigma^2)(T-t)}. \tag{3.8}$$

The quoted ATM value is the implied volatility of an option with this strike K_{ATM},

$$ATM=\sigma_{imp}(K_{ATM},T). \tag{3.9}$$

We will also use the notation σ_{ATM}.

A 25-delta call is a call option with $\Delta=0.25$ and a 25-delta put is a put option with $\Delta=-0.25$. The 25Δ-Risk Reversal is a portfolio consisting of a long 25-delta call and a short 25-delta put with the same expiry T but with different strikes (these strikes can be calculated from the expression for delta; in the Black-Scholes model, $\Delta=\mathcal{N}(d_1)$ for a call option, see Björk[5]), see the payoff diagram in figure 3.6. Let $\sigma_{25\Delta call}=\sigma_{imp}(K_{25\Delta-call},T)$, the implied volatility of a 25Δ-call option, and let $\sigma_{25\Delta put}=\sigma_{imp}(K_{25\Delta-put},T)$, the implied volatility of the 25Δ-put option. Then the quote 25Δ-RR is the implied volatility of this call option minus the implied volatility of this put option,

$$RR=\sigma_{25\Delta call}-\sigma_{25\Delta put}.$$

Finally, the 25Δ-Strangle is a portfolio consisting of long both a 25Δ-call and a 25Δ-put option with the same expiry but with different strikes (again these strikes follow from the values of delta), see the payoff diagram in figure 3.6. The quote 25Δ-STR is the average of the implied volatilities of the call and the put, minus the implied volatility of the ATM,

$$STR=\frac{1}{2}\left(\sigma_{25\Delta call}-\sigma_{25\Delta put}\right)-ATM.$$

From these three quotes we can obtain the implied volatilities for the 25Δ-call and 25Δ-put:

$$\sigma_{25\Delta call} = STR+ATM+\frac{1}{2}RR \tag{3.10}$$

$$\sigma_{25\Delta put} = STR+ATM-\frac{1}{2}RR \tag{3.11}$$

Now we are able to construct the volatility smile as function of strike. We have three options available to do this, the ATM option, a 25Δ-call and a 25Δ-put. First calculate the strike that

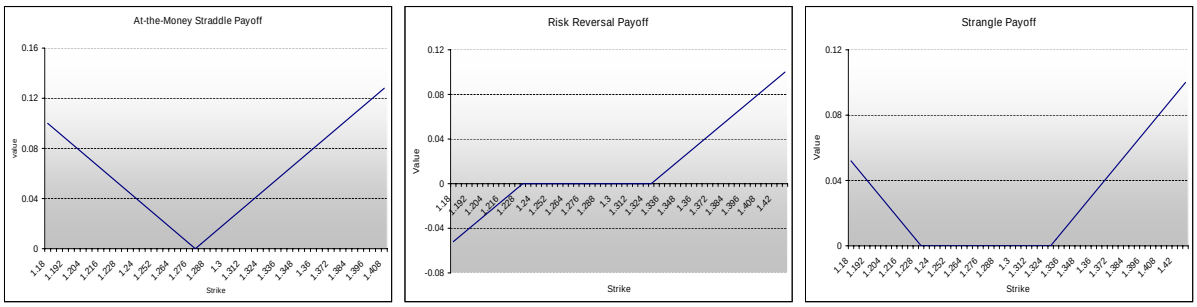

Figure 3.6: Payoff diagrams for the at-the-money Straddle, Risk Reversal and Strangle portfolio. The strikes are given by $K_{ATM} = 1.28$, $K_{25\Delta C} = 1.33$ and $K_{25\Delta P} = 1.23$.

corresponds to a value of delta equal to 0.25 for the call, and -0.25 for the put. For the three available strikes there holds $K_{25\Delta put} < K_{ATM} < K_{25\Delta call}$. For these strikes we have three implied volatilities. We can then interpolate between these points to obtain a complete smile.

The ATM, RR and STR quotes contain information about the volatility smile. First of all, the ATM gives a starting point for the smile, and it determines the general level of the smile. See figure 3.7. The RR gives information about the skewness (i.e., about the level of non-symmetry), see figure 3.8.

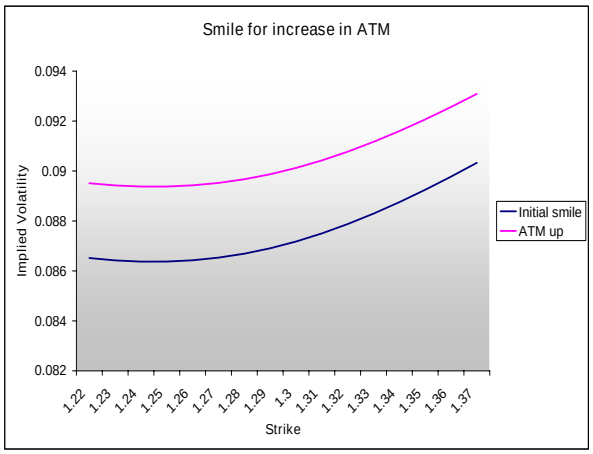

Figure 3.7: Volatility smile for an increase in the ATM quote from $ATM = 8.7\%$ to $ATM = 9.0\%$. The ATM strike is $K_{ATM} = 1.29$.

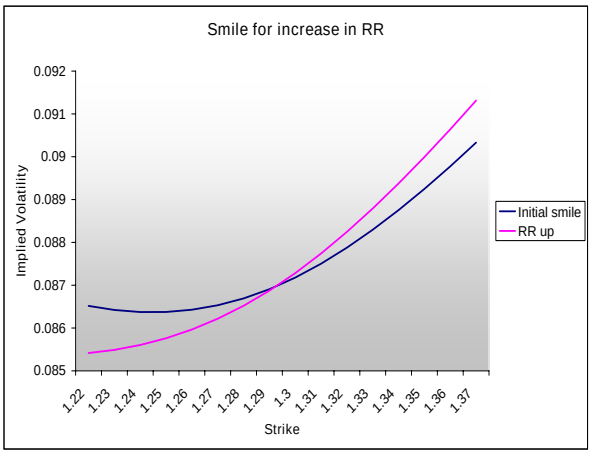

Figure 3.8: Volatiliy smile for an increase in RR from $RR = 0.38\%$ to $RR = 0.60\%$. The 25Δ-call and -put strikes are given by $K_{25\Delta C} = 1.22$, $K_{25\Delta C} = 1.37$.

For RR > 0 the implied volatility of the call is higher than for the put, so the smile is right skewed and for RR < 0 the opposite holds, so the smile is left skewed. For RR equal to zero the smile is symmetric. If market participants consider it equally likely that the exchange rate could move by a specific percentage in either direction, the risks incurred at both positions (the long call and the short put) cancel each other out, leaving the risk reversal price at zero. By contrast, a RR > 0 means that 'the market' considers the probability of a rising currency as being higher than the probability of a falling currency. This implies a greater demand for $25 - \Delta - calls$ than

for $25-\Delta puts$, and hence a higher volatility and a higher price. For a negative risk reversal the opposite holds true.

The STR tells us something about the curvature of the smile, see figure 3.9.

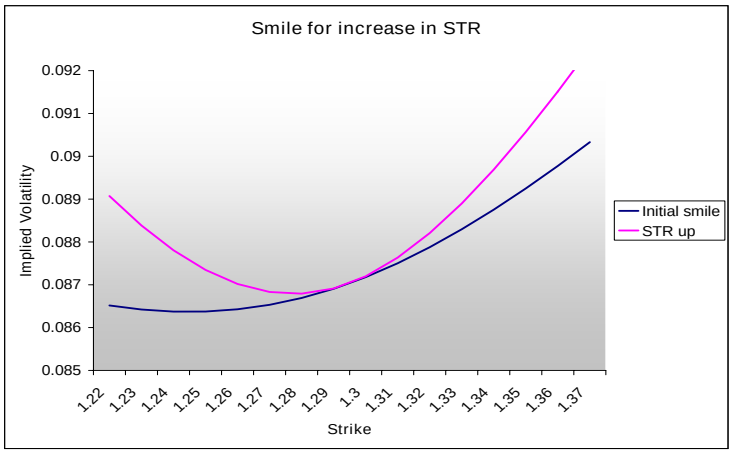

Figure 3.9: Volatiliy smile for an increase in STR from $STR = 0.15\%$ to $STR = 0.40\%$. The 25Δ-call and -put strikes are given by $K_{25\Delta C} = 1.22$, $K_{25\Delta C} = 1.37$, the ATM strike is equal to $K_{ATM} = 1.29$.

A low value of STR means that the average implied volatility of put and call is close to the ATM volatility, so we have little curvature. For high values of STR this distance is large and therefore there is more curvature. Put in other words, the higher the value of STR, the more expensive (in terms of implied volatility) out-of-the-money options are. Since the payoff at maturity is only received if the exchange rate is above the strike price of the call options or below that of the put option, the strangle can be considered as a measure of substantial exchange rate fluctuations expected by market participants.

How do the smile dynamic models relate to these quotes? First of all, the sticky strike rule implies that, as the spot changes, the smile remains the same. This implies that the the RR, ATM and STR do change. This can be seen in figure 3.10, which shows the sticky strike and sticky delta rule (see also section 3.4). On the other hand, the sticky delta rule implies that, as the spot changes, the smile moves along the strike axis. Hence, the RR, ATM and STR remain the same in this case, see again figure 3.10.

Finally, a comment on the relationship between the quotes and the shape of the density function. We have already seen that the volatility smile is a measure of the deviation from lognormality. This is therefore also reflected in the risk reversal and the strangle. With respect to the risk reversal, the calculated density function reflects the risk reversal in the skewness: for $\text{RR} < 0$ the implied density leans to the right, putting its peak to the right of the average expected spot rate, thus making an appreciation of the exchange rate more likely than a depreciation of the same size.

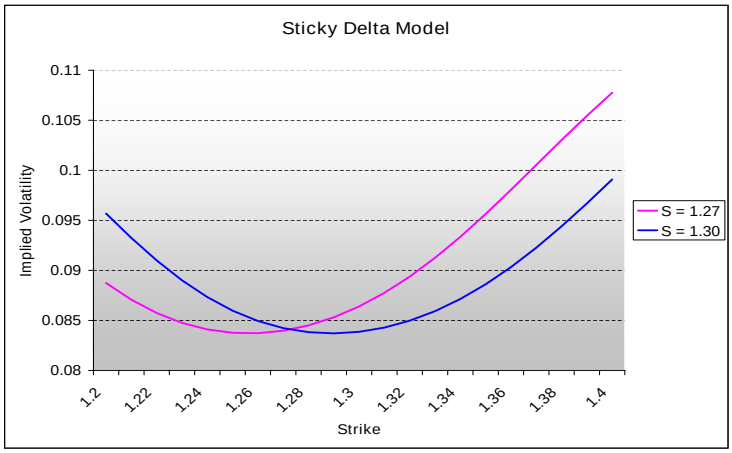

Figure 3.10: Smile Dynamics: when spot rises from $S = S_0 = 1.27$ to $S = 1.30$, the smile shifts to the right along the strike axis for the sticky delta model. In the initial state we have $K^{S_0}_{ATM} = 1.292$, $K^{S_0}_{25\Delta C} = 1.222$ and $K^{S_0}_{25\Delta P} = 1.370$. For the new state we have $K^{S}_{ATM} = 1.326$, $K^{S}_{25\Delta C} = 1.406$ and $K^{S}_{25\Delta P} = 1.254$.

With respect to the strangle, the calculated density function reflects the strangle in the fatness of the tails, see figures 3.2, 3.3 and 3.1.

3.7 Empirical Smile Dynamics

The smile dynamics that can be observed in the market are discussed in Baker, Beneder and Zilber[2] and in Carr and Wu[8]. They find the following observations.

With respect to the market quotes, it is found that the ATM typically fluctuates around levels between 5% and 10%, RR between -2% and 2% and STR is reasonably stable around a level of 0.3%. In general, short dated maturities have traded at higher levels of volatilities than the longer dated maturities.

The above findings refer to the shape of the smile. Now we turn to the smile dynamics. There are two observations that seem to be most important to describing the dynamic.

The first feature that is seen is the strong, positive correlation between changes in the spot exchange rate with changes in the RR quote. As spot increases, the risk reversal tends to increase also. This corresponds to distributions with fatter right tails and thinner left tails. For out-of-the-money calls this means that, as the implied volatility has changed to a higher value, the probability of getting in-the-money gets higher. For in-the-money calls this means that, as the implied volatility now takes a lower value, the probability of getting out-of-the-money get smaller. For put options the converse is true: out-of-the-money put options have a lower probability of getting in-the-money, and in-the-money put options have a higher probability of getting out-of-

the-money.

This correlation between spot and RR is seen to be stronger for short maturities.

Secondly, it is observed that the spot and ATM are correlated also. This correlation may be positive or negative. It is observed that the RR quote gives a good indication of the sign of the historical correlation: a negative RR corresponds to a negative correlation between spot and ATM, a positive RR corresponds to a positive correlation between spot and ATM.

A good model should be able to capture the above mentioned smile dynamics. Does this hold for the sticky strike rule and the sticky delta rule? For the sticky delta rule, when spot increases, the smile moves along the strike axis and this means that the ATM, the RR and the STR remain the same, so this is not in agreement with empirical observations.

For the sticky strike rule the implied volatility smile stays the same when spot changes. This means that the ATM, the RR and the STR will change when spot changes. This is in line with the observations, although we would need more information about the smile to determine if there is indeed a positive correlation.

Part II

Option Pricing Models

Chapter 4

Local Volatility Model

4.1 Outline

The implied volatility displays a smile pattern. Quoted option prices result in implied volatilities that vary with both strike and maturity. This means that the volatility is not constant as is assumed in the Black-Scholes model. Many alternative models have been suggested to accommodate the observed market prices. The simplest of these adjusted Black-Scholes models is the *Local Volatility Model*. In the local volatility model it is assumed that the volatility of the underlying is a deterministic function of time and of the value of the underlying itself, i.e., $\sigma = \sigma(S(t), t)$.

This chapter discusses the local volatility model. In section 4.2 we derive expressions for the local volatility in two cases: first, when the local volatility is assumed to be a function of time only, and second when it is assumed to be a function of both spot and time. Section 4.3 gives an overview of comments on the model that can be found in the literature. Section 4.4 explains how to calculate an option price using this model. Section 4.5 discusses the numerical implementation.

4.2 Local Volatility

The simplest adjustment to the Black-Scholes model that accounts for the observed smile pattern is the Local Volatility Model by Dupire[12]. In the local volatility model it is assumed that the volatility of the underlying is a deterministic function of time and of the value of the underlying itself, i.e., $\sigma = \sigma(S(t), t)$. The risk neutral dynamics for the asset are then given by

$$dS(t) = rS(t)dt + \sigma(S(t), t)S(t)dW(t)$$

In Dupire[12] it is shown how the local volatility function can be determined from observed European call option prices. Here we will also show how this function can be calculated. First we will consider the simpler case when we only have a term structure, $\sigma = \sigma(t)$. It can be shown (see Wilmott[25]) that the Black-Scholes formulae are still valid in this case, but we have to replace σ

in these formulae by

$$\sqrt{\frac{1}{T-t}\int_t^T \sigma(\tau)^2 d\tau}, \tag{4.1}$$

and now we have to make sure that this expression is equal to the implied volatilities as function of the time to maturity,

$$\sqrt{\frac{1}{T-t}\int_t^T \sigma(\tau)^2 d\tau} = \sigma_{imp}(T-t).$$

A simple calculation shows that we can achieve this by taking the square and differentiate with respect to t to obtain the result,

$$\sigma(t) = \sqrt{\sigma_{imp}(T-t)^2 - 2(T-t)\sigma_{imp}(T-t)\frac{\partial \sigma_{imp}(T-t)}{\partial t}}. \tag{4.2}$$

We can use this expression for $\sigma(t)$ and plug it into equation (4.1). Then vanilla option prices are calculated by inserting (4.1) in the Black Scholes formulae. In case of pricing the option numerically, we can insert (4.2) in the PDE that is to be solved.

Now we will continue with constructing a *local volatility surface* $\sigma(S,t)$ that matches the implied volatility surface. We will back out this local volatility surface from the observed market prices of European call options, which will be denoted by $C(S,t;K,T)$: the call price at the current time t and current spot S for strike K and maturity T. Assume that these prices are known for all possible strikes and maturities. We have seen in section 3.3 that these call prices enable us to derive an expression for the density of the underlying at maturity. To repeat:

$$f_{S_T}(S) = e^{r(T-t)}\frac{\partial^2 C(S_t,t;K,T)}{\partial K^2}|_{K=S},$$

where $f_{S_T}(S)$ is the density function of S_T in the point S. This result is the first step in finding the local volatility. What we want is to find a diffusion process that generates this density.

It is known (for example, see Björk[5]) that if the coefficients $a(x,t)$ and $b(x,t)$ of the diffusion process

$$dX(t) = a(X(t),t)dt + b(X(t),t)dW(t)$$

are known, then we can obtain the transition density $f = f(x_0,s;x,T)$ of X through the Fokker-Planck equation

$$\frac{1}{2}\frac{\partial^2\left[b(x,T)^2 f(x_0,s;x,T)\right]}{\partial x^2} - \frac{\partial\left[a(x,T)f(x_0,s;x,T)\right]}{\partial x} = \frac{\partial f(x_0,s;x,T)}{\partial T},$$

where we have to solve this equation for the density function f. Our goal is to find a (risk neutral) diffusion process that generates the density, this is exactly the converse problem: we have a known

density $f_{S_T}(S,T)$, and we want to find σ. Again we turn to the Fokker-Planck equation, but now the coefficient $\sigma(S,T)$ is the unknown quantity:

$$\frac{\partial f_{S_T}(S,T)}{\partial T} = -\frac{\partial}{\partial S}\left[rSf_{S_T}(S,T)\right] + \frac{1}{2}\frac{\partial^2}{\partial S^2}\left[\sigma^2(S,T)S^2 f_{S_T}(S,T)\right]. \tag{4.3}$$

Our starting point is the expression for the value of a call option,

$$C(S,t;K,T) \quad = \quad e^{-r(T-t)}\int_K^\infty (s-K)f_{S_T}(s)ds. \tag{4.4}$$

We can calculate the derivative of this expression with respect to T, and we will show that this will lead us to the local volatility $\sigma(S,t)$. Denote $C(S,t;K,T)$ by C for notational convenience. Differentiation with respect to T results in

$$\frac{\partial C}{\partial T} = -rC + e^{-r(T-t)}\int_K^\infty (S-K)\frac{\partial}{\partial T}f_{S_T}(S,T)dS$$

$$= -rC + e^{-r(T-t)}\int_K^\infty (S-K)\left(-\frac{\partial}{\partial S}\left(rSf_{S_T}(S,T)\right) + \frac{\partial^2}{\partial S^2}\left(\frac{1}{2}\sigma^2(S,T)S^2 f_{S_T}(S,T)\right)\right)dS, \tag{4.5}$$

where we have used the Fokker-Planck equation (4.2) from the first to the second line. Now we assume that f as well as $\frac{\partial f}{\partial S_T}$ approach zero fast enough, such that the boundary terms vanish. We calculate both terms in the integrand on the right hand side (by partial integration). For the first term:

$$\int_K^\infty (S-K)\frac{\partial^2}{\partial S^2}\left(\frac{1}{2}\sigma^2(S,T)S^2 f_{S_T}(S,T)\right)dS$$

$$= (S-K)\frac{\partial}{\partial S}\left(\frac{1}{2}\sigma^2(S,T)S^2 f_{S_T}(S,T)\right)|_K^\infty - \int_K^\infty \frac{\partial}{\partial S}\left(\frac{1}{2}\sigma^2(S,T)S^2 f_{S_T}(S,T)\right)dS$$

$$= \frac{1}{2}\sigma^2(K,T)K^2 f_{S_T}(K,T)$$

$$= \frac{1}{2}\sigma^2(K,T)K^2 e^{r(T-t)}\frac{\partial^2 C}{\partial K^2}, \tag{4.6}$$

where the final expression follows from equation (4.3). The other term of the integrand can be calculated as (again by partial integration)

$$\int_K^\infty (S-K)\frac{\partial}{\partial S}\left(rSf_{S_T}(S,T)dS\right)$$

$$= (S-K)rSf_{S_T}(S,T)\,|_K^\infty - \int_K^\infty rSf_{S_T}(S,T)dS$$

$$= -r\left[\int_K^\infty (S-K)f_{S_T}(S,T)dS + \int_K^\infty Kf_{S_T}(S,T)dS\right]$$

$$= -re^{r(T-t)}\left[C(S,t;K,T) - K\frac{\partial C(S,t;K,T)}{\partial K}\right], \tag{4.7}$$

where the final expression follows from equations (3.1) and (4.3). Finally, we can substitute (4.6) and (4.7) back into equation (4.5) to arrive at

$$\begin{aligned}\frac{\partial C}{\partial T} &= -rC + e^{r(T-t)}\int_K^\infty (S-K)\left(-\frac{\partial}{\partial S}\left(rSf_{S_T}(S,T)\right) + \frac{\partial^2}{\partial S^2}\left(\frac{1}{2}\sigma^2(S,T)S^2 f_{S_T}(S,T)\right)\right)dS \\ &= -rC + e^{-r(T-t)}\left[\frac{1}{2}\sigma^2(K,T)K^2 e^{r(T-t)}\frac{\partial^2 C}{\partial K^2} + re^{r(T-t)}(C - K\frac{\partial C}{\partial K})\right], \qquad (4.8)\end{aligned}$$

and we can solve this expression for σ to obtain

$$\sigma^2_{loc}(K,T) = \frac{\frac{\partial C(S,t;K,T)}{\partial T} + rK\frac{\partial C(S,t;K,T)}{\partial K}}{\frac{1}{2}K^2\frac{\partial^2 C(S,t;K,T)}{\partial K^2}}.$$

To extend this to the foreign exchange market we also have to include to foreign rate r_f. The derivation is similar, but now the Fokker Planck equation reads

$$\frac{\partial f_{S_T}(S,T)}{\partial T} = -\frac{\partial}{\partial S}\left((r_d - r_f)Sf_{S_T}(S,T)\right) + \frac{1}{2}\frac{\partial^2}{\partial S^2}\left(\sigma^2(S,T)S^2 f_{S_T}(S,T)\right),$$

From this we can find $\sigma_{loc}(K,T)$, and by relabelling, the result is then given by $\sigma_{loc}(S,t)$:

$$\sigma^2_{loc}(S,t) = \frac{\frac{\partial C}{\partial T} + (r_d - r_f)K\frac{\partial C}{\partial K} + r_f C}{\frac{1}{2}K^2\frac{\partial^2 C}{\partial K^2}}, \qquad (4.9)$$

where $C = C(S_0, t_0; K, T, \sigma(K,T))|_{K=S,T=t}$, given that we are currently at time $t = t_0, S = S_0$. This expression is called *Dupire's formula.*

In Jackson[20] it is shown that the local volatility term can be written in terms of the implied volatility instead of in terms of call prices. A simplified version of Dupire's formula is derived, which is specified directly in terms of the known market implied volatility surface. The result is as follows:

$$\sigma^2_{loc}(S,t) = \left(\frac{\frac{\partial\left(\sigma^2_{imp}T\right)}{\partial T}}{\left(1 - \frac{X}{\sigma_{imp}}\frac{\partial\sigma_{imp}}{\partial X}\right)^2 + T\sigma_{imp}\frac{\partial^2\sigma_{imp}}{\partial X^2} - \left(\frac{1}{2}T\sigma_{imp}\frac{\partial\sigma_{imp}}{\partial X}\right)^2}\right), \qquad (4.10)$$

where the implied volatility is used for a strike equal to S and maturity equal to t, $\sigma_{imp} = \sigma_{imp}(K,T)|_{K=S,T=t}$. Further,

$$\begin{aligned}X &= log\left(\frac{F}{K}\right), \\ F &= S(t)e^{(r_d - r_f)(T-t)}\end{aligned}$$

The partial differential equation for the price $V = V(S,t)$ of an option in the FX market is now given by

$$\frac{\partial V}{\partial t} + S[r_d - r_f]\frac{\partial V}{\partial S} + \frac{1}{2}S^2\sigma^2_{loc}(S,t)\frac{\partial^2 V}{\partial S^2} - r_d V = 0.,$$

where the local volatility term $\sigma^2_{loc}(S,t)$ can be calculated using formula (4.9) or (4.10).

4.3 Literature Review: Comments

The local volatility model generates volatilities that completely matches the market implied volatilities (and as such, the observed market prices). An advantage of this model is that it maintains market completeness. We have one tradable asset and because the local volatility is a deterministic function of the underlying stock itself, we also have one source of randomness. This means that we can always set up a replicating portfolio with the underlying stock. Risk neutral valuation will then give rise to a unique option price.

However, there are also some major drawbacks of the model. This section presents an overview of the comments on the local volatility model that can be found in the literature. See also Derman[10], Dumas et al.[11] and Hagan et al.[13].

The first problem is that it is never possible to obtain a *complete* set of options prices. Therefore, we have to use an interpolation technique to construct a complete smile surfaces. The problem is that different interpolation techniques can lead to very different local volatility functions. In our implementation, we use a third order polynomial to approximate the market smile. Using this we can then calculate the local volatility term as in equation (4.9) or (4.10).

Another problem of the local volatility model is that the shape of the local volatility surface may sometimes look very surprising and counterintuitive. For example (see Ayache et al.[1]) future volatilities predicted by the model have a tendency to flatten out. Far in the future, the local volatilities are roughly constant. So the model results in future smiles that are far flatter than the current smile, which is not observed in practice.

In Dumas et al.[11] the local volatility model is examined. In particular, its predictive and hedging performance is investigated for a call option. In an out-of-sample test it is investigated if the volatility function implied by option prices today, is the same one as embedded in option prices tomorrow. Today's call option prices are used to estimate the parameters of the underlying process. Then, after stepping forward in time, option prices are calculated. It turns out that the estimated volatility function is not stable through time, which means that pricing and hedging using this model is unreliable. Out-of-sample option values are inaccurate. This implies that the model does not specify the true volatility function (or the true stochastic process for the underlying asset).

But the main problem of the local volatility model is that the model predicts the wrong smile *dynamics*. This has consequences for both the pricing of exotic options as well as for hedging results. See for example Hull et al.[18], in which the local volatility model is used to calculate the prices of different exotic options and to perform a hedge test.

First a word about the pricing of exotic options. We have seen that we can extract the density at maturity from observed market prices (or, from the observed volatility smile). So if we have a model that completely matches this observed smile, then it produces the right density at maturity. This in turn means that this model always correctly prices a derivative when its payoff is contingent on the asset price at only one time. Since the local volatility model matches the observed market smile, it produces correct vanilla option prices.

But many exotic options do not only depend on the density at maturity, but also on the transition density from one time in the future to a further time in the future (i.e., on the value of the asset on more than one time). However, it is not guaranteed that the local vol model correctly prices derivatives where the payoff is contingent on the asset price at more than one time. This is because the joint distribution of the asset price at times T_1 and T_2 is not uniquely determined from the marginal distributions at times T_1 and T_2. This information about joint distributions is not contained in vanilla prices. Just as the volatility smile implies the terminal density, the smile *dynamics* determine these transition densities. We will return to this point in the next chapter about stochastic volatility models. For now it is important to note that wrong smile dynamics result in wrong transition densities, and therefore wrong prices of options that depend on these transition densities.

So, predicting the wrong smile dynamics is the main point of issue for the local volatility model. In fact, the dynamics as predicted by the model may be more extreme, or even completely *opposite* to what is observed in the real world. Once the local volatility term has been calculated according to equation (4.9), the smile dynamics are implicitly determined. In Hagan et al.[13] it is shown that the smile dynamics implied by the local volatility model are given by

$$\sigma_{impl}(K,T;S_1) \approx \sigma_{local}\left(\frac{1}{2}(S_1+K);S_0\right) \approx \sigma_{impl}(K+\Delta S,T;S_0),$$

where $S_1 = S_0 + \Delta S$. This shows that when the price of the underlying decreases, local volatility models predict that the smile shifts to higher prices (the smile shifts to the right); and when the price of the underlying increases, local volatility models predict that the smile shifts to lower prices (the smile shifts to the left). This is exactly opposite to the observed market behavior.

But not only do these wrong smile dynamics influence exotic option prices. It is also a problem in hedging, because this requires the calculation of (some of) the greeks. If we look at the value of delta again,

$$\Delta = \frac{\partial BS}{\partial S} + Vega_{BS}\frac{\partial \sigma}{\partial S},$$

then the result of the volatility dynamics implied by the local volatility model is that the term $\frac{\partial \sigma}{\partial S}$ may have the wrong sign. For example, if in the market it can be observed that $\frac{\partial \sigma}{\partial S}$ is positive,

for the local volatility model might be negative. Therefore, even the original Black-Scholes model can yield more accurate hedges than the local volatility model. An example of this behavior is given in Hagan [13] to illustrate this point.

4.4 Option Price Calculation

The value of an option can now be calculated by solving the partial differential equation (PDE) (4.11) with the corresponding payoff as the 'initial' condition. This can be done using a finite difference (FD) grid. The next section will discuss the implementation in more detail. Using an FD grid option prices are calculated by starting at expiry where we have an initial condition, the payoff, so the option value can be calculated for every gridpoint at expiry. Then we move to the next time step, and we calculate the option prices in every grid point, where the coefficient with the local volatility is calculated as in equation (4.9) or (4.10). This is repeated until we arrive at time $t = 0$.

Consider a forward start option. Let T_1 be the fixing date at which the strike is set, and let T_2 be the expiry date. For a forward start option, the strike depends on the spot value at time T_1. This means that when we start in a grid at time T_2, the strike is unknown. To resolve this, we solve the PDE in two grids separately. Grid 1 extends from time T_2 to time T_1, grid 2 from time T_1 to time $t = 0$. We start on Grid 2. We do not know what the spot will be at time T_1, so we do not know the strike. But if we *assume* that we know the spot value S_{fixed} at T_1, then we can calculate the payoff at T_2 and work our way back through the grid up to time T_1. Given that we came from the point S_{fixed}, we can now calculate the option value in this point: for a call option, $C(S_{fixed}, T_1; K(S_{fixed}); T_2)$. To obtain the option value in all the grid points at time T_1 we have to repeat this step, each time assuming a different spot value at fixing date. So, the number of times we have to solve the PDE from T_2 to T_1 is equal to the number of grid points we use. Finally we have to solve the PDE one more time, from T_1 to time $t = 0$, to obtain the option value at the current time. For this, we use the call value as our payoff at T_1.

Next consider a compound option with expiry T_1 on an underlying option with expiry $T_2 > T_1$. The payoff of the compound option depends on the value of the underlying option at T_1. Therefore, first we solve PDE (4.11) for the underlying option with payoff $max(S_{T_2} - K_2, 0)$ on an FD grid from T_2 to T_1. Then we obtain the underlying option price at T_1 for all possible choices of spot at that time. These values can be used in the payoff at T_1 of the compound option, and in the second step the PDE is solved again, now using the payoff $max(C(S_{T_1}, T_1; K_2, T_2) - K_1, 0)$.

4.5 Numerical Implementation: Crank-Nicholson

To calculate the price $V = V(S,t)$ of an option under the local volatility model, we have to solve the PDE

$$\frac{\partial V}{\partial t} + a(S,t)\frac{\partial^2 V}{\partial S^2} + b(S,t)\frac{\partial V}{\partial S} + c(S,t)V = 0,$$

where

$$\begin{aligned} a(S,t) &= \frac{1}{2}\sigma_{loc}^2(S,t)S^2 \\ b(S,t) &= [r_d(t) - r_f(t)]\,S \\ c(S,t) &= r_d(t). \end{aligned}$$

We will solve this equation using finite differences. In the previous section it has been explained how to use a finite difference grid for the compound option and the forward start option. For these options it is necessary to construct two grids and solve the equation on both grids. In this section we will show how the value of an option can be obtained on a single grid.

We estimate the price given by the local volatility model by using a Crank-Nicholson scheme (see for example Wilmott[25]). For this, a grid is constructed in spot direction and in time direction. In time direction, the grid extends from time zero to the maturity T of the option being priced. In spot direction, the grid extends from a low enough value $S = S_{min}$ to a high enough value $S = S_{max}$. Let N_s and N_t be equal to one plus the number of interior grid points in spot- and time direction, respectively. Then the step sizes δS and δt in time and spot direction respectively are given by

$$\begin{aligned} \delta t &= \frac{T}{N_t} \\ \delta S &= \frac{S_{max} - S_{min}}{N_s} \end{aligned}$$

The numerical approximation of the option value in the grid points is given by $V_n^k = V(S_n, t_k)$, where

$$\begin{aligned} S_n &= S_{min} + n\delta S, & n &= 0, 1, \ldots, N_s \\ t_k &= T - k\delta t & k &= 0, 1, \ldots, N_t \end{aligned}$$

The solving procedure starts at expiry, so we have an initial condition at $t = T$ ($k = 0$), which is given by the payoff of the option. The value of the option can be calculated at any grid point at $t = T$ using this payoff. Further we also have boundary conditions for the lower and upper boundaries of the spot. These depend on the option under consideration and will be given in the next subsection.

For the spot derivatives we use central differences both for the first and second derivative. The Crank-Nicholson scheme is given by

$$\frac{V_n^{k-1}-V_n^k}{\delta t}+\frac{1}{2}\left[a_n^k\frac{V_n^k-2V_n^k+V_{n-1}^k}{\delta S^2}+a_n^{k-1}\frac{V_{n+1}^{k-1}-2V_n^{k-1}+V_{n-1}^{k-1}}{\delta S^2}\right]+$$

$$\frac{1}{2}\left[b_n^k\frac{V_{n+1}^k-V_{n-1}^k}{2\delta S}+b_n^{k-1}\frac{V_{n+1}^{k-1}-V_{n-1}^{k-1}}{2\delta S}\right]+\frac{1}{2}\left[c_n^kV_n^k+c_n^{k-1}V_n^{k-1}\right]=0$$

$$k=1,\ldots,N_t$$

$$n=1,\ldots,(N_s-1).$$

Here, the coefficients are given by

$$\begin{aligned}a_n^k &= \frac{1}{2}\sigma_{loc}(S_{min}+n\delta S,T-k\delta t)^2(S_{min}+n\delta S)^2\\ b_n^k &= \left[r_d(T-k\delta t)-r_f(T-k\delta t)\right](S_{min}+n\delta S)\\ c_n^k &= r_d(T-k\delta t).\end{aligned}$$

Note that the time derivative is backwards, since we are solving the equation starting at maturity and ending at time zero:

$$\begin{aligned}V(S,t) &\approx V(S,t-\delta t)-\delta t\frac{\partial V(S,t)}{\partial t}\\ \frac{\partial V(S,t)}{\partial t} &\approx \frac{V(S,t)-V(S,t-\delta t)}{\delta t}=\frac{V^{k-1}-V^k}{\delta t}\end{aligned}$$

Rearranging terms, we find

$$\left[\frac{\delta t}{2\delta S^2}a_n^k-\frac{\delta t}{2\delta S}b_n^k\right]V_{n-1}^k+\left[1-\frac{\delta t}{\delta S^2}a_n^k+\frac{\delta t}{2}c_n^k\right]V_n^k+\left[\frac{\delta t}{2\delta S^2}a_n^k+\frac{\delta t}{4\delta S}b_n^k\right]V_{n+1}^k$$

$$=$$

$$\left[\frac{\delta t}{2\delta S^2}a_n^{k-1}-\frac{\delta t}{2\delta S}b_n^{k-1}\right]V_{n-1}^{k-1}+\left[1-\frac{\delta t}{\delta S^2}a_n^{k-1}+\frac{\delta t}{2}c_n^{k-1}\right]V_n^{k-1}+\left[\frac{\delta t}{2\delta S^2}a_n^{k-1}+\frac{\delta t}{4\delta S}b_n^{k-1}\right]V_{n+1}^{k-1}.$$

If we define

$$\begin{aligned}A_n^k &= \left[\frac{\delta t}{2\delta S^2}a_n^k-\frac{\delta t}{2\delta S}b_n^k\right]\\ B_n^k &= \left[1-\frac{\delta t}{\delta S^2}a_n^k+\frac{\delta t}{2}c_n^k\right]\\ C_n^k &= \left[\frac{\delta t}{2\delta S^2}a_n^k+\frac{\delta t}{4\delta S}b_n^k\right],\end{aligned}$$

then we can write

$$\begin{pmatrix} A_1^k & B_1^k & C_1^k & 0 & 0 & 0 & \cdots\\ 0 & A_2^k & B_2^k & C_2^k & 0 & 0 & \cdots\\ \vdots & & & \ddots & \ddots & \ddots & \\ & & & & A_{N_s-1}^k & B_{N_s-1}^k & C_{N_s-1}^k \end{pmatrix}\begin{pmatrix} V_0^k\\ V_1^k\\ V_2^k\\ \\ \vdots\\ \\ V_{N_s-2}^k\\ V_{N_s-1}^k\\ V_{N_s}^k\end{pmatrix}=$$

$$\begin{pmatrix} A_1^{k-1} & B_1^{k-1} & C_1^{k-1} & 0 & 0 & 0 & \dots \\ 0 & A_2^{k-1} & B_2^{k-1} & C_2^{k-1} & 0 & 0 & \dots \\ \vdots & & & \ddots & \ddots & \ddots & \\ & & & & A_{N_s-1}^{k-1} & B_{N_s-1}^{k-1} & C_{N_s-1}^{k-1} \end{pmatrix} \begin{pmatrix} V_0^{k-1} \\ V_1^{k-1} \\ V_2^{k-1} \\ \vdots \\ V_{N_s-2}^{k-1} \\ V_{N_s-1}^{k-1} \\ V_{N_s}^{k-1} \end{pmatrix}$$

The above matrix equation holds for $k = 1, \dots, N_t$; V_n^0 corresponds to the value of the option at maturity, for $n = 0, \dots, N_s$. These can be computed from the payoff function of the option contract. The matrix has $N_s + 1$ columns and $N_s - 1$ rows. At this point, the boundary conditions can be applied in order to obtain a square matrix of size $(N_s - 1)$ by $(N_s - 1)$. Using the boundary conditions, we can remove the first and the last column of the matrix, and the first and last element of the vector on the left hand side of the equation. At each time step k, the values at the previous time step $k - 1$ are known, so the right hand side of the equation can be calculated by simply deleting the first and last column of the matrix and first and last element of the vector (which is known) . This results in a system of the form

$$\mathbf{M^k v^k} \quad = \quad \mathbf{M^{k-1} v^{k-1}} \quad := \quad \mathbf{q^{k-1}}.$$

The matrix $\mathbf{M^k}$ is a tridiagonal matrix. At each time step this system of equations can be solved by making use of an LU-decomposition.

4.5.1 Boundary Conditions

In this section we will give the initial and boundary conditions that are needed to solve the partial differential equation.

Initial Conditions

The initial condition is given by the payoff of the option. For the forward start option with expiry T_2,

$$V_n^k = \max[\phi(S_n^k - K(S_n^{T_1})), 0], \qquad k = 0, n = 0, \dots, N_s.$$

The term $S_n^{T_1}$ denotes the value of the underlying at time T_1 in the grid point S_n. In this condition ϕ is equal to one for a call option, and equal to minus one for a put option. It has been explained that the value of a forward start option makes use of two grids. The above initial condition holds for the grid extending from time time T_2 (expiry) to T_1 (fixing date). In the grid from time $t = T_1$ to $t = 0$, the payoff is simply given by the value of the option at T_1.

For the compound option we also solve the PDE in two grids. First, we solve for the underlying option. This grid extends from expiry of the underlying option T_2 to expiry of the compound option

T_1. Let ϕ be defined the same as above for the compound option, and let θ be defined the same as above, but for the underlying option. The initial condition for the underlying option is given by:

$$U_n^k = \max[\theta(S_n^0 - K_2), 0], \qquad k = 0, n = 0, \ldots, N_s$$

Here, U_n^k is the value of the underlying option and $k = 0$ corresponds to $t = T_2$. Using this, the value of the underlying option at time T_1 can be calculated. This value can then be used in the payoff of the compound option at time T_1:

$$V_n^k = \max[\phi(U_n^{T_1} - K_1), 0], \qquad k = 0, n = 0, \ldots, N_s$$

With $U_n^{T_1}$ we mean the value of the underlying option at time T_1, $U_n^{T_1} = U_n^{T_1}(S_n, T_1; K_2, T_2)$. Further, $k = 0$ now corresponds to $t = T_1$.

Boundary Conditions

Both for the forward start option as for the compound option we can use the same boundary conditions. For the compound option have two options: the underlying and the compound itself. For both options we use the same boundary conditions, and therefore we will not treat them separately here.

Again, let ϕ be equal to one for a call option, and minus one for a put option. When $S = 0$ we have $dS = 0$, and therefore the value of the underlying at expiry is also equal to zero. Therefore, both for the forward start option as for the compound option, we have a Dirichlet boundary condition

$$V(S, t) = \frac{1 - \phi}{2} K e^{-r_d(T-t)}, \qquad S \to 0$$

In terms of our discrete equation this can be written as

$$V_n^t = \frac{1 - \phi}{2} K e^{-r_d k}, \qquad n = 0, k = 0, \ldots, N_t$$

When the spot goes to infinity, we can use a zero-convexity boundary condition for a call option, i.e., the second derivative of with respect to spot is equal to zero. This can be seen easily from a plot of the option value at any time before expiry; for large values of spot we have (for a call option)

$$C(S, t) \approx S, \qquad S \to \infty$$

For a put option, (...) In discrete terms, this results both for the forward start option as for the compound option in the boundary condition

$$V_n^t = 2V_{n-1}^t - V_{n-2}^t, \qquad n = N_s, k = 0, \ldots, N_t$$

Here, we have used backward difference in calculating the second derivative at the boundary of the grid.

Chapter 5

Stochastic Volatility Smile Dynamics Model

5.1 Outline

The second category of models that we include are the *Stochastic Volatility Models*. It is widely accepted that the volatility is not deterministic and therefore, has to be modelled as a stochastic process. Let the dynamics of the asset and the volatility, under the objective probability measure, be given by

$$\begin{aligned} dS(t) &= \alpha S(t)dt + \sigma(t)S(t)d\overline{W}_1(t) \\ d\sigma(t) &= p(S,\sigma,t)dt + q(S,\sigma,t)d\overline{W}_2(t), \end{aligned}$$

with a correlation between the Wiener processes of ρdt.

Since the volatility is not a tradable asset, S is the only tradable asset while there are two sources of randomness: stochastic volatility introduces market incompleteness.

This chapter discusses the Stochastic Volatility Smile Dynamics Model proposed in Rosien[24], which actually is a combination of local volatility and stochastic volatility. In section 5.2 an overview is given of a few models that can be found in the literature. These models will not be treated very detailed, but they do give insight into some important aspects of stochastic volatility models. Hestons model[15] and the Stochastic Volatility Smile Dynamics Model described in Zilber[26] will be presented. Also the model described in Blacher[6] will be addressed shortly. A more extensive overview can be found, for example, in Rosien[23]. In section 5.3 we turn to the Stochastic Volatility Smile Dynamics Model proposed in Rosien[24]. This model is an extension of the model used in Zilber[26] (and therefore has the same name). In section 5.4 we explain how to determine the model parameters. Section 5.5 handles on the option price calculation and finally section 5.6 gives a detailed description of the numerical implementation.

5.2 Overview of Models With Stochastic Volatility

In general, for Stochastic Volatility models the price process for the asset, S, under the objective probability measure, is given by

$$dS(t) = \alpha S(t)dt + \sigma(t)S(t)d\overline{W}_1(t),$$

and it is assumed that the volatility satisfies (also under the objective probability measure)

$$d\sigma(t) = p(S,\sigma,t)dt + q(S,\sigma,t)d\overline{W}_2(t).$$

The two Wiener processes have correlation ρdt. Observe that since volatility is not a tradable asset, there is only one tradable asset while there are two sources of randomness: stochastic volatility models result in incomplete markets. As a result, an option cannot be hedged by the underlying alone anymore. We need to include a benchmark option into our portfolio and the concept of *market price of volatility risk* will be introduced. We can derive the partial differential equation that the option value should satisfy, the derivation is similar to the Black-Scholes case for incomplete markets, see section 2.8. There we constructed a portfolio consisting of the option, the underlying and a benchmark option, and we showed how this resulted in the market price of risk. In that case we only had one source of randomness and no tradable assets.

We can set up the same construction for two random sources together with one tradable asset and one non-tradable asset. Again we form a portfolio based on the underlying (tradable) asset S, the option and a benchmark option. The derivation of the PDE for the price of an option is similar as in the case discussed before and is therefore deleted. See Wilmott[25] for a derivation. In this case the value of a claim is a function of both S and σ, $\Pi(t;\mathcal{X}) = F(S(t),\sigma(t),t)$ and Itô's formula can be applied. We find that the function $F(s,\sigma,t)$ should satisfy the partial differential equation

$$F_t + \frac{1}{2}\sigma^2 S^2 F_{ss} + \rho\sigma q S F_{\sigma s} + \frac{1}{2}q^2 F_{\sigma\sigma} + rSF_s + (p-\lambda q)F_\sigma - rF = 0, \tag{5.1}$$

where the function $\lambda = \lambda(S(t),\sigma(t),t)$ is the *market price of volatility risk*. We have seen this also in chapter 2. The risk neutral dynamics of spot and volatility are given by

$$\begin{aligned} dS_t &= rSdt + \sigma S dW_t \\ d\sigma_t &= [p(S,\sigma,t) - \lambda(S,\sigma,t)q(S,\sigma,t)]\,dt + q(S,\sigma,t)dW_t. \end{aligned}$$

In pricing an option we are interested in the risk neutral dynamics only. Therefore, the models that we will discuss specified directly in terms of the risk-neutral dynamics. This eliminates the need to specify the market price of risk explicitly.

Finally a note on the dynamics implied by a stochastic volatility model. We have explained the dynamic behavior of the sticky strike and sticky delta rules in chapter 3. By making a change

of variables we can show that the value of an option in a stochastic volatility model depends not on S and K separately, but on the ratio $\frac{S}{K}$. To see this, introduce the variable $\mu(t) = \frac{S(t)}{K}$. Then

$$\begin{aligned} \frac{\partial V}{\partial S} &= \frac{\partial V}{\partial \mu}\frac{\partial \mu}{\partial S} = \frac{1}{K}\frac{\partial V}{\partial \mu}, \\ \frac{\partial^2 V}{\partial S^2} &= \frac{1}{K^2}\frac{\partial^2 V}{\partial \mu^2}. \end{aligned}$$

So we can substitute this in equation (5.1), to see that $V(\mu, \sigma, t)$ satisfies the PDE.

We have seen this ratio $\frac{S}{K}$ before and we recognize it as the sticky delta rule. For this reason, stochastic volatility models also display sticky delta behavior. In addition, we also have a correlation between spot and volatility, and this implies that in response to an increase in spot, the smile will shift to the right (sticky delta), and to a higher level (due to the correlation).

5.2.1 Heston

In the stochastic volatility model introduced in Heston[15], the dynamics of the stock price under the risk neutral measure are given by

$$\begin{aligned} dS(t) &= rSdt + \sqrt{v(t)}Sd\overline{W}_1(t) \\ dv(t) &= \kappa[\theta - v(t)]dt + \xi\sqrt{v(t)}d\overline{W}_2(t) \\ Corr(d\overline{W}_1, d\overline{W}_2) &= \rho dt, \end{aligned}$$

where $v(t)$ is the variance, θ is the long-run mean of the variance, and κ is the mean reversion speed. The partial differential equation for the price of an option V is given by

$$V_t + \frac{1}{2}vS^2V_{ss} + v\rho\xi SV_{sv} + \frac{1}{2}v\xi^2V_{vv} + rSV_s + \kappa(\theta - v)V_v - rV = 0.$$

This equation can be solved with appropriate boundary conditions to calculate option prices. In his paper, Heston derives a closed-form solution for the price of a European call option on an asset with stochastic volatility.

Heston explains the effects that stochastic volatility has on option prices, and he puts this in contrast with the results of the Black-Scholes model. This can very well be explained in terms of the underlying distribution of the spot returns. When $\rho = 0$ the two Wiener processes are uncorrelated. In this case, an increase in ξ (the volatility of volatility) leads to a higher kurtosis (fatter tails), and it does not affect the skewness. This implies an increase in the price of far out-of-money and far in-the-money options, relative to at-the-money (or near-the-money) options. Or, equivalently, a higher value of ξ implies as stronger smile shape.

When the correlation is nonzero, this affects the skewness of spot returns. When $\rho > 0$, this implies that the variance will be higher when the spot rises. This results in a fat right tail and a thin left tail. Prices of out-of-money call options and in-the-money put options rise, and

prices of in-the-money call options and out-of-the-money put options decrease, compared to the Black-Scholes model.

For a negative correlation $\rho < 0$, the converse is true: out-of-the-money options are priced below the Black-Scholes price, while in-the-money options have prices above the Black-Scholes price. So, a positive correlation results in a volatility smile that is increasing as function of the strike, a negative correlation results in a smile that is decreasing as function of the strike.

The intuition behind these effects can be explained by the impact of the correlation on the distributions of stock prices at maturity (see also Hull et al.[18]). For positive correlation we know that high stock prices are associated with high volatilities. When stock prices rise, the probability of large positive changes increases. This means that very high stock prices become more probable than when the volatility is fixed. The other way around, low stock prices are associated with low volatilities. So if stock prices fall, it becomes less likely that large changes take place. Low stock prices become like absorbing states, and it becomes more likely that the stock price at maturity will be low.

For negative correlation, the opposite holds true: price increases reduce the volatility so that it is unlikely that very high stock prices will result. Price decreases increase volatility, so that there is an increasing probability of large positive price changes, and very low prices become less likely.

5.2.2 The SVSD Model by Zilber

The Stochastic Volatility Smile Dynamics (SVSD) model proposed by Zilber[26] is motivated by an investigation of empirical observations regarding the smile dynamics. These observations show two important things (this was also discussed in section 3.7): spot is correlated with both ATM and risk reversal. From this, Zilber concludes that in order to price exotic options correctly, and to calculate correct values for the greeks (needed for hedging purposes), it is important that a model is able to capture this dynamic behavior.

Zilber explains that the dynamics implied by the sticky strike and sticky delta rule, the local volatility model and a pure stochastic volatility model do not meet these criteria. As we have seen in the previous chapter, the local volatility model results in dynamics that are more extreme than what is observed in practice. In a sticky delta model both ATM and RR remain unchanged. In a sticky strike model, these quotes do change. The magnitude of change depends on the shape of the smile. But it cannot be concluded that the sticky strike model reflects reality, as the shift in RR and ATM may be very different from what can be observed in the market. A pure stochastic volatility model displays sticky delta dynamics. Moreover, the correlation parameter impacts the level of the smile. Therefore, such a model does incorporate the correlation between spot and ATM, but it still leaves the RR unchanged.

This motivates Zilber to extend the pure stochastic volatility model with an extra term that explicitly accounts for the dynamics. This is done by directly linking the volatility to the spot: a local volatility term is added.

The SVSD model is specified in forward terms, which enables him to use analytic formulae for European vanillas. This is based on the results derived in Hagan et al.[13], to which we refer for details. Under the risk neutral measure, the dynamics of the forward exchange rate and the stochastic volatility σ are given by

$$\begin{aligned} df &= C_{loc}(f)\sigma dW_1 \qquad f(0) = f_0 \\ d\sigma &= \xi\sigma dW_2, \qquad \sigma(0) = \sigma_0 \\ < dW_1, dW_2 > &= \rho dt, \end{aligned}$$

where f is the forward on the exchange rate with expiry T, and the function C_{loc} is a local volatility term,

$$C_{loc}(f) = f\left[1 + \alpha\left(1 - \frac{f}{f_0}\right) + \beta\left(1 - \frac{f}{f_0}\right)^2\right],$$

where α and β are constants. Using $\alpha = \beta = 0, \xi \neq 0$ we have a pure stochastic volatility model (as explained, with sticky delta dynamics). By setting $\xi = 0$ only, we are left with a local volatility model. By adjusting these three parameters it is possible to specify whole range of dynamics, from local volatility dynamics at the one end, to sticky delta dynamics at the other end.

Zilber specifies the values for α and β by calibrating them to historical data. The next section discusses the SVSD model proposed by Rosien[24]. As we will see, an important difference between these models is calibration for α and β.

The SVSD model by Zilber resembles the Reech Stochastic Volatility model described by Blacher[6] very much. We will therefore not discuss this model in detail. The model is set up with the same objective as the SVSD model, that is, to be able to control the smile dynamics through the use of a local volatility term. The link between the model parameters and the market quantities that they want to match is shown in table 5.1 (see also Blacher[6]). In this table the following notation is used:

- σ_{ATM}: the volatility for an option with strike $K = S_0$.
- $\sigma'_{ATM} = \frac{\partial \sigma_{ATM}}{\partial K}|_{K=S_0}$: slope of the smile at the money.

Both Blacher and Zilber describe the meaning of the parameters, it is as follows:

- σ_0 = starting value of the volatility at t_0. It influences σ_{ATM} and determines the general level of the volatility smile.

Theoretical Quantities	σ_{ATM}	$\frac{\partial \sigma_{ATM}}{\partial S_0} \mid_{\sigma=\sigma_0}$	$\frac{\partial \sigma'_{ATM}}{\partial S_0} \mid_{\sigma=\sigma_0}$	σ'_{ATM}	$\frac{\partial \sigma'_{ATM}}{\partial K}$
Market Quantities	σ_{ATM}	$\frac{\partial \sigma_{ATM}}{\partial S_0} \mid_{\sigma=\sigma_0}$	$\frac{\partial RR}{\partial S_0} \mid_{\sigma=\sigma_0}$	RR	STR
Model Parameters	σ_0	α	β	ρ	ξ

Table 5.1: Interpretation of the model parameters in the Reech model.

- $\xi(t)$ = the volatility of volatility at time t. It creates smile curvature (strangle).
- $\rho(t)$ = the correlation between spot and volatility at time t. It creates the skew (risk reversal) of the smile.
- α = generates the sensitivity of the ATM volatilities to changes in spot, $\frac{\partial \sigma_{ATM}}{\partial S_0}$. It also impacts the slope of the smile (risk reversal).
- β = generates the sensitivity of the RR to changes in spot: $\frac{\partial \sigma'_{ATM}}{\partial S_0}$. It also impacts the curvature of the smile (strangle).

5.3 Stochastic Volatility Smile Dynamics Model

The *Stochastic Volatility Smile Dynamics (SVSD) Model* proposed in Rosien[24] is an adjustment of the SVSD model of Zilber[26]. It is a stochastic volatility model with a local volatility term to have complete control over the smile dynamics.

There are a number of differences with Zilber. The most important difference has to do with the calibration. While Zilber uses prespecified dynamics, which he obtains by inspecting historical data, Rosien obtains these dynamics directly from the market. This is achieved by calibrating the model to barrier options. Rosien shows that calibration to vanillas only is not sufficient to extract the smile dynamics from the market. It is well-known that models may agree on the complete vanilla market, and yet give rise to different smile dynamics (see Rosien[24]). Rosien illustrates that, in order to get this dynamic behavior directly from the market, exotic options are needed in the calibration. In section 5.4.2 this will be discussed in more detail.

Two other differences are that a mean-reverting drift term is included, and a term structure is added to make (some of) the parameters time dependent, since empirical observations show that implied volatilities vary with both strike *and* maturity. By including the term structure it is possible to match the smile for more than one maturity.

Under the risk-neutral measure, the SVSD model for the spot foreign exchange rate is given

by

$$
\begin{aligned}
dS &= [r_d(t) - r_f(t)]Sdt + C_{loc}(S,t)\sigma S dW_t^{(1)} \qquad S(t_0) = S_0 && (5.2)\\
d\sigma &= \kappa[m(t) - \sigma]dt + \xi(t)\sigma dW_t^{(2)} \qquad \sigma(t_0) = \sigma_0 && (5.3)\\
< dW_t^{(1)}, dW_t^{(2)} > &= \rho(t)dt, && (5.4)
\end{aligned}
$$

where

- σ_0 = volatility level at time $t = 0$
- $r_d(t)$ = domestic interest rate at time t
- $r_f(t)$ = foreign interest rate at time t
- $C_{loc}(S,t)$ = local volatility function
- $m(t)$ = mean-reversion level at time t
- κ = mean-reversion speed
- $\xi(t)$ = volatility of volatility at time t
- $\rho(t)$ = correlation between the two Wiener processes at time t

The local volatility function is given by

$$C_{loc}(S,t) = \left(1 + \alpha\left[\frac{Se^{(t_0-t)(r_d(t)-r_f(t))}}{S_0} - 1\right] + \beta\left[\frac{Se^{(t_0-t)(r_d(t)-r_f(t))}}{S_0} - 1\right]^2\right),$$

where α and β are constants.

The parameters in the SVSD model have a clear and intuitive meaning. We distinguish between the directly observable parameters and the non-observable parameters. The directly observable parameters are the domestic interest rate at time t, $r_d(t)$, the foreign interest rate at time t, $r_f(t)$, and the spot exchange rate at time t_0, S_0. The list of non-observable parameters and their meanings was presented in the previous subsection. We repeat them here:

- σ_0 = starting value of the volatility at t_0. It determines the general level of the volatility smile.
- $m(t)$ = the mean-reversion level of the volatility process at time t.
- κ = the mean-reversion speed of the volatility process.
- $\xi(t)$ = the volatility of volatility at time t. It impacts the curvature (strangle) of the smile.
- $\rho(t)$ = the correlation between the two Wiener processes at time t. It impacts the skew (risk reversal) of the smile.

- α = generates the sensitivity of the ATM volatilities to changes in spot, $\frac{\partial ATM}{\partial S}$. It also impacts the slope of the smile (risk reversal).
- β = generates the sensitivity of the RR to changes in spot: $\frac{\partial RR}{\partial S}$. It also impacts the curvature of the smile (strangle).

In this model we have complete control over the smile dynamics through the local volatility function. Some attention needs to be paid to the explanation of the parameters α and β that are present in this local volatility function. We need to distinguish between the static and the dynamic behavior of the local volatility. Statically, the parameters affect the *shape* of the smile, α for the risk reversal and β for the curvature. High values of S imply a different local volatility function than low values of S, depending on the values of the parameters. The function is linear in α and quadratically in β. For the dynamic behavior we need to look at the derivative of C_{loc} with respect to S,

$$\frac{\partial C_{loc}(S,t))}{\partial S} \sim \alpha + \beta S.$$

When the spot changes, the local volatility changes with a constant (relative to) α plus a change depending on the spot level. Then we can see that the parameter α generates the sensitivity of the ATM volatility to changes in spot, and β the sensitivity of the risk reversal to changes in spot.

Note that the model has two parameters affecting the risk reversal (ρ and α), and two parameters affecting the strangle (ξ and β). This is not desirable from a calibration point of view because the calibration to the smile dynamics will now affect the calibration to the current smile. We will return to this point in the next section.

Under the SVSD model, option prices $V(S_t, \sigma_t, t)$ must satisfy the PDE

$$\frac{\partial V}{\partial t} + [r_d(t) - r_f(t)]\, S\frac{\partial V}{\partial S} + \frac{1}{2}\sigma^2 S^2 C_{loc}^2(S,t)\frac{\partial^2 V}{\partial S^2} + \kappa(t)\,[m(t) - \sigma]\,\frac{\partial V}{\partial \sigma} +$$

$$\frac{1}{2}\xi(t)^2\sigma^2\frac{\partial^2 V}{\partial \sigma^2} + \rho(t)\xi(t)\sigma^2 S C_{loc}(S,t)\frac{\partial^2 V}{\partial S \partial \sigma} - r_d(t)V = 0$$

$$V(T, s, \sigma) = \phi(s, \sigma),$$

where ϕ is the payoff of the derivative at maturity and $C_{loc}(S,t)$ is the local volatility term given by equation (5.5).

Finally, we note that the SVSD model has many parameters. In general, the more parameters a models has, the better the model can be fitted to market data. However, including too many parameters may lead to over-parameterization. In this case the model gives a good fit to the market, but we are actually modelling the noise as well. We have to be careful with our conclusions and keep in mind the fact that may be over-fitting the market.

5.4 Calibration: Including Barrier Options

The model parameters are estimated in the calibration procedure. The parameters $r_d(t)$, $r_f(t)$ and S_0 can directly be observed in the market, so they need not be included in the calibration procedure. The parameters that are then left to be determined are σ_0, κ, $m(t)$, $\xi(t)$, $\rho(t)$, α and β. For the SVSD model, the calibration procedure consists of two parts: calibration to the vanilla market in order to match the smile, and calibration to barrier option prices in order to obtain the right smile dynamics. This section explains both parts of the calibration.

5.4.1 Vanilla calibration

We start with the remark that the mean reversion speed of the volatility, κ, will not be included in the calibration procedure. Instead, a constant value is chosen. This is done because there is a scale invariance present in the model. On the one hand, the higher the volatility of volatility ξ, the more volatile the volatility process is. On the other hand the mean reversion speed κ also affects the volatility of the volatility, but in opposite direction: the higher κ, the *less* volatile the volatility process. Rosien shows that the value of an option depends on $\frac{\xi}{\kappa}$ only, and not on both parameters separately. For details we refer to Rosien[24].

A second remark is that we also do not include the initial volatility level σ_0 in the calibration. Instead, we set the value of σ_0 equal to the mean reversion level m of the volatility process. Our mean reversion level is time dependent, $m = m(t)$. We will only calibrate our model to a limited number of maturities, and therefore we assume that m is piecewise constant between these maturities. We will return to this point later. The value of σ_0 is set equal to the mean reversion level up to the first maturity.

Excluding these two parameters from the calibration procedure gives us an advantage. The parameters α and β are used in order to match the smile dynamics, they are estimated in the barrier calibration (this will be explained in the next subsection). This leaves three parameters for the vanilla calibration: the mean reversion level $m(t)$, the volatility of volatility $\xi(t)$ and the correlation $\rho(t)$. In chapter 3, section 3.6, we discussed the quotes that are available in the FX market: the ATM, the RR and the STR. These quotes determine the shape of the market smile. So, we have three parameters that need to be specified, and three quotes to calibrate them to. We are left with a root finding problem.

Also, the parameters are linked to the quotes in a natural way. The volatility of volatility ξ determines the curvature of the smile, this corresponds to the STR quote. The correlation ρ determines the skewness, this corresponds to the RR quote. Finally, the mean reversion level determines the level of the ATM option and the general level of the smile, this corresponds to the ATM quote.

We will first explain how this is done for the model without term structure. After that, we extend the procedure to include time-dependence in the parameters.

For the model without term structure, we calibrate the model to one maturity only. This is done as follows. For given values of the parameters, we can use the model to calculate the ATM value, the RR and the STR. The goal of the calibration is to find values for the parameters such that these quotes calculated using the model, exactly match the market quotes:

$$\begin{aligned} ATM_{SVSD}(\sigma_0^*, \xi^*, \rho^*) &= ATM_{market} \\ STR_{SVSD}(\sigma_0^*, \xi^*, \rho^*) &= STR_{market} \\ RR_{SVSD}(\sigma_0^*, \xi^*, \rho^*) &= RR_{market} \end{aligned}$$

Here, ATM_{SVSD} is the ATM quote calculated using the SVSD model. We can calculate the price of an option with the ATM strike K_{ATM} (as explained in section 3.6) with the SVSD model for varying parameter values σ_0, ξ and ρ. From this we can calculate the implied volatility, $ATM_{SVSD}(\sigma_0, \xi, \rho)$. Further ATM_{market} is the ATM quote that can be observed in the market. Similar definitions hold for the STR and the RR. Then σ_0^* , ξ^* and ρ^* are the specific values of σ_0 , ξ and ρ respectively, for which the ATM, STR *and* RR quotes under the SVSD model are exactly equal to the ATM, STR *and* RR quotes in the market. This is a root-finding problem. To solve this, Broyden's method is used. This method will be explained in the next subsection.

Now we can extend this procedure to include a term structure in the parameters. Doing this, we are able to match the vanilla quotes for more than one maturity. So, the first step is to choose a set of maturities that we want to include in our term structure. Further, we assume that the parameters are piecewise constant between these maturities. So if we have a total of n different maturities, then the parameters would take constant values between the different dates:

$$\xi(t) = \begin{cases} \xi_1 & t \leq M_1 \\ \xi_2 & M_1 < t \leq M_2 \\ \vdots & \\ \xi_n & M_{n-1} < t \leq M_n \\ \xi_{n+1} & t > M_n \end{cases}$$

where M_i denotes maturity i with $M_i < M_{i+1}$, and ξ_i is constant, for $i = 1, \ldots, n$. For ρ and m similar definitions hold.

We start with the smallest maturity M_1 and we find the values of ξ_1, ρ_1 and m_1 such that the the ATM, RR and STR values calculated with the model exactly match the market quotes for this maturity. We set σ_0 equal to the calibrated value of m_1. This part is exactly the same as described above for the model without term structure.

Then we set the maturity equal to the second date M_2. We search for the values ξ_2, ρ_2 and m_2 in the same way as before, but we use the fact that we know the values up until the first maturity.

So, in solving from time M_1 to time zero we use the already calibrated values. In this way, we find ξ_2, ρ_2 and m_2.

In the next step, we find the values ξ_3, ρ_3 and m_3 for the time interval M_2 to M_3, and we use the values ξ_2, ρ_2 and m_2 in solving from M_2 to M_1, and the values ξ_1, ρ_1 and m_1 in solving from M_1 to time zero, etcetera. We can repeat this procedure until we find the final result of the parameters with term structure. The result of the vanilla calibration is that the model matches the market quotes for a number of maturities.

Broyden's Method

In the vanilla calibration we have to solve a system of three equations:

$$\mathbf{F(x) = 0},$$

where

$$\mathbf{F(x)} = \begin{pmatrix} f_1(x_1, x_2, x_3) \\ f_2(x_1, x_2, x_3) \\ f_2(x_1, x_2, x_3) \end{pmatrix}.$$

The functions f_1, f_2 and f_3 are given in the previous section, we will repeat them here:

$$\begin{aligned} f_1(x_1, x_2, x_3) &= ATM_{SVSD}(x_1, x_2, x_3) - ATM_{market} \\ f_2(x_1, x_2, x_3) &= STR_{SVSD}(x_1, x_2, x_3) - STR_{market} \\ f_3(x_1, x_2, x_3) &= RR_{SVSD}(x_1, x_2, x_3) - RR_{market}, \end{aligned}$$

so we have $x_1 = \sigma_0$, $x_2 = \xi$ and $x_3 = \rho$. This section gives a description of the Broyden method, a detailed discussion can be found in Press[22].

Broyden's method combines Newton's method with the Secant method. First we will consider the one dimensional problem of finding the root of a function f. Starting from an initial point x_0, the next improvement of Newton's method is given by the point x_1, which is the intercept with the axis of the tangent line of f at the point x_0. Using a Taylor polynomial for f, we have

$$f(x + \delta x) = f(x) + \delta x f'(x) + \frac{1}{2}(\delta x)^2 f''(\chi),$$

where $\chi \in (x, x + \delta x)$. For δx small we may neglect the second order term. Then $f(x + \delta x) = 0$ implies that

$$\delta x = -\frac{f(x)}{f'(x)}.$$

Starting from a point x_0 which is close to the root, the next point is given by

$$x_1 = x_0 + \delta x_0 = x_0 - \frac{f(x_0)}{f'(x_0)},$$

and in general,

$$x_{i+1} = x_i - \frac{f(x_i)}{f'(x_i)}, \tag{5.5}$$

The Newton method converges quadratically, given that we start at a point close enough near the root. If not, then we can see from the Taylor expansion that the higher order terms become important, in which case the method can fail.

Although Newton's method is a powerful technique, the drawback of the method is that is requires the computation of the derivative of f at each approximation, which can be far more difficult than to evaluate the function value itself.

The Secant method can be used in order to avoid the problem of derivative evaluation. In the Secant method the the function is assumed to be approximately linear in the local region of interest. Starting from an initial interval $[x_0, x_1]$ that contains a root for the function f, the next improvement x_2 is taken as the point where the approximating linear line between $f(x_0)$ and $f(x_1)$ crosses the axis. The new interval is given by $[x_1, x_2]$ and again the linear approximation between x_1 and x_2 can be set equal to zero to find x_3, and so on. In formulas:

$$x_{i+1} = x_i - f(x_i)\frac{(x_i - x_{i-1})}{f(x_i) - f(x_{i-1})}. \tag{5.6}$$

Comparing with the Newton method, equation (5.5), we see that the Secant method uses the same scheme,

$$x_{i+1} = x_i - \frac{f(x_i)}{f'(x_i)},$$

but the difference is that the derivative of f in the point x_i is approximated by

$$f'(x_i) = \lim_{x \to x_i} \frac{f(x_i) - f(x)}{x_i - x} \approx \frac{f(x_i) - f(x_{i-1})}{x_i - x_{i-1}}. \tag{5.7}$$

Now we proceed by giving the extension of the methods to the multidimensional case. We want to find the root of a system of N equations $F_i, i = 1, \ldots, N$, and N variables $x_i, i = 1, \ldots, N$: find $\mathbf{x}$ such that $\mathbf{F}(\mathbf{x}) = \mathbf{0}$. Each of the functions F_i can be expanded by its Taylor series,

$$F_i(\mathbf{x} + \delta\mathbf{x}) = F_i(\mathbf{x}) + \sum_{j=1}^{N} \frac{\partial F_i}{\partial x_j}\delta x_j + O\left((\delta\mathbf{x})^2\right).$$

In matrix equations this amounts to

$$\mathbf{F}(\mathbf{x} + \delta\mathbf{x}) = \mathbf{F}(\mathbf{x}) + \mathbf{J}\delta\mathbf{x} + O\left((\delta\mathbf{x})^2\right),$$

where $\mathbf{J}$ is the Jacobian matrix. For $\delta\mathbf{x}$ small enough, $\mathbf{F}(\mathbf{x} + \delta\mathbf{x}) = 0$ implies that

$$\delta\mathbf{x} = -\mathbf{J}(\mathbf{x})^{-1}\mathbf{F}(\mathbf{x}).$$

The multidimensional scheme for Newton's method is now given by

$$\mathbf{x}_{i+1} = \mathbf{x}_i + \delta\mathbf{x} = \mathbf{x}_i - \mathbf{J}(\mathbf{x}_i)^{-1}\mathbf{F}(\mathbf{x}_i).$$

Broyden's method is the multidimensional equivalent of the Secant method. Similar to the one dimensional case, the Jacobian matrix is approximated by a matrix $\mathbf{B}$ such that

$$\mathbf{B}_i\left[\mathbf{x}_i - \mathbf{x}_{i-1}\right] = \mathbf{F}(\mathbf{x}_i) - \mathbf{F}(\mathbf{x}_{i-1}), \tag{5.8}$$

compare with equation (5.7). The updating scheme for Broyden's method is given by

$$\mathbf{B}_i\left[\mathbf{x}_{i+1} - \mathbf{x}_i\right] = -\mathbf{F}(\mathbf{x}_i),$$

where $\mathbf{B}$ satisfies equation (5.8).

However, equation (5.8) does not define the matrix $\mathbf{B}$ uniquely. The best performing algorithm in practice results from Broyden's formula, see Press[22], which specifies $\mathbf{B}$ as follows:

$$\mathbf{B}_{i+1} = \mathbf{B}_i + \frac{\mathbf{y}_i + \mathbf{B}_i\mathbf{s}_i}{\mathbf{s}_i \cdot \mathbf{s}_i}\mathbf{s}_i,$$

where

$$\begin{aligned}\mathbf{y}_i &= \mathbf{F}(\mathbf{x}_i) - \mathbf{F}(\mathbf{x}_{i-1})\\ \mathbf{s}_i &= \mathbf{x}_i - \mathbf{x}_{i-1}.\end{aligned}$$

5.4.2 Barrier Calibration

After giving a motivation for the use of barrier options in the first part, the second subsection describes the barrier calibration procedure.

Motivation

The SVSD model attempts to capture the right smile dynamics, and to get these dynamics directly from the market. This is done by including exotic options in the calibration procedure. In the FX market, barrier options are liquid products and can be used in the calibration procedure. As is shown in Baker et al.[2] and Hull and Suo[18], and Ayache et a.[1], market prices of barrier options contain information about the smile dynamics and can therefore serve our goal of matching these dynamics.

When a model prices European options correctly (i.e., when it matches the smile), this means that the risk-neutral probability distribution of the asset price at any time in the future is always correct. For options that depend only on the density of the asset at one time (maturity), such a model will calculate the correct price. So, by calibrating a model to the vanilla market we are able to recover the correct density of the underlying asset maturity. However, the vanilla market does not give any information about the smile dynamics that are observed in the market. As long

as we use a model only to price vanilla options, this will cause no problem, since these prices only depend on the smile. But for many exotic options, the prices depend not only on the current smile, but also on the smile dynamics.

We can illustrate this with the local volatility model that was discussed in the previous chapter. The model is designed as to match the market smile exactly. Once the local volatility term is calculated with formula (5.5), the model is fully specified and the smile dynamics are determined implicitly. However, it is a known fact that the model generates smile dynamics that are more extreme compared to what can be observed in the market. A clear example of this is given in Hagan et al.[13]. So while the local volatility model completely matches the observed market smile, and therefore correctly prices European options, it fails to predict the right smile dynamics, and therefore will not be able to calculate correct prices for exotic options.

Just as the current market smile is determined by the density of the underlying at maturity, the smile dynamics are determined by the transition density of the underlying from a certain future date to some further future date. The transition densities cannot be obtained by calibrating to the vanilla market only. Compound options and forward start options, for example, depend not only on the density of the underlying at maturity, but also on the transition density from one time in the future to a further time in the future. Let $\phi_n(T_1, T_2, \ldots, T_n)$ be the joint density of the asset price at times T_1, T_2, $\ldots$, T_n. The fact that $\phi_1(T_1)$ is correct for all T_1 (for example, as in the local volatility model) does not imply that $\phi_n(T_1, T_2, \ldots, T_n)$ is correct for $n > 1$. Consider a call-on-call compound option. In chapter 1 we have seen that the value C_{call} of this option is given by

$$\begin{aligned} C_{call}(S_t, t; K_1, T_1) &= e^{-r(T_2-t)}\mathbb{E}_t\left[S_{T_2}1_{S_{T_2}>K_2}1_{S_{T_2}>S^*}\right] \\ &\quad -K_2e^{-r(T_2-t)}\mathbb{E}_t\left[1_{S_{T_2}>K_2}1_{S_{T_2}>S^*}\right] \\ &\quad -K_1e^{-r(T_1-t)}\mathbb{E}_t\left[1_{S_{T_2}>S^*}\right]. \end{aligned}$$

So, the option price depends on $\phi_2(T_1, T_2)$. But this density is not uniquely determined from the marginal densities of the asset price at times T_1 and T_2. Rosien[24] explains this by considering a discrete world, in which the densities are the probabilities to move from one state to another. Different models are considered with the same marginal densities at times T_1 and T_2 (i.e., the probabilities from time 0 to time T_1 as well as the probabilities from time 0 to time T_2 are the same for both models), but with different transition probabilities from time T_1 to T_2. It is shown that while these models calculate the same price for European options, the prices for exotic options are different. We refer to Rosien, in which a detailed example is given in Rosien to illustrate this.

There are many derivatives for which the dependence on the joint density is much more complex. This is the case for a barrier option, for example. Consider an up-and-out barrier call option

with strike K and maturity T_n. Let T_1, T_2, ..., T_n be the times at which the asset price is observed in order to determine if the barrier B has been hit. The price of the barrier option is then given by

$$e^{-rT_n}\mathbb{E}\left[\max(S_{T_n}-K,0)|S_{T_1}<B,\ldots,S_{T_n}<B\right].$$

So the option price depends on $\phi_n(T_1,\ldots,T_n)$. As Hull and Suo[18] argue, when a model is not able to compute the correct price for a compound option, it will not be able to compute the price of a barrier option. In other words, if a model is not able to recover the joint density at two times $\phi_n(T_1,T_2)$, it will surely not be able to recover a more complex joint density $\phi_n(T_1,\ldots,T_n)$. We may conclude that barrier option prices hold information on these joint densities.

This is also shown in Baker et al.[2]. They show that the main factor determining the barrier price is the forward smile along the trigger level, more specifically, the slope of the smile. For a detailed treatment we refer to Baker et al. They show that barrier option prices are mainly affected by the risk reversal. Therefore one may say that barrier prices in the market reflect the market's feeling about the volatility smile at the trigger level at hit time (i.e., the smile at hit time, assuming a spot close to the trigger at that time).

So, in short, the motivation to use barrier options is the believe that barrier option prices hold information on these joint densities, and therefore about the dynamics. For this reason, it is a good idea to include them in the calibration procedure. In this way, the smile dynamics are not imposed by the model being used, instead they are inferred from the market. For the SVSD model, we have complete control over the smile dynamics through the local volatility term. The idea of the barrier calibration is to choose the parameters α and β to match the prices of barrier options.

Calibration Procedure

In order to extract as much information as possible about the smile dynamics from the market, it seems best to include as many barrier option quotes as possible. Rosien[24] investigated the effect on the values of α and β using many different combinations of barrier quotes. Attention was paid to three different aspects: quantity, maturity and barrier level. It was found that it is not straightforward to calculate the 'correct' values for the two parameters, as different combinations of barrier options in the calibration procedure can lead to very different parameter values. But it can be concluded that we should include barrier option prices in our calibration with maturities and trigger level that are spread, i.e., using barrier options with that have different maturities and trigger levels. Further, a minimum number of barriers should be included in the calibration. It is found that including 2 barriers does not give enough information, but 4 barriers do give good results (and including more barriers does not substantially improve this any further).

Ideally the two calibration procedures would be independent. Then we could first perform the vanilla calibration to fit the the current market smile, and next calibrate it to barrier option prices to match the smile dynamics that are observed in the market as well. However, this is not the case. At this point, we should recall the remark that was made about the smile dynamic parameters. In section 5.3 it has been noticed that α and β do not only affect the smile dynamics, but also the the shape of the smile. Therefore, calibrating the parameters α and β will spoil the result of the vanilla calibration. As the values of α and β are changed in the barrier calibration, this will affect the value of the vanilla calibration parameters simultaneously. Therefore, the barrier calibration procedure actually represents the total calibration procedure. It is carried out as follows. To start the procedure, we need as input the market quotes (ATM, RR, STR) of vanilla options for all maturities that we want to include in the vanilla calibration, and the market prices and specifications (strike, barrier level, etc.) of all barrier options that we want to include. The following steps describe the total calibration procedure:

1. Choose starting values for α and β.
2. Perform the vanilla calibration as described in section 5.4.1 to find σ_0, $\xi(t)$, $\rho(t)$ and $m(t)$.
3. Using the parameter values from steps 1 and 2, calculate the SVSD model prices of all barrier options.
4. For every barrier option, compare the calculated barrier model price with the market price. If the difference is small enough, stop. Otherwise, change the values of α and β and repeat step 2, 3 and 4.

The price difference is measure using an average relative squared error function:

$$E = \frac{1}{N}\sum_{i=1}^{N}\left(\frac{V_i^{market} - V_i^{model}}{V_i^{market}}\right)^2,$$

where

$$\begin{aligned} E &= \text{error value} \\ N &= \text{number of barrier options} \\ V_i^{market} &= \text{market price of barrier } i \\ V_i^{model} &= \text{model price of barrier } i \end{aligned}$$

For the right choices of α and β a minimization method is used: the Powell method. This method is discussed in the next subsection.

Powell Method

A function of one variable can be minimized in various ways, for example using Golden Section Search or Brent's method, see Press[22]. Assume we have a function f of N variables that we

want to minimize, starting from a specific N-dimensional point $\mathbf{P}$. We can minimize this function along some direction $\mathbf{n}$ by a one dimensional minimization method. A very general description for this can be given by:

> Input: starting point $\mathbf{P}$, direction $\mathbf{n}$ and the function f.
>
> Find the scalar λ such that $f(\mathbf{P} + \lambda\mathbf{n})$ is minimized. Replace $\mathbf{P}$ by $\mathbf{P} + \lambda\mathbf{n}$.

This is called *line minimization*. There exist many line minimization algorithms that differ from each other only by how, at each stage, the next direction $\mathbf{n}$ is chosen. For example, one could take the unit vectors $\mathbf{e}_1, \ldots, \mathbf{e}_N$ as a *set of directions*, and use the line minimization to move along the first direction to its minimum, from there along the second direction to *its* minimum, and so on. This means cycling through the whole set of directions as many times as necessary, until the function stops decreasing. This is an example of a *direction set method*. Direction set methods consist of prescriptions for updating the set of directions as the method proceeds.

Powell's method is one of these algorithms. In this method, the choice of the successive directions does not involve explicit computation of the function's gradient. The updating set of directions for Powell's method includes a number of 'non-interfering' directions (called *conjugate directions*) with the property that minimization along one is not spoiled by subsequent minimizations along another, so that interminable cycling through the set of directions can be avoided. In Powell's method a set of directions is chosen that produces N mutually conjugate directions. We will give a short description of the method, the method is covered in more detail in Press[22], to which we refer for more information.

To start, choose the initial set of directions $\mathbf{u}_i$ equal to the basis vector,

$$\mathbf{u}_i \quad = \quad \mathbf{e}_i, \qquad i = 1, \ldots, N.$$

Choose a starting point $\mathbf{P}_0$ and repeat the following steps until the function stops decreasing:

- For $i = 1, \ldots, N$: find λ that minimizes $f(\mathbf{P}_{i-1} + \lambda\mathbf{u}_i)$, and set $\mathbf{P}_i = \mathbf{P}_{i-1} + \lambda\mathbf{u}_i$.
- For $i = 1, \ldots, N-1$: set $u_i = u_{i+1}$.
- Set $\mathbf{u}_N = \mathbf{P}_N - \mathbf{P}_0$.
- Move $\mathbf{P}_N$ along direction $\mathbf{u}_N$ to its minimum and call this point $\mathbf{P}_0$.

In the barrier calibration the function f is chosen to be the average relative squared error function $E = E(\alpha, \beta)$ (presented in the previous subsection).

5.5 Option Price Calculation

The option price calculation is essentially the same as for the local volatility model, discussed in section 4.4. The difference with the local volatility model is the extra direction in the grid. But

besides this option prices are calculated in the same way, and it will therefore not be repeated in this section.

5.6 Numerical Implementation: Alternating Direction Implicit Method

To calculate the price $V(S,\sigma,t)$ of an option under the SVSD model, we have to solve the PDE

$$\frac{\partial V}{\partial t} + a(S,\sigma,t)\frac{\partial^2 V}{\partial S^2} + b(S,\sigma,t)\frac{\partial V}{\partial S} + c(S,\sigma,t)V + d(S,\sigma,t)\frac{\partial^2 V}{\partial \sigma^2} + e(S,\sigma,t)\frac{\partial V}{\partial \sigma} + f(S,\sigma,t)\frac{\partial^2 V}{\partial S \partial \sigma} = 0,$$

where

$$\begin{aligned} a(S,\sigma,t) &= \frac{1}{2}\sigma^2 S^2 C_{loc}^2(S,t) \\ b(S,\sigma,t) &= \left[r_d(t) - r_f(t)\right] S \\ c(S,\sigma,t) &= -r_d(t) \\ d(S,\sigma,t) &= \frac{1}{2}\xi(t)^2\sigma^2 \\ e(S,\sigma,t) &= \kappa(t)\left[m(t) - \sigma\right] \\ f(S,\sigma,t) &= \rho(t)\xi(t)\sigma^2 S C_{loc}(S,t) \end{aligned}$$

As with the local volatility model, we will solve this using the finite difference method. Now we have three dimensions: time, spot and volatility. At every time step we construct a grid in spot and volatility direction. Let N_t, N_s and N_σ be equal to one plus the number of interior grid points in time, spot and volatility direction, respectively. The stepsizes in each direction are given by

$$\begin{aligned} \delta t &= \frac{T}{N_t} \\ \delta S &= \frac{S_{max} - S_{min}}{N_s} \\ \delta \sigma &= \frac{\sigma_{max} - \sigma_{min}}{N_\sigma} \end{aligned}$$

Besides the initial condition and the boundary conditions at S_{min} and S_{max}, we also have boundary conditions at σ_{min} and σ_{max}. The numerical approximation of the option value in the grid points is given by $V_{n,m}^k = V(S_n, \sigma_m, t_k)$, where

$$S_n = S_{min} + n\delta S, \qquad n = 0, 1, \ldots, N_s \tag{5.9}$$

$$\sigma_m = \sigma_{min} + m\delta\sigma \qquad m = 0, 1, \ldots, N_\sigma \tag{5.10}$$

$$t_k = T - k\delta t \qquad k = 0, 1, \ldots, N_t \tag{5.11}$$

The numerical scheme we use to solve the problem, is the *alternating direction implicit (ADI) method*. The original ADI scheme for initial-boundary value problems for convection-diffusion equations as described, for example, in Wilmott[25], is only applicable when there is no cross-derivative term present. Because we do have a cross-derivative term, we use a modification of the

ADI scheme that that accounts for this term.

Before explaining this modified scheme, we will first review the original ADI scheme. The idea of the ADI method is as follows. To avoid the use of an implicit scheme both for the spot and volatility in one time step, every time step is split into two parts. In the first part the values at the new time step are calculated with an explicit scheme in spot direction, and an implicit scheme for the volatility direction (using Crank-Nicholson). The second step is the other way around: an implicit scheme is used for the spot (again using Crank-Nicholson), and an explicit scheme is used for the volatility.

The advantage of the method is that, since we only have an implicit scheme in one variable at a time, we have a system involving a tridiagonal matrix at every time step, which can easily be solved using an LU decomposition. However, at this point it is not yet clear how to handle the cross-derivative term since it cannot be split into a separate spot or volatility derivative term. To solve this problem we use a modification of the ADI method, which uses a predictor and a corrector step (as described in Craig and Sneyd[9] and in Hout and Welfert[19]).

In the predictor step, we follow the procedure for the standard ADI method described above and we use an explicit scheme for the cross-derivative term. We use the result of the predictor step in the corrector step. In the corrector step we repeat the procedure for the ADI method, but now we use an implicit scheme for the cross-derivative term. We calculate the value of this cross-derivative term using the result of the predictor step. So while it is an implicit scheme, it can treated explicitly since the predictor values are already known.

For $k = 1, \ldots, N_t$, $n = 1, \ldots, (N_s - 1)$ and $m = 1, \ldots, (N_\sigma - 1)$, define

$$\begin{aligned}
D_{SS}V^k_{n,m} &= a^k_{n,m}\frac{V^k_{n+1,m} - 2V^k_{n,m} + V^k_{n-1,m}}{\delta S^2} \\
D_{S}V^k_{n,m} &= b^k_{n,m}\frac{V^k_{n+1,m} - V^k_{n-1,m}}{2\delta S} \\
D_{0}V^k_{n,m} &= c^k_{n,m}V^k_{n,m} \\
D_{\sigma\sigma}V^k_{n,m} &= d^k_{n,m}\frac{V^k_{n,m+1} - 2V^k_{n,m} + V^k_{n,m-1}}{\delta \sigma^2} \\
D_{\sigma}V^k_{n,m} &= e^k_{n,m}\frac{V^k_{n,m+1} - V^k_{n,m-1}}{2\delta \sigma} \\
D_{S\sigma}V^k_{n,m} &= f^k_{n,m}\frac{V^k_{n+1,m+1} - V^k_{n-1,m+1} - V^k_{n+1,m-1} + V^k_{n-1,m-1}}{4\delta S \delta \sigma}
\end{aligned}$$

The coefficients are given by

$$\begin{aligned} a^k_{n,m} &= \frac{1}{2}\sigma_m^2 S_n^2 C^2_{loc}(S_n, t_k) \\ b^k_{n,m} &= [r_d(t_k) - r_f(t_k)]\, S_n \\ c^k_{n,m} &= -r_d(t_k) \\ d^k_{n,m} &= \frac{1}{2}\xi(t_k)^2\sigma_m^2 \\ e^k_{n,m} &= \kappa(t_k)\,[m(t_k) - (\sigma_m)] \\ f^k_{n,m} &= \rho(t_k)\xi(t_k)\sigma_m^2 S_n C_{loc}(S_n, t_k), \end{aligned}$$

where S_n, σ_m and t_k are given by equations (5.9), (5.10) and (5.11) respectively. In Hout and Welfert[19], the modified ADI scheme is written in the general form:

Predictor step:

$$\begin{aligned} Y_0 &= V^{k-1} + \delta t\,[D_{SS} + D_S + D_0 + D_{\sigma\sigma} + D_\sigma + D_{S\sigma}]\, V^{k-1}_{n,m} \\ Y_1 &= Y_0 + \theta\delta t\,[D_{SS} + D_S + D_0]\left(Y_1 - V^{k-1}\right) \\ Y_2 &= Y_1 + \theta\delta t\,[D_{\sigma\sigma} + D_\sigma]\left(Y_2 - V^{k-1}\right) \end{aligned} \tag{5.12}$$

Corrector step:

$$\begin{aligned} \tilde{Y}_0 &= Y_0 + \phi\delta t D_{S\sigma}\left(Y_2 - V^{k-1}\right) \\ \tilde{Y}_1 &= \tilde{Y}_0 + \theta\delta t\,[D_{SS} + D_S + D_0]\left(\tilde{Y}_1 - V^{k-1}\right) \\ \tilde{Y}_2 &= \tilde{Y}_1 + \theta\delta t\,[D_{\sigma\sigma} + D_\sigma]\left(\tilde{Y}_2 - V^{k-1}\right) \\ V^k &= \tilde{Y}_2 \end{aligned} \tag{5.13}$$

Here, V^k denotes the option value at time t_k in the grid, $V^k = \left\{V^k_{n,m}\right\}_{\forall n,m}$. Both in the predictor and in the corrector step, an explicit step is followed by two implicit but unidirectional steps (with the purpose of stabilizing the explicit step). By choosing $\theta = \phi = \frac{1}{2}$, we have an implicit Crank-Nicholson scheme for spot and volatility as well as for the cross derivative term. A more intuitive formulation for our partial differential equation is given as follows:

Predictor step 1: The option value $V^{k-1}_{n,m}$ at the previous time step $k-1$ is known. Solve from time $k-1$ to k implicitly in spot and explicitly in volatility, and use an explicit scheme for the cross-derivative term, to find $(U^k_{n,m})^*$:

$$\frac{(U^k_{n,m})^* - V^{k-1}_{n,m}}{\delta t} + [D_{SS} + D_S + D_0]\,\frac{(U^k_{n,m})^* + V^{k-1}_{n,m}}{2} + [D_{\sigma\sigma} + D_\sigma + D_{S\sigma}]\, V^{k-1}_{n,m} = 0$$

Predictor step 2: Solve from time step $k-1$ to k explicitly in spot and implicitly in volatility. Also, use an explicit schemes for the cross-derivative term. We find the prediction $U^k_{n,m}$:

$$\frac{U^k_{n,m} - V^{k-1}_{n,m}}{\delta t} + [D_{SS} + D_S + D_0]\,\frac{(U^k_{n,m})^* + V^{k-1}_{n,m}}{2} + [D_{\sigma\sigma} + D_\sigma]\,\frac{U^k_{n,m} + V^{k-1}_{n,m}}{2} + D_{S\sigma}V^{k-1}_{n,m} = 0$$

We can see that we use the result of the first predictor step for the spot derivative in the second predictor step. In that sense, the result of step 1 can itself be considered to be a predictor for step 2.

Corrector step 1: Now the prediction value $U^k_{n,m}$ at time step k is known. Solve from time $k-1$ to k implicitly in spot and explicitly in volatility, and use an implicit scheme for the cross-derivative (for which we use the result of the predictor step - note that this term can be treated explicitly). In this way, we find $(V^k_{n,m})^*$:

$$\frac{(V^k_{n,m})^* - V^{k-1}_{n,m}}{\delta t} + [D_{SS} + D_S + D_0] \frac{(V^k_{n,m})^* + V^{k-1}_{n,m}}{2} + D_{S\sigma} \frac{U^k_{n,m} + V^{k-1}_{n,m}}{2} + [D_{\sigma\sigma} + D_\sigma] V^{k-1}_{n,m} = 0$$

Corrector step 2: Solve from time step $k-1$ to k explicitly in spot and implicitly in volatility, using the same implicit scheme for the cross-derivative as in the previous corrector step. The result is the option value at the new time, $V^k_{n,m}$:

$$\frac{V^k_{n,m} - V^{k-1}_{n,m}}{\delta t} + [D_{SS} + D_S + D_0] \frac{(V^k_{n,m})^* + V^{k-1}_{n,m}}{2} + D_{S\sigma} \frac{U^k_{n,m} + V^{k-1}_{n,m}}{2} + [D_{\sigma\sigma} + D_\sigma] \frac{V^k_{n,m} + V^{k-1}_{n,m}}{2} = 0$$

The implementation of the method is carried out in the general form (5.12) and (5.13). Calculating Y_0 and $\tilde{Y}_0$ is a matter of matrix multiplications. Calculating Y_1, Y_2 and $\tilde{Y}_1$, $\tilde{Y}_2$ amounts to solving systems of equations in a similar way as the one dimensional case of the local volatility model. Y_1 and $\tilde{Y}_1$ are steps implicit in spot and explicit in volatility. Therefore, in this step we need to solve a system of equations for each *column* of the state matrix in the previous time step:
$\forall m$, solve

$$\mathbf{M^k}(Y_1)_m = \tilde{\mathbf{M}}^{\mathbf{k-1}}(V^{k-1})_m,$$

where $(Y_1)_m$ and $(V^{k-1})_m$ denote the m-th column of the matrix. The matrix entries of $\mathbf{M^k}$ and $\tilde{\mathbf{M}}^{\mathbf{k-1}}$ can be derived by writing out the discretisation (similar as in section 4.4).

Y_2 and $\tilde{Y}_2$ are steps explicit in spot and implicit in volatility. Therefore, in this step we need to solve a system of equations for each *row* of the state matrix in the previous time step:
$\forall n$, solve

$$\mathbf{N^k}(Y_2)_n = \tilde{\mathbf{N}}^{\mathbf{k-1}}(V^{k-1})_n,$$

where $(Y_2)_n$ and $(V^{k-1})_n$ denote the n-th row of the matrix.

5.6.1 Boundary Conditions

In this section we will give the initial and boundary conditions that are needed to solve the partial differential equation. We will specify the conditions for all option that will be evaluated with the model: the compound option and the forward start option, and also vanilla and barrier options

since the prices of these options will be calculated in the calibration procedure.

For the barrier option we will only discuss knock-out options. This is enough, since we can obtain the value of a knock-in option through the relation

$$KO(S,t;K,T,B) + KI(S,t;K,T,B) = V(S,t;K,T)$$

Here, $KO(S,t;K,T,B)$ and $KI(S,t;K,T,B)$ are knock-out and knock-in options respectively, and $V(S,t;K,T)$ is a vanilla option, all options evaluated at time t and spot S, with strike K, maturity T and barrier level B. This relation holds for call as well as for put options.

To see that this relation holds true, consider the payoff of the respective options: the payoff of a knock-out option is equal to the payoff of the corresponding vanilla option, given that the barrier level has not been crossed at any time before or at expiry. The payoff of a knock-in option is equal to the payoff of the corresponding vanilla option, given that there has been some point in time before or at expiry when the barrier level has been crossed.

We start by defining the following:

$$\phi = \begin{cases} 1 & \text{(vanilla/compound) call option} \\ -1 & \text{(vanilla/compound) put option} \end{cases}$$

$$\theta = \begin{cases} 1 & \text{compound underlying call option} \\ -1 & \text{compound underlying put option} \end{cases}$$

$$\eta = \begin{cases} 1 & \text{up-and-out barrier option} \\ -1 & \text{down-and-out barrier option} \end{cases}$$

Initial conditions

The conditions all hold for $k = 0$ and $n = 0, \ldots, N_s$, $m = 0, \ldots, N_\sigma$, so below we will not state them explicitly.

Forward Start option with expiry T_2 and fixing date T_1:

$$V^k_{n,m} = \max\left[\phi\left(S^k_n - K(S^{T_1}_n)\right), 0\right],$$

where $S^{T_1}_n$ is the asset value at time T_1 in for $S = n\delta S$.

Underlying of the compound option:

$$U^k_{n,m} = \max\left[\theta\left(S^k_n - K_2\right), 0\right]$$

Compound option:

$$V^k_{n,m} = \max\left[\phi\left(U^{T_1}_{n,m} - K_1\right), 0\right]$$

Vanilla option:

$$V^k_{n,m} = \max\left[\phi\left(S^k_n - K\right), 0\right]$$

Barrier knock-out option:

$$V_{n,m}^k = \begin{cases} \max\left[\phi\left(S_n^k - K\right), 0\right], & \eta S_n^k \leq \eta B \\ 0 & \text{otherwise} \end{cases}$$

For the payoff of the barrier option we assume that the option has not yet been knocked out before expiry; otherwise, the option value would be equal to zero. Therefore the payoff is equal to the payoff of a vanilla option, conditional on not reaching the barrier level at expiry.

Boundary conditions for spot

Lower boundary: we use the same spot lower boundary conditions for forward start options, compound options, vanilla options and up-and-out barrier options. For $n = 0$ and for $m = 0, \ldots, N_\sigma$, $k = 1, \ldots, N_t$,

$$V_{n,m}^k = \frac{1-\phi}{2} K e^{-r_d k}, \qquad S \to 0$$

For down-and-out barrier options, we have $S_0 = S_{min} = B$ and

$$V_{n,m}^k = 0, \qquad n = 0,\ m = 0, \ldots, N_\sigma,\ k = 1, \ldots, N_t$$

Upper boundary: we use the same upper boundary conditions for forward start options, compound options, vanilla options and down-and-out barrier options: the zero-convexity condition. For $n = N_s$ and for $m = 0, \ldots, N_\sigma$, $k = 1, \ldots, N_t$,

$$V_{n,m}^k = 2V_{n-1,m}^k - V_{n-2,m}^k$$

For up-and-out barrier options, we have $S_{N_s} = S_{max} = B$ and

$$V_{n,m}^k = 0, \qquad n = N_s,\ m = 0, \ldots, N_\sigma,\ k = 1, \ldots, N_t$$

Boundary conditions for volatility

We use the same volatility boundary conditions for all options.

Lower boundary: we determine the boundary condition by the PDE itself. When the volatility is equal to zero the PDE still has to be satisfied, so we can substitute $\sigma = 0$ into the partial differential equation to find:

$$\frac{\partial V}{\partial t} + b(S,0,t)\frac{\partial V}{\partial S} + c(S,0,t)V + e(S,0,t)\frac{\partial V}{\partial \sigma} = 0,$$

In discrete terms this amounts to the following:

Predictor step 1:

$$\frac{(U_{n,m}^k)^* - V_{n,m}^{k-1}}{\delta t} + [D_S + D_0]\frac{(U_{n,m}^k)^* + V_{n,m}^{k-1}}{2} + \widetilde{D_\sigma} V_{n,m}^{k-1} = 0$$

Predictor step 2:

$$\frac{U^k_{n,m} - V^{k-1}_{n,m}}{\delta t} + [D_S + D_0]\frac{(U^k_{n,m})^* + V^{k-1}_{n,m}}{2} + \widetilde{D_\sigma}\frac{U^k_{n,m} + V^{k-1}_{n,m}}{2} = 0,$$

and with similar equations in the corrector steps. Note that we use $\widetilde{D_\sigma}$, which is different from D_σ. Since we are on the zero volatility boundary we cannot use a central difference scheme for the volatility derivative. We use a forward difference scheme that is of the same order of accuracy. We can derive this scheme using a Taylor series:

$$\begin{aligned} V(S,\sigma+\delta\sigma,t) &= V(S,\sigma,t) + \delta\sigma\frac{\partial V}{\partial\sigma} + \delta\sigma^2\frac{\partial^2 V}{\partial\sigma^2} + O\left(\delta\sigma^3\right) \\ V(S,\sigma+2\delta\sigma,t) &= V(S,\sigma,t) + 2\delta\sigma\frac{\partial V}{\partial\sigma} + 4\delta\sigma^2\frac{\partial^2 V}{\partial\sigma^2} + O\left(\delta\sigma^3\right) \end{aligned}$$

Multiplying the first series by minus 4, adding it to the second series and rearranging term results in

$$\frac{\partial V}{\partial\sigma} = \frac{-3V(S,\sigma,t) + 4V(S,\sigma+\delta\sigma,t) - V(S,\sigma+2\delta\sigma,t)}{2\delta\sigma} + O\left(\delta\sigma^2\right)$$

So, for $m = 0$ and $n = 0,\ldots,N_s$, $k = 1,\ldots,N_t$ we define the operator $\widetilde{D_\sigma}$ by

$$\widetilde{D_\sigma}V^k_{n,m} = e^k_{n,m}\frac{-3V^k_{n,m} + 4V^k_{n,m+1} - V^k_{n,m+2}}{2\delta\sigma}$$

Upper boundary: we can take a look at the Black-Scholes formulae (2.6) and (2.7) to see that the call and put option value are proportional to spot for large values of the volatility. Therefore, we use the zero-convexity boundary condition for the upper volatility boundary: for $m = N_\sigma$ and $n = 0,\ldots,N_s$, $k = 1,\ldots,N_t$,

$$V^k_{n,m} = 2V^k_{n,m-1} - V^k_{n,m-2}$$

Chapter 6

dVega/dVol dVega/dSpot Method

6.1 Outline

In this chapter we discuss the dVega/dVol, dVega/dSpot method. Unlike the previously discussed local and stochastic volatility model, the dVega/dVol dVega/dSpot model is not based on some specific assumption for the process of the underlying stock. Instead, in this model option prices are calculated by providing a smile correction on top of the Black-Scholes option price.

Section 5.2 explains how this smile correction is calculated. In this section no term structure is taken into account. Many exotic option, however, depend on more than one point in time; this is the case for both compound and forward start options. Section 5.3 explains the so-called bucketed dVega/dVol dVega/dSpot method which accounts for this time dependence. Finally section 5.4 explains how the method can be used to calculate option prices.

6.2 dVega/dVol dVega/dSpot Price Adjustment

The dVega/dVol dVega/dSpot method, or in short the *dVdVdVdS method* (see Hoogerwerf[16], Zilber[27], and Beneder[4]) is a method with which (exotic) FX option prices are calculated in the presence of a volatility smile. The method is not based on some specific assumption for the process of the underlying stock, e.g. a local or stochastic volatility model. Instead, it is based on a thorough understanding of the market from a hedging point of view. Market practitioners tend to stick to the Black-Scholes model with its constant volatility, but since it is known that volatility is in fact stochastic, they also adapt some rules of thumb to include the effect of the volatility smile. It is an empirical procedure based on hedging arguments.

In chapter 2 we have seen that the price of a call option in the Black-Scholes model can be derived by constructing a dynamic delta hedge, whose initial value matches the option price. However, in real financial markets it is known that the volatility is not constant, but follows a stochastic process itself. Traders hedge the associated volatility risk by constructing a hedging

portfolio that is not only vega-neutral, but also neutral with respect to some higher order greeks like volga, which is the sensitivity of the vega of the option with respect to changes in implied volatility, and vanna, which is the sensitivity of vega with respect to changes in spot. Volga can be thought of as a sensitivity with respect to the volatility of the implied volatility; vanna can be thought of as a sensitivity with respect to the correlation between the underlying asset and the implied volatility. Traders try to minimize the model risk by setting the vega, the volga and the vanna of the hedged portfolio equal to zero.

The procedure for calculating an option price using the dVdVdVdS method can be summarized as follows. The first step is to price the exotic option with the Black-Scholes formula using the ATM volatility. Then the vega, volga and vanna of this option are calculated. These exposures can then be hedged by deriving a hedging portfolio consisting of three European vanilla options. The next step is to calculate the value of this hedging portfolio. This is done in two ways: the value is calculated using the corresponding implied volatilities, yielding the true market value of the portfolio, and then using the ATM volatility. Then the difference between the two values is added to the Black-Scholes exotic option price. The exotic option price is thus defined by adding to the 'flat smile' Black-Scholes price the difference in cost of the hedging portfolio induced by the market implied volatilities compared to the constant volatility.

Using formulas, the price of the exotic option V_{exotic} is given by

$$\begin{aligned} V_{exotic} &= V_{BS}(S,t;K,T,\sigma_{imp}(K,T)) \\ &= V_{BS}(S,t;K,T,\sigma_{ATM}) + \text{smile adjustment}, \end{aligned} \tag{6.1}$$

where $V_{BS}(S,t;K,T,\sigma)$ is the Black-Scholes price of the option with strike K and expiry T, using a volatility equal to σ.

Note that the method can also be viewed at as an interpolation method. From the above equation we can see that once the smile adjustment is calculated, the implied volatility for some strike K can be obtained by solving equation (6.1) for the implied volatility.

The dVdVdVdS method uses the three sensitivity parameters vega, volga and vanna:

$$\begin{aligned} \text{vega} &= \frac{\partial V}{\partial \sigma} \\ \text{volga} &= \frac{\partial^2 V}{\partial \sigma^2} \\ \text{vanna} &= \frac{\partial^2 V}{\partial S \partial \sigma}, \end{aligned}$$

where V denotes the option value. The price adjustment is then calculated by matching the sensitivities of the exotic option with the sensitivities of a portfolio consisting of three plain vanilla options. The three vanilla options that make up the vanilla portfolio are an ATM option,

a 25Δ-call option and a 25Δ-put option. The implied volatilities of these options are given in chapter 3, equations (3.9), (3.10) and (3.11). To each vanilla option a weight is assigned in order to match the sensitivities of the exotic. The weights can be determined by solving the matrix equation:

$$\begin{pmatrix} \text{vega}_{ATM} & \text{vega}_{25\Delta-C} & \text{vega}_{25\Delta-P} \\ \text{volga}_{ATM} & \text{volga}_{25\Delta-C} & \text{volga}_{25\Delta-P} \\ \text{vanna}_{ATM} & \text{vanna}_{25\Delta-C} & \text{vanna}_{25\Delta-P} \end{pmatrix} \begin{pmatrix} w_1 \\ w_2 \\ w_3 \end{pmatrix} = \begin{pmatrix} \text{vega}_{exotic} \\ \text{volga}_{exotic} \\ \text{vanna}_{exotic} \end{pmatrix}$$

The sensitivities are calculated for the ATM volatility, so vega $= \frac{\partial V(K,T;\sigma)}{\partial \sigma}|_{\sigma=sigma_{ATM}}$, for all options.

Then we calculate the price of this vanilla portfolio in two ways: one price where we assume a flat volatility (the ATM volatility), and one price where we use the implied volatilities for each option in the portfolio.

Finally, the smile adjustment for the price of the exotic option is then equal to the difference between the two prices of the vanilla portfolio (with and without smile):

$$\begin{aligned} A_{exotic} &= [w_1 (P_{ATM,smile} - P_{ATM,flat}) + w_2 (P_{25\Delta C,smile} - P_{25\Delta P,flat}) + w_3 (P_{25\Delta P,smile} - P_{25\Delta P,flat})] \\ &= [w_2 (P_{25\Delta C,smile} - P_{25\Delta C,flat}) + w_3 (P_{25\Delta P,smile} - P_{25\Delta P,flat})] , \end{aligned}$$

where A_{exotic} is the smile adjustment and P denotes the price of the vanilla option.

The price of the exotic option V_{exotic} is then given by

$$V_{exotic}(S,t;K,T) = V_{BS}(S,t;K,T,\sigma_{ATM}) + A_{exotic} \tag{6.2}$$

6.3 Bucketed dVega/dVol dVega/dSpot Method

The method described in the previous section can be applied to options that depend only on one maturity. However, path-dependent options may depend on more than one maturity, we have seen this for the compound and forward start options, for example. In these cases, the dVdVdVdS procedure can be extended in the following way.

The bucketed dVdVdVdS method can be applied in general for any number of buckets, but as we are dealing with two buckets only for the compound and forward start options, we will restrict ourselves to this case. Let $V_{exotic}(\sigma_1,\sigma_2) = V_{exotic}(S,t;K,T;\sigma_1,\sigma_2)$ denote the price of our (exotic) option at time t and spot S, with strike K and maturity T. For brevity we will only show the dependence on the volatilities, where σ_1 and σ_2 are the volatilities corresponding to the first and second maturity pillars ('buckets'), respectively. The price of the option is given by

$$V_{exotic}(\sigma_1^{imp},\sigma_2^{imp}) = V_{exotic}(\sigma_1^{ATM},\sigma_2^{ATM}) + \text{adjustment}$$

As in the standard dVdVdVdS method, the first step is to calculate the exotic option price using the ATM volatility, and to calculate the three sensitivities, also using the ATM volatility.

Let σ_1 and σ_2 denote the ATM volatilities:

$$\begin{aligned} \sigma_1 &= \sigma_1^{ATM} \\ \sigma_2 &= \sigma_2^{ATM} \end{aligned}$$

In our bucketed method, we have vegas, volgas, and vannas for every maturity. For vega and vanna this is simply given by

$$\begin{aligned} \text{vega}_1(\sigma_1, \sigma_2) &= \frac{\partial V}{\partial \sigma_1}(\sigma_1, \sigma_2) \\ \text{vega}_2(\sigma_1, \sigma_2) &= \frac{\partial V}{\partial \sigma_2}(\sigma_1, \sigma_2) \\ \text{vanna}_1(\sigma_1, \sigma_2) &= \frac{\partial^2 V}{\partial S \partial \sigma_1}(\sigma_1, \sigma_2) \\ \text{vanna}_2(\sigma_1, \sigma_2) &= \frac{\partial^2 V}{\partial S \partial \sigma_2}(\sigma_1, \sigma_2) \end{aligned}$$

For volga we have to take into account the fact that there exists a correlation between the volatilities for different maturities. A bump in σ_1 implied a certain perturbation of the whole term structure of volatility. In the bucketed dVdVdVdS method, this is included in the following way:

$$\begin{aligned} \text{volga}_1(\sigma_1, \sigma_2) &= \frac{d\text{vega}_1}{d\sigma_1}(\sigma_1, \sigma_2) \\ &= \frac{\partial \text{vega}_1}{\partial \sigma_1}(\sigma_1, \sigma_2) + E\left[\Delta\sigma_2 | \Delta\sigma_1 = 1\right] \frac{\partial \text{vega}_1}{\partial \sigma_2}. \end{aligned}$$

So this can be defined as a sensitivity to an expected bump in the volatility term structure given a unit change in volatility. A similar relation holds for volga_2.

These bumping weights are expressed via correlations and relative volatility of ATM options:

$$E\left[\Delta\sigma_2 | \Delta\sigma_1 = 1\right] = \rho_{12}\sqrt{\frac{T_2}{T_1}}.$$

Here, the term $\sqrt{\frac{T_2}{T_1}}$ is the 'square root rule' that is used in practice for the relative volatility of the ATM options, and ρ_{12} is the correlation between the volatilities. We do not know this correlation, but we can estimate it using an historical estimation.

Having calculated these sensitivities, the procedure continues in the same way as the standard case, with the difference that a price adjustment is calculated for each bucket. So, both for maturity T_1 and T_2 a portfolio of European vanilla options is constructed and the weights of these portfolios are determined by solving equation (6.2) for the corresponding bucket. Then the total smile adjustment is the sum of these two adjustments per bucket:

$$V_{exotic}(\sigma_1^{imp}, \sigma_2^{imp}) = V_{exotic}(\sigma_1^{ATM}, \sigma_2^{ATM}) + \text{adjustment}_1 + \text{adjustment}_2,$$

where adjustment_1 and adjustment_2 are the price adjustments for buckets 1 and 2, respectively.

6.4 Option Price Calculation

Using the dVdVdVdS method the option can be priced in two steps. First the Black-Scholes value of the option is calculated using the ATM volatility. This can be done using an analytical formula if available, or by using a finite difference method otherwise.

For the compound option an analytical formula has been derived in section 2.6; for a call-on-call compound option:

$$C_{call}(S,t) = S\mathcal{N}_2(a_+, b_+; \rho) - K_2 e^{-rT_2}\mathcal{N}_2(a_-, b_-; \rho) - K_1 e^{-rT_1}\mathcal{N}(a_-),$$

with

$$\begin{aligned} \rho &= \frac{Cov(W_{T_1}, W_{T_2})}{\sqrt{Var(W_{T_1})Var(W_{T_2})}} \\ &= \frac{Var(W_{T_1})}{\sqrt{Var(W_{T_1})Var(W_{T_2})}} = \sqrt{\frac{T_1}{T_2}}. \end{aligned}$$

$$\begin{aligned} a_+ &= \frac{log(\frac{S}{S^*}) + \left(r + \frac{1}{2}\sigma^2\right)T_1}{\sigma\sqrt{T_1}} \qquad & a_- &= a_+ - \sigma\sqrt{T_1} \\ b_+ &= \frac{log(\frac{S}{K_2}) + \left(r + \frac{1}{2}\sigma^2\right)T_2}{\sigma\sqrt{T_2}} \qquad & b_- &= b_+ - \sigma\sqrt{T_2}, \end{aligned}$$

where $\mathcal{N}$ is the standard normal distribution, $\mathcal{N}_2$ is the bivariate standard normal distribution and ρ is the correlation coefficient.

For the forward start option with a relative strike there also is an analytical formula available:

$$FS(S,0) = S_0 C_{BS}(1, T_1; \alpha, T_2; \sigma_{12}^{ATM}, r),$$

where $FS(S,0)$ is the price of the forward start option at time zero and spot S, $C_{BS}(1, T_1; \alpha, T_2; \sigma_{12}^{ATM}, r)$ is the Black-Scholes price for a call option with spot $S = 1$, strike $K = \alpha$, time to maturity $T2 - T_1$, interest rate r and volatility σ_{12}^{ATM}, which is the ATM forward volatility:

$$\sigma_{12}^{ATM} = \sqrt{\frac{\left(\sigma_2^{ATM}\right)^2 T_2 - \left(\sigma_1^{ATM}\right)^2 T_1}{T_2 - T1}}.$$

When the strike is given in absolute rather than relative terms, we do not have an analytical formula. We can calculate the price using finite differences.

The second parts consists of calculating the price adjustment according to the dVdVdVdS method. The option price is is then given by equation (6.2).

Chapter 7

Forward Smile Model

7.1 Outline

The final option pricing model that we will discuss is the *Forward Smile Model* by Nauta and Zilber[21]. The objective of this model is *not* to specify a fundamental evolution model for the price process of an asset (e.g. a local or stochastic volatility model), but instead to specify the transition density directly. In fact, two models will be presented, one using the sticky strike smile dynamics, and one using the sticky delta smile dynamics.

In section 7.2 we will discuss the notation that will be used throughout the chapter. In section 7.3 the specification of the transition density is given. In section 7.4 and 7.5 the derivations of the forward smile are given for the sticky strike and sticky delta model, respectively. Finally, section 7.6 explains how the model can be used to calculate option prices.

7.2 Notation

Let S_1 denote the spot at time T_1 so ($S_1 = S(T_1)$) and S_2 the spot at time T_2. Throughout the chapter, $C(S,t;K,T)$ denotes the value of a call option at time t and spot S, with strike K and maturity T. Sometimes we will also show the dependence on the volatility; then we will use $C(S,t;K,T;\sigma)$. For the volatilities, we will use the following notations:

$$\begin{aligned} \sigma_{imp}(K,T) &= \text{implied volatility for strike } K \text{and maturity } T \\ \sigma_{01,ATM} &= \text{ATM volatility for maturity } T_1 \\ \sigma_{02,ATM} &= \text{ATM volatility for maturity } T_2 \end{aligned}$$

Let $\rho_{S_1}(s_1)$, $\rho_{S_2}(s_2)$ be the densities of S_1 and of S_2 in the points s_1 and s_2, respectively. As we know, these can be obtained from vanilla prices,

$$\rho_{S_T}(s) = e^{r_d(T-t)} \frac{\partial^2 C(S_t,t;K,T)}{\partial K^2}|_{K=s}. \tag{7.1}$$

The transition densities are determined in such a way that they are consistent with these densities. Let $G_{S_2|S_1}(s_1, T_1; s_2, T_2)$ be the transition density of S_2 conditional on S_1 in the points s_2 and s_1 (the probability density of ending up in s_2 at T_2 given that we start in s_1 at T_1). A transition density consistent with the smiles at T_1 and T_2 means that the following constraint should be satisfied:

$$\rho_{S_2}(s_2) = \int G_{S_2|S_1}(s_1, T_1; s_2, T_2)\rho_{S_1}(s_1)ds_1. \tag{7.2}$$

Sometimes it may be more convenient to work with a transformation to the 'log-space'; therefore let $X_1 = log(S_1)$ and $X_2 = log(S_2)$. Let F_{S_1} denote the cumulative distribution function of S_1, and F_{X_1} the cumulative distribution function of X_1. Then we know that

$$\begin{aligned} F_{S_1}(s) &= \mathbb{P}(S_1 < s) \\ &= \mathbb{P}(X_1 < log(s)) \\ &= F_{X_1}(log(s)). \end{aligned}$$

Then for the density functions ρ_{S_1} and ρ_{X_1} of S_1 and X_1 respectively, we have

$$\begin{aligned} \rho_{S_1}(s) &= \frac{d}{ds}F_{S_1}(s) \\ &= \frac{d}{ds}F_{X_1}(log(s)) \\ &= \rho_{X_1}(log(s))\frac{1}{s}, \end{aligned}$$

where we simply apply the chain rule in the final step. For X_2 we have a similar relation. Let $G_{X_2|X_1}(x_1, T_1; x_2, T_2)$ be the transition density of X_2 conditional on X_1. A transition density consistent with the smiles at T_1 and T_2 means that we should have

$$\rho_{X_2}(x_2, T_2) = \int G_{X_2|X_1}(x_1, T_1; x_2, T_2)\rho_{X_1}(x_1, T_1)dx_1. \tag{7.3}$$

This expression is exactly the same as equation (7.2); to see this, we can write both the right- and the left hand side of this equation in terms of 'log-space'. The left hand side of equation (7.2) can be written as

$$\begin{aligned} \rho_{S_2}(s_2) &= \frac{1}{s_2}\rho_{X_2}(log(s_2)) \\ &= e^{-x_2}\rho_{X_2}(x_2), \end{aligned}$$

where $x_2 = log(s_2)$. For the right hand side we have

$$\begin{aligned} \int G_{S_2|S_1}(s_1, T_1; s_2, T_2)\rho_{S_1}(s_1)ds_1 &= \int \frac{1}{s_2}G_{X_2|X_1}(log(s_1), T_1; log(s_2), T_2)\frac{1}{s_1}\rho_{X_1}(log(s_1))ds_1 \\ &= \int e^{-x_2}G_{X_2|X_1}(x_1, T_1; x_2, T_2)\rho_{X_1}(x_1)dx_1, \end{aligned}$$

where $x_1 = log(s_1)$ and again $x_2 = log(s_2)$.

Two other constraints that a density should satisfy are

$$\int G(x_1, T_1; x_2, T_2) dx_2 = 1 \qquad \forall x_1 \tag{7.4}$$

$$G(x_1, T_1; x_2, T_2) > 0 \qquad \forall x_1, x_2 \tag{7.5}$$

Now we have introduced the notation that will be used, and we have established three constraints that the transition density should satisfy.

7.3 Transition Density

The transition density in terms of spot is given by

$$G_{S_2|S_1}(s_1, T_1; K, T_2) = e^{r_d(T_2-T_1)} \frac{d^2 C_{BS}(s_1, T_1; K, T_2; \sigma_{12}(K, \Delta_{BS}))}{dK^2},$$

where $\sigma_{12}(K, \Delta_{BS})$ is the implied volatility , which is the forward volatility at T_2, seen from T_1. The Black-Scholes delta Δ_{BS} is calculated for the at-the-money forward volatility σ_{12}^{ATM}. The transition density has the same form as the density of the underlying at maturity, and it can be derived in a similar manner as has been done in section 3.3.

The relation between the transition density in terms of spot and the transition density in terms of 'log-spot' can be derived in a similar way as the relation between the densities of the underlying at maturity; the result is

$$G_{S_2|S_1}(s_1, T_1; K, T_2) \quad = \quad \frac{1}{K} G_{X_2|X_1}(log(s_1), T_1; log(K), T_2). \tag{7.6}$$

7.4 Sticky Strike Forward Smile

The first model is the *Sticky Strike Forward Smile Model*. In this model, the forward volatility σ_{12} depends only on the strike, $\sigma_{12}(K, \Delta_{BS}) = \sigma_{12}(K)$. So the smile that is seen for expiry at T_2 does not depend on the spot level at T_1. For this model, the transition density is given by

$$G_{S_2|S_1}(s_1, T_1; K, T_2) \quad = \quad e^{r_d(T_2-T_1)} \frac{d^2 C_{BS}(s_1, T_1; K, T_2; \sigma_{12}(K))}{dK^2}. \tag{7.7}$$

Our goal is to find the forward volatility under the sticky strike rule, $\sigma_{12}(K)$. We will show that it can be found by applying the constraint (7.2), which says that the transition density must be consistent with the smiles observed at T_1 and T_2. To achieve this, we plug our sticky strike

transition density (7.7) into constraint (7.2),

$$\begin{aligned}
\rho_{S_2}(K) &= \int G_{S_2|S_2}(s_1, T_1; K, T_2)\rho_{S_1}(s_1)ds_1 \\
&= \int e^{r_d(T_2-T_1)}\frac{d^2C_{BS}(s_1, T_1; K, T_2; \sigma_{12}(K))}{dK^2}\rho_{S_1}(s_1)ds_1 \\
&= \int e^{r_d(T_2-T_1)}\frac{d^2C_{BS}(s_1, T_1; K, T_2; \sigma_{12}(K))}{dK^2}\rho_{X_1}(log(s_1))\frac{1}{s_1}ds_1 \\
&= \int e^{r_d(T_2-T_1)}\frac{d^2C_{BS}(e^{x_1}, T_1; K, T_2; \sigma_{12}(K))}{dK^2}\rho_{X_1}(x_1)dx_1, \qquad (7.8)
\end{aligned}$$

where we have made the change of variables $x_1 = log(s_1)$ in the final step. We will show that this equation can be solved to obtain $\sigma_{12}(K)$.

We will rewrite equation (7.8), using the previously discussed dVdVdVdS model. We will start with the left hand side of this equation. To see how we apply the dVdVdVdS model, recall that the densities can be obtained by twice differentiating the call option price so that we may write,

$$\begin{aligned}
\rho_{S_2}(K) &= e^{r_dT_2}\frac{d^2C(S, t; K, T_2)}{dK^2} \\
&= e^{r_dT_2}\frac{d^2C_{BS}(S, t; K, T_2; \sigma_{imp}(K, T_2))}{dK^2} \\
&= e^{r_dT_2}\frac{d^2}{dK^2}\left[C_{BS}(S, t; K, T_2; \sigma_{02,ATM}) + \text{smile adjustment}\right] \\
&= \rho_{BS,S_2}(K; \sigma_{02,ATM}) + e^{r_dT_2}\left[\frac{d^2}{dK^2}(\text{smile adjustment})\right]. \qquad (7.9)
\end{aligned}$$

From the previous chapter we know that the smile adjustment A_{exotic} for an exotic option is given by

$$A_{exotic} = w_1\left(f^{smile}_{ATM} - f^{flat}_{ATM}\right) + w_2\left(f^{smile}_{25\Delta C} - f^{flat}_{25\Delta C}\right) + w_3\left(f^{smile}_{25\Delta P} - f^{flat}_{25\Delta P}\right), \qquad (7.10)$$

where f is the price of the vanilla with maturity T_2. The weights w_i, for $i = 1, 2, 3$, are determined by solving

$$\mathbf{Vw} = \mathbf{d}C_{BS}(S, t; K, T_2; \sigma_{02,ATM}),$$

where

$$\mathbf{V} = \begin{pmatrix} \text{vega}_1 & \text{vega}_2 & \text{vega}_3 \\ \frac{\partial \text{vega}_1}{\partial \sigma} & \frac{\partial \text{vega}_2}{\partial \sigma} & \frac{\partial \text{vega}_3}{\partial \sigma} \\ \frac{\partial \text{vega}_1}{\partial S} & \frac{\partial \text{vega}_2}{\partial S} & \frac{\partial \text{vega}_3}{\partial S} \end{pmatrix}, \quad \mathbf{w} = \begin{pmatrix} w_1 \\ w_2 \\ w_3 \end{pmatrix}, \quad \mathbf{d} = \begin{pmatrix} \frac{\partial}{\partial \sigma} \\ \frac{\partial^2}{\partial \sigma^2} \\ \frac{\partial^2}{\partial S \partial \sigma} \end{pmatrix}$$

If we define

$$\delta\mathbf{f} = \begin{pmatrix} f_{ATM,smile} - f_{ATM,flat} \\ f_{25\Delta C,smile} - f_{25\Delta C,flat} \\ f_{25\Delta P,smile} - f_{25\Delta P,flat} \end{pmatrix}$$

Then the price adjustment given by equation (7.10) can be written as

$$\begin{aligned} A_{exotic} &= \delta\mathbf{f}\cdot\mathbf{w} \\ &= \delta\mathbf{f}\cdot\mathbf{V}^{-1}\mathbf{d}C_{BS}(S,t;K,T_2;\sigma_{02,ATM}) \end{aligned}$$

We can insert this result in equation (7.9); then the density can be written as

$$\begin{aligned} \rho_{S_2}(K) &= \rho_{BS,S_2}(K;\sigma_{02,ATM}) + e^{r_d T_2}\left[\frac{d^2}{dK^2}(\text{smile adjustment})\right] \\ &= \rho_{BS,S_2}(K;\sigma_{02,ATM}) + e^{r_d T_2}\left[\frac{d^2}{dK^2}\delta\mathbf{f}_{T_2}\cdot\mathbf{V}_{T_2}^{-1}\mathbf{d}_{02}C_{BS}(S,t;K,T_2,\sigma_{02,ATM})\right] \\ &= \rho_{BS,S_2}(K;\sigma_{02,ATM}) + \delta\mathbf{f}_{T_2}\cdot\mathbf{V}_{T_2}^{-1}\mathbf{d}_{02}e^{r_d T_2}\left[\frac{d^2}{dK^2}C_{BS}(S,t;K,T_2,\sigma_{02,ATM})\right] \\ &= \rho_{BS.S_2}(K;\sigma_{02,ATM}) + \delta\mathbf{f}_{T_2}\cdot\mathbf{V}_{T_2}^{-1}\mathbf{d}_{02}\left(\rho_{BS,S_2}(K;\sigma_{02,ATM})\right) \\ &= \left(1+\delta\mathbf{f}_{T_2}\cdot\mathbf{V}_{T_2}^{-1}\mathbf{d}_{02}\right)\rho_{BS,S_2}(K;\sigma_{02,ATM}). \end{aligned}$$

Here we have used the subscript T_2 to point out that this applies to options with expiry T_2. Further,

$$\mathbf{d}_{02} = \begin{pmatrix} \frac{\partial}{\partial\sigma_{02,ATM}} \\ \\ \frac{\partial^2}{\partial\sigma_{02,ATM}^2} \\ \\ \frac{\partial^2}{\partial S\partial\sigma_{02,ATM}} \end{pmatrix},$$

i.e., the sensitivities with respect to the ATM volatility for expiry T_2. So, using the dVdVdVdS method, we can write the the density on the left hand side of equation (7.8) in terms of a Black-Scholes density for the ATM volatility:

$$\rho_{S_2}(K) = \left(1+\delta\mathbf{f}_{T_2}\cdot\mathbf{V}_{T_2}^{-1}\mathbf{d}_{02}\right)\rho_{BS,S_2}(K;\sigma_{02,ATM}). \tag{7.11}$$

We can do the same for $\rho_{S_1}(s_1)$, and write it in terms of 'log-spot' to obtain $\rho_{X_1}(log(s_1))$ so that we can insert it into the expression on the right hand side of equation (7.8). We have

$$\rho_{S_1}(K) = \left(1+\delta\mathbf{f}_{T_1}\cdot\mathbf{V}_{T_1}^{-1}\mathbf{d}_{01}\right)\rho_{BS,S_1}(K;\sigma_{01,ATM}), \tag{7.12}$$

so in log space this becomes

$$\frac{1}{K}\rho_{X_1}(log(K)) = \frac{1}{K}\left(1+\delta\mathbf{f}_{T_1}\cdot\mathbf{V}_{T_1}^{-1}\mathbf{d}_{01}\right)\rho_{BS,X_1}(log(K);\sigma_{01,ATM}).$$

Then we can write equation (7.8) as

$$\left(1+\delta\mathbf{f}_{T_2}\cdot\mathbf{V}_{T_2}^{-1}\mathbf{d}_{02}\right)\rho_{BS,S_2}(K;\sigma_{02,ATM}) =$$

$$\int e^{r_d(T_2-T_1)}\frac{d^2}{dK^2}C_{BS}(e^{x_1},T_1;K,T_2;\sigma_{12}(K))\left(1+\delta\mathbf{f}_{T_1}\cdot\mathbf{V}_{T_1}^{-1}\mathbf{d}_{01}\right)\rho_{BS,X_1}(x_1;\sigma_{01,ATM})dx_1 =$$

$$\frac{d^2}{dK^2}\left(1+\delta\mathbf{f}_{T_1}\cdot\mathbf{V}_{T_1}^{-1}\mathbf{d}_{01}\right)\int e^{r_d(T_2-T_1)}C_{BS}(e^{x_1},T_1;K,T_2;\sigma_{12}(K))\rho_{BS,X_1}(x_1;\sigma_{01,ATM})dx_1. \tag{7.13}$$

In this expression we can now write the call value in the integrand as the discounted value of its expected payoff:

$$\begin{aligned} e^{r_d(T_2-T_1)}C(e^{x_1},T_1;K,T_2;\sigma_{12}(K)) &= \mathbb{E}^Q\left[\max(S_{T_2}-K,0)|S_{T_1}=e^{x_1}\right] \\ &= \int \max(s_2-K,0)\rho_{BS,S_{T_2}|S_{T_1}}(s_2|e^{x_1};\sigma_{12}(K))ds_2 \\ &= \int \max(s_2-K,0)\rho_{BS,X_{T_2}|X_{T_1}}(log(s_2)|x_1;\sigma_{12}(K))\frac{1}{s_2}ds_2 \\ &= \int \max(e^{x_2}-K,0)\rho_{BS,X_{T_2}|X_{T_1}}(x_2|x_1;\sigma_{12}(K))dx_2. \end{aligned}$$

We can insert this back into equation (7.13) to have

$$\left(1+\delta\mathbf{f}_{T_2}\cdot\mathbf{V}_{T_2}^{-1}\mathbf{d}_{02}\right)\rho_{BS,S_2}(K;\sigma_{02,ATM}) =$$

$$\frac{d^2}{dK^2}\left(1+\delta\mathbf{f}_{T_1}\cdot\mathbf{V}_{T_1}^{-1}\mathbf{d}_{01}\right)\int\left(\int max(e^{x_2}-K,0)\rho_{BS,X_{T_2}|X_{T_1}}(x_2|x_1;\sigma_{12}(K))dx_2\right)\rho_{BS,X_1}(x_1;\sigma_{01,ATM})dx_1 =$$

$$\frac{d^2}{dK^2}\left(1+\delta\mathbf{f}_{T_1}\cdot\mathbf{V}_{T_1}^{-1}\mathbf{d}_{01}\right)\int max(e^{x_2}-K,0)\left(\int\rho_{BS,X_{T_2}|X_{T_1}}(x_2|x_1;\sigma_{12}(K))\rho_{BS,X_1}(x_1;\sigma_{01,ATM})dx_1\right)dx_2 =$$

$$\frac{d^2}{dK^2}\left(1+\delta\mathbf{f}_{T_1}\cdot\mathbf{V}_{T_1}^{-1}\mathbf{d}_{01}\right)\int max(e^{x_2}-K,0)\rho_{BS,X_{T_2}}(x_2;\tilde{\sigma}_{02}(K))dx_2. \tag{7.14}$$

In the last line we use the fact that the convolution of two normal densities is again a normal density. In this case, the volatility $\tilde{\sigma}_{02}(K)$ is given by

$$\tilde{\sigma}_{02}(K)=\sqrt{\frac{T_1(\sigma_{01,ATM})^2+T_{12}(\sigma_{12}(K))^2}{T_2}}, \tag{7.15}$$

where $T_{12}=T_2-T_1$. Note that one the right hand side of equation (7.14) (the last line) the integral is the (undiscounted) value of a call option with volatility $\tilde{\sigma}_{02}(K)$, so that we can reduce the expression further to

$$\left(1+\delta\mathbf{f}_{T_2}\cdot\mathbf{V}_{T_2}^{-1}\mathbf{d}_{02}\right)\rho_{BS,S_2}(K;\sigma_{02,ATM}) = \frac{d^2}{dK^2}\left(1+\delta\mathbf{f}_{T_1}\cdot\mathbf{V}_{T_1}^{-1}\mathbf{d}_{01}\right)C_{BS}(S_0,0;K,T_2,\tilde{\sigma}_{02}(K))e^{r_dT_2}$$

Integrating twice on both sides results in

$$\begin{aligned} &\left(1+\delta\mathbf{f}_{T_2}\cdot\mathbf{V}_{T_2}^{-1}\mathbf{d}_{02}\right)C_{BS}(S,t;K,T_2,\sigma_{02,ATM})e^{r_dT_2} = \\ &\qquad\left(1+\delta\mathbf{f}_{T_1}\cdot\mathbf{V}_{T_1}^{-1}\mathbf{d}_{01}\right)C_{BS}(S,t;K,T_2,\tilde{\sigma}_{02}(K))e^{r_dT_2}+aK+b \end{aligned}$$

Now use the boundary condition that for $K\to\infty$ we have $C_{BS}(S,t;K,T_2,\sigma_{02,ATM})\to 0$ and $C_{BS}(S,t;K,T_2,\tilde{\sigma}_{02}(K))\to 0$, so that $a=b=0$. The final result is given by:

$$\left(1+\delta\mathbf{f}_{T_2}\cdot\mathbf{V}_{T_2}^{-1}\mathbf{d}_{02}\right)C_{BS}(S,t;K,T_2,\sigma_{02,ATM}) = \left(1+\delta\mathbf{f}_{T_1}\cdot\mathbf{V}_{T_1}^{-1}\mathbf{d}_{01}\right)C_{BS}(S,t;K,T_2,\tilde{\sigma}_{02}(K)) \tag{7.16}$$

This equation can now be solved for $\tilde{\sigma}_{02}(K)$ and finally we can obtain $\sigma_{12}(K)$ through equation (7.15).

It still needs to be checked if this transition density satisfies the constraints (7.2), (7.4) and (7.5). The first one is obvious because that is what we have used to calculate the implied volatility. A simple calculation shows that the second constraint is also satisfied. It is unknown if also the third constraint is satisfied.

7.5 Sticky Delta Forward Smile

The second model is the *Sticky Delta Forward Smile Model*. In this model, the forward volatility σ_{12} depends only on the delta, $\sigma_{12}(K, \Delta_{BS}) = \sigma_{12}(\Delta_{BS})$. For this model, the transition density in log-space is given by

$$\begin{aligned} G_{X_2|X_1}(log(s_1), T_1; log(K), T_2) &= K G_{S_2|S_1}(s_1, T_1; K, T_2) \\ &= K e^{r_d(T_2-T_1)} \frac{d^2 C_{BS}(s_1, T_1; K, T_2; \sigma_{12}(\Delta_{BS}))}{dK^2}. \end{aligned}$$

Our goal is to find the forward volatility $\sigma_{12}(\Delta)$. First of all, note that the delta does not depend on S and K separately, but only as a function of $log\left(\frac{S}{K}\right)$. Therefore we can write the volatility as $\sigma_{12}(\Delta_{BS}) = \sigma_{12}(log(\frac{S}{K}))$ and the transition density is a function of $log(s_2) - log(s_1)$ only. In 'log-space',

$$\begin{aligned} G_{X_2|X_1}(log(s_1), T_1; log(K), T_2) &= G_{X_2|X_1}(log(K) - log(s_1), T_1, T_2) \\ &= K e^{r_d(T_2-T_1)} \frac{d^2 C_{BS}(s_1, T_1; K, T_2; \sigma_{12}(log(K) - log(s_1)))}{dK^2}. \end{aligned}$$

We will show how the implied forward volatility σ_{12} can be derived through the use of Fourier transforms. For $x_1 = log(s_1)$ and $x_2 = log(s_2)$ the transition density is a function of $x_2 - x_1$. As in the sticky strike forward smile model, we will derive this implied volatility by using the consistency constraint (in log-space),

$$\rho_{X_2}(x_2) = \int G_{X_2|X_1}(x_2 - x_1, T_1, T_2) \rho_{X_1}(x_1) dx_1. \tag{7.17}$$

The Fourier transform $\hat{\rho}_{X_2}(k, T_2)$ of $\rho_{X_2}(x_2)$ is defined by

$$\hat{\rho}_{X_2}(k, T_2) = \int \rho_{X_2}(x_2) e^{ikx_2} dx_2,$$

and a similar expression holds for $\hat{\rho}_{X_1}(k, T_1)$. Then we can write the Fourier transform of equation

(7.17) as

$$\begin{aligned}
\hat{\rho}_{X_2}(k,T_2) &= \int e^{ikx_2}\rho_{X_2}(x_2)dx_2 \\
&= \int e^{ikx_2}\left(\int G_{X_2|X_1}(x_2-x_1,T_1,T_2)\rho_{X_1}(x_1)dx_1\right)dx_2 \\
&= \int \rho_{X_1}(x_1)\left(\int e^{ikx_2}G_{X_2|X_1}(x_2-x_1,T_1,T_2)dx_2\right)dx_1 \\
&= \int \rho_{X_1}(x_1)e^{ikx_1}\left(\int e^{ik(x_2-x_1)}G_{X_2|X_1}(x_2-x_1,T_1,T_2)dx_2\right)dx_1 \\
&= \hat{G}_{X_2|X_1}(k)\int \rho_{X_1}(x_1)e^{ikx_1}dx_1 \\
&= \hat{G}_{X_2|X_1}(k)\hat{\rho}_{X_1}(k,T_1),
\end{aligned}$$

For brevity, let $\hat{G}(k) = \hat{G}_{X_2|X_1}(k)$, $\hat{\rho}_{X_2}(k,T_2) = \hat{\rho}_{X_2}(k)$, and $\hat{\rho}_{X_1}(k,T_1) = \hat{\rho}_{X_1}(k)$. The transition density $\hat{G}(k)$ is given by

$$\hat{G}(k) = \frac{\hat{\rho}_{X_2}(k)}{\hat{\rho}_{X_1}(k)}$$

We can write this in terms of Fourier transforms of the Black-Scholes density. From the previous subsection we know that we can write the density $\rho_{X_2}(x_2)$ in terms of the Black-Scholes density, using the dVdVdVdS method:

$$\rho_{X_2}(x_2) = (1 + \delta\mathbf{f}_{T_2}\cdot\mathbf{V}_{T_2}^{-1}\mathbf{d}_{02})\rho_{BS,X_2}(x_2,\sigma_{02,ATM}), \tag{7.18}$$

where $\rho_{BS,X_2}(x_2,\sigma_{02,ATM})$ is the Black-Scholes density for the ATM volatility (for maturity T_2). We want to find the Fourier transform of the right hand side of equation (7.18). For this we have to calculate the Fourier transform of $\rho_{BS,X_2}(x_2)$ and of $\mathbf{d}_{02}\rho_{BS,X_2}(x_2)$.

Using the Black-Scholes model for the ATM volatility, the asset price S_2 at T_2 is given by

$$S_2 = S_0 e^{\left((r_d - r_f - \frac{1}{2}\sigma_{02,ATM}^2)T_2 - \sigma_{02,ATM}W_{T_2}\right)}.$$

Let $X_2 = log(S_2)$. Then

$$X_2 = log(S_0) + (r_d - r_f - \frac{1}{2}\sigma_{02,ATM}^2)T_2 - \sigma_{02,ATM}W(T_2),$$

so X_2 has a normal density with mean μ_{02} and variance Σ_{02} given by

$$\begin{aligned}
\mu_{02} &= log(S_0) + (r_d^{02} - r_f^{02} - \frac{1}{2}\sigma_{02,ATM}^2)T_2 \\
\Sigma_{02} &= \sigma_{02,ATM}^2 T_2
\end{aligned}$$

So the Black-Scholes density $\rho_{BS,X_2}(x_2)$ is given by

$$\rho_{BS,X_2}(x_2) = \frac{1}{\sqrt{2\pi\Sigma_{02}}}e^{-\frac{-1}{2\Sigma_{02}}(x_2-\mu_{02})^2}.$$

Now the Fourier transform of this Black-Scholes density can be calculated

$$\begin{aligned}
\hat{\rho}_{BS,X_2}(k,T_2) &= \int_{-\infty}^{\infty} \rho_{BS,X_2}(x_2;\mu_{02},\Sigma_{02}) e^{ikx_2} dx_2 \\
&= \int \frac{1}{\sqrt{2\pi\Sigma_{02}}} e^{\frac{-1}{2\Sigma_{02}}(x_2-\mu_{02})^2} e^{ikx_2} dx_2 \\
&= e^{\left(ik\mu_{02}-\frac{1}{2}\Sigma_{02}k^2\right)} \int \frac{1}{\sqrt{2\pi\Sigma_{02}}} e^{\frac{-1}{2\Sigma_{02}}[x_2-(ik\Sigma_{02}+\mu_{02})]^2} dx_2 \\
&= e^{\left(ik\mu_{02}-\frac{1}{2}\Sigma_{02}k^2\right)}
\end{aligned}$$

Next, calculate the Fourier transform of

$$\mathbf{d}_{02}\rho_{BS,X_2}(x_2) = \begin{pmatrix} \frac{\partial}{\partial\sigma_{02,ATM}} \\ \\ \frac{\partial^2}{\partial\sigma_{02,ATM}^2} \\ \\ \frac{\partial^2}{\partial S\partial\sigma_{02,ATM}} \end{pmatrix} \rho_{BS,X_2}(x_2),$$

we treat the components of this vector separately. For notational convenience, we will use the following notation in the rest of the chapter:

$$\sigma_{01} = \sigma_{01,ATM}$$

$$\sigma_{02} = \sigma_{02,ATM}$$

The transform of the first component of $\hat{\rho}_{BS,X_2}(k,T_2)$ is equal to

$$\begin{aligned}
\widehat{\left(\frac{\partial}{\partial\sigma}\rho_{BS,X_2}\right)}(k,T_2) &= \int e^{ikx_2} \frac{\partial}{\partial\sigma}\rho_{BS,X_2}(x_2)dx_2 \\
&= \frac{\partial}{\partial\sigma}\int e^{ikx_2}\rho_{BS,X_2}(x_2)dx_2 \\
&= \frac{\partial}{\partial\sigma}\hat{\rho}_{BS,X_2}(k,T_2) \\
&= \frac{\partial}{\partial\sigma} e^{\left(ik\mu_{02}-\frac{1}{2}\Sigma_{02}k^2\right)} \\
&= \left(-\sigma_{02}k^2T_2 - i\sigma kT_2\right)\hat{\rho}_{BS,X_2}(k,T_2).
\end{aligned}$$

The second and the third term can be handled in a similar manner; the result is given by

$$\begin{aligned}
\widehat{\left(\frac{\partial^2}{\partial\sigma^2}\rho_{BS,X_2}\right)}(k,T_2) &= \left[(-\sigma k^2T - i\sigma kT)^2 - (k^2T + ikT)\right]\hat{\rho}_{BS,X_2}(k,T_2), \\
\widehat{\left(\frac{\partial^2}{\partial S\partial\sigma}\rho_{BS,X_2}\right)}(k,T_2) &= \frac{ik}{S}\left[-\sigma k^2T - i\sigma kT\right]\hat{\rho}_{BS,X_2}(k,T_2).
\end{aligned}$$

So, we can write

$$\hat{\rho}_{X_2}(k,T_2) = \left(1 + \delta\mathbf{f}_{T_2}\cdot\mathbf{V}_{T_2}^{-1}\mathbf{d}_{k,T_2}\right)\hat{\rho}_{BS,X_2}(k,T_2),$$

where

$$\mathbf{d}_{k,T_2} = \begin{pmatrix} -\sigma_{02}T_2k^2 - ik\sigma_{02}T_2 \\ \\ (-\sigma_{02}T_2k^2 - ik\sigma_{02}T_2)^2 - T_2k^2 - ikT_2 \\ \\ \frac{ik}{S_0}\left(-\sigma_{02}T_2k^2 - ik\sigma_{02}T_2\right) \end{pmatrix}.$$

In this way the Fourier transform of the transition density can be stated in terms of the Fourier transforms of the Black-Scholes density:

$$\hat{G}(k) = \frac{\left(1 + \delta\mathbf{f}_{T_2} \cdot \mathbf{V}_{T_2}^{-1}\mathbf{d}_{k,T_2}\right)}{\left(1 + \delta\mathbf{f}_{T_1} \cdot \mathbf{V}_{T_1}^{-1}\mathbf{d}_{k,T_1}\right)} \frac{\hat{\rho}_{BS}(k,T_2)}{\hat{\rho}_{BS}(k,T_1)}$$

Next, we can approximate this by using the fact that $\frac{1}{1+x} \approx 1 - x$, so that

$$\begin{aligned}
\hat{G}(k) &\approx \left(1 + \delta\mathbf{f}_{T_2} \cdot \mathbf{V}_{T_2}^{-1}\mathbf{d}_{k,T_2} - \delta\mathbf{f}_{T_1} \cdot \mathbf{V}_{T_1}^{-1}\mathbf{d}_{k,T_1}\right) \frac{\hat{\rho}_{BS}(k,T_2)}{\hat{\rho}_{BS}(k,T_1)} \\
&\approx \left(1 + \delta\mathbf{f}_{T_2} \cdot \mathbf{V}_{T_2}^{-1}\mathbf{d}_{k,T_2} - \delta\mathbf{f}_{T_1} \cdot \mathbf{V}_{T_1}^{-1}\mathbf{d}_{k,T_1}\right) e^{-\frac{1}{2}(\Sigma_{T_2} - \Sigma_{T_1})k^2 + i(\mu_{T_2} - \mu_{T_1})k} \\
&= \left(1 + \delta\mathbf{f}_{T_2} \cdot \mathbf{V}_{T_2}^{-1}\mathbf{d}_{k,T_2} - \delta\mathbf{f}_{T_1} \cdot \mathbf{V}_{T_1}^{-1}\mathbf{d}_{k,T_1}\right) e^{-\frac{1}{2}\Delta\Sigma k^2 + i\Delta\mu k},
\end{aligned}$$

where

$$\begin{aligned}
\Delta\Sigma &= \sigma_{02}^2 T_{02} - \sigma_{01}^2 T_{01} \\
&:= \sigma_{12}^2 T_{12}
\end{aligned}$$

$$\begin{aligned}
\Delta\mu &= (r_d^{02} - r_f^{02} - \frac{1}{2}\sigma_{02}^2)T_{02} - (r_d^{02-} r_f^{02} - \frac{1}{2}\sigma_{01}^2)T_{01} \\
&:= (r_d^{12} - r_f^{12} - \frac{1}{2}\sigma_{12}^2)T_{12}
\end{aligned}$$

Now we can apply the inverse Fourier transform to obtain an expression for the transition density G as function of $x = log(S_2) - log(S_1)$. For this, first rewrite $\mathbf{d}_{k,T}$ in terms of volatility derivatives. Note that we have

$$\begin{aligned}
\frac{\partial}{\partial\sigma_{02}} e^{-\frac{1}{2}\Delta\Sigma k^2 + i\Delta\mu k} &= (-\sigma_{02}T_{02}k^2 - ik\sigma_{02}T_{02}) e^{-\frac{1}{2}\Delta\Sigma k^2 + i\Delta\mu k} \\
\frac{\partial^2}{\partial\sigma_{02}^2} e^{-\frac{1}{2}\Delta\Sigma k^2 + i\Delta\mu k} &= \left[(-T_{02}k^2 - ikT_{02}) + (-\sigma_{02}T_{02}k^2 - ik\sigma_{02}T_{02})^2\right] e^{-\frac{1}{2}\Delta\Sigma k^2 + i\Delta\mu k}
\end{aligned}$$

so that we have

$$\mathbf{d}_{k,T_2} = \begin{pmatrix} -\sigma_{02}T_2k^2 - ik\sigma_{02}T_2 \\ (-\sigma_{02}T_2k^2 - ik\sigma_{02}T_2)^2 - T_2k^2 - ikT_2 \\ \frac{ik}{S_0}\left(-\sigma_{02}T_2k^2 - ik\sigma_{02}T_2\right) \end{pmatrix} = \begin{pmatrix} \frac{\partial}{\partial\sigma_{02}} \\ \frac{\partial^2}{\partial\sigma_{02}^2} \\ \frac{ik}{S_0}\frac{\partial}{\partial\sigma_{02}} \end{pmatrix}$$

For $\mathbf{d}_{k,T_1}$ we can do the same, this results in

$$\mathbf{d}_{k,T_1} = \begin{pmatrix} -\sigma_{01}T_1k^2 - ik\sigma_{01}T_1 \\ (-\sigma_{01}T_1k^2 - ik\sigma_{01}T_1)^2 - T_1k^2 - ikT_1 \\ \frac{ik}{S_0}\left(-\sigma_{01}T_1k^2 - ik\sigma_{01}T_1\right) \end{pmatrix} = \begin{pmatrix} -\frac{\partial}{\partial\sigma_{01}} \\ \frac{\partial^2}{\partial\sigma_{01}^2} - \frac{2}{\sigma_{01}\frac{\partial}{\partial\sigma_{01}}} \\ -\frac{ik}{S_0}\frac{\partial}{\partial\sigma_{01}} \end{pmatrix}$$

Further, remember that $-ik\hat{f}(k)$ is the Fourier transform of $\frac{df(x)}{dx}$ (this can be verified with partial integration). Then the inverse Fourier transform is given by

$$G(x) = \left(1 + \delta\mathbf{f}_{T_2} \cdot \mathbf{V}_{T_2}^{-1}\hat{\mathbf{d}}_{\sigma_{02}} - \delta\mathbf{f}_{T_1} \cdot \mathbf{V}_{T_1}^{-1}\hat{\mathbf{d}}_{\sigma_{01}}\right) \frac{1}{\sqrt{2\pi\Delta\Sigma}} e^{-\frac{1}{2\Delta\Sigma}(x-\Delta\mu)^2},$$

where we now have

$$\hat{\mathbf{d}}_{\sigma_{01}} = \begin{pmatrix} -\frac{\partial}{\partial\sigma_{01}} \\ \frac{\partial^2}{\partial\sigma_{01}^2} - \frac{2}{\sigma_{01}\frac{\partial}{\partial\sigma_{01}}} \\ \frac{1}{S_0}\frac{\partial}{\partial\sigma_{01}}\frac{\partial}{\partial x} \end{pmatrix} \qquad \hat{\mathbf{d}}_{\sigma_{02}} = \begin{pmatrix} \frac{\partial}{\partial\sigma_{02}} \\ \frac{\partial^2}{\partial\sigma_{02}^2} \\ -\frac{1}{S_0}\frac{\partial}{\partial\sigma_{02}}\frac{\partial}{\partial x} \end{pmatrix}$$

Or, in terms of call option prices,

$$C(S_1, T_1; K, T_2, \sigma_{12}(\Delta)) = \left(1 + \delta\mathbf{f}_{T_2} \cdot \mathbf{V}_{T_2}^{-1}\hat{\mathbf{d}}_{\sigma_{02}} - \delta\mathbf{f}_{T_1} \cdot \mathbf{V}_{T_1}^{-1}\hat{\mathbf{d}}_{\sigma_{01}}\right) C(S_1, T_1; K, T_2, \sigma_{12}) \quad (7.19)$$

$$\sigma_{12} = \sqrt{\frac{\sigma_{02}^2 T_2 - \sigma_{01}^2 T_1}{T_2 - T_1}}.$$

7.6 Option price calculation

We will start with the forward start option. Suppose we have a forward start call option with fixing date T_1 and expiry T_2, and strike $K = K(S_{T_1})$.

When we we use the sticky delta model, the forward volatility is a function of Δ. This means that the forward volatility depends on $log\left(\frac{S_{T_1}}{K}\right)$:

$$\sigma_{12} = \sigma_{12}\left(log\left(\frac{S_{T_1}}{K(S_{T_1})}\right)\right).$$

Therefore, when the strike is given in relative terms, $K = \alpha S_{T_1}$, the forward volatility is independent of the spot at time T and we can use the formula that was derived in section 2.7,

$$FS(S, 0) = SC_{BS}(1, T_1; \alpha, T_2; \sigma_{12}),$$

where $FS(S_0, 0)$ is the price of the forward start option at time zero and for spot S_0. We calculate σ_{12} according to the sticky delta forward smile model, equation (7.19).

On the other hand, when we use the sticky strike model, the forward volatility is a function of the strike. For our forward start option this means that the forward volatility is a function of the spot level at time T_1,

$$\sigma_{12} = \sigma_{12}(K) = \sigma_{12}(S_{T_1}).$$

Because of this dependence we cannot use the formula as above. Instead, we can obtain our option price by calculating an integral,

$$FS(S_0, 0) = e^{-r_d T_1}\int_0^\infty C_{BS}(s_1, T_1; K = \alpha s_1, \sigma_{12}(\alpha s_1))\,\rho_{S_{T_1}}(s_1)ds_1.$$

We calculate the forward volatility according to the sticky strike forward smile model, i.e., equation (7.16). Further, the density of S_{T_1} is given by equation (7.12).

We can also use this formula in case the strike is given in absolute terms, $K = \alpha + S_{T_1}$, in the sticky strike as well as the sticky delta model.

The value CC of a call on a call compound option with expiry T_1 and strike K_1 on an underlying option with expiry T_2 and strike K_2 can also be obtained by evaluating an integral:

$$CC(S_0, 0) = e^{-r_d T_1} \int_{s*}^{\infty} [C(s_1, T_1; K_2, T_2; \sigma_{12}) - K_1] \, \rho_{S_{T_1}}(s_1) ds_1$$

where σ_{12} is calculated from the forward smile model. Here $s*$ is the critical asset price such that the underlying option value at T_1 is larger than K_1.

Part III

Model Comparison

Chapter 8

Pricing Results: a Model Comparison

8.1 Outline

We have seen various different models that can be used to price options in the FX market. In this chapter, we will perform a price comparison of these models, applied to two types of exotic options: the compound option and the forward start option. We will perform tests for two currency pairs: EUR/USD and USD/JPY. As these markets may display very different smiles, the results for the models may also be different for the two markets.

In section 9.2 the market data is given that will be used in the tests. We will start the comparison by specifying a specific compound and forward start contract and compare the model prices. These contracts will serve as our 'base case'. After that, we will perform different tests, varying some specific element of the contract and keeping the other contract specifications constant (equal to the values of our base case), to see the effect of these changes. We will also compare the greeks for the base case. (...)

8.2 Market Data

First we note that in this chapter we will make use of the following shorthand notation:

- LV model = Local volatility model
- dVdS model = dVdVdVdS model
- SS model = Forward smile sticky strike model
- SD model = Forward smile sticky delta model
- SV model = Stochastic volatility model with $\alpha = \beta = 0$
- SVSD model = Stochastic volatility smile dynamics model

Currency Pair	EUR/USD
Spot	1.2668 (USD)

Volatility Quotes (in %)			
Maturity	**ATM**	**RR25**	**STR25**
1 day	5.25	0.00	0.13
1 week	7.10	0.00	0.13
2 weeks	7.65	0.00	0.13
3 weeks	7.55	0.10	0.13
1 month	7.55	0.15	0.13
2 months	7.90	0.23	0.13
3 months	8.05	0.30	0.13
6 months	8.35	0.35	0.13
1 year	8.70	0.38	0.15

Currency Pair	USD/JPY
Spot	116.75 (JPY)

Volatility Quotes (in %)			
Maturity	**ATM**	**RR25**	**STR25**
1 day	4.75	-1.00	0.14
1 week	7.15	-1.00	0.15
2 weeks	8.00	-1.00	0.15
1 month	7.85	-0.85	0.15
2 months	8.03	-0.90	0.15
3 months	8.15	-0.95	0.16
6 months	8.20	-1.05	0.18
1 year	8.30	-1.35	0.21

Table 8.1: Volatility Quotes for currency pairs EUR/USD (left) and USD/JPY (right).

Interest Rates (in %)							
CCY	**1w**	**1m**	**2m**	**3m**	**6m**	**9m**	**1y**
EUR	3.09	3.11	3.24	3.30	3.49	3.60	3.66
USD	5.34	5.35	5.37	5.39	5.39	5.35	5.28
JPY	0.32	0.33	0.35	0.39	0.45	0.51	0.57

Table 8.2: Interest Rates for all currencies.

Barrier Options Currency Pair EUR/USD					
Barrier	**Maturity**	**put/call**	**Strike (USD)**	**Trigger (USD)**	**Market price** (bp)
1	3 months	call	1.27	1.24	179.2
2	3 months	put	1.27	1.30	157.2
3	6 months	call	1.28	1.25	144.6
4	6 months	put	1.28	1.29	157.5
5	1 year	call	1.30	1.25	142.1
6	1 year	put	1.25	1.30	150.0

Table 8.3: Barrier Options for the EUR/USD currency pair (Date 08-09-2006).

Barrier Options Currency Pair USD/JPY					
Barrier	**Maturity**	**put/call**	**Strike (JPY)**	**Trigger (JPY)**	**Market price**
1	3 months	call	115	112	1.916
2	3 months	put	115	120	1.603
3	6 months	call	115	110	1.970
4	6 months	put	110	125	1.224
5	1 year	call	115	110	1.722
6	1 year	put	110	118	1.187

Table 8.4: Barrier Options for the USD/JPY currency pair (Date 08-09-2006).

Before we can start our price comparison, we need to get the market data. We use market data of 08/09/2006. This includes the spot, the domestic and foreign rates, the volatility quotes, and also barrier option market prices[1] are needed in order to perform the calibration of the SVSD model.

In table 8.1 the spot and the volatility quotes are displayed for the USD/JPY currency pair. Table 8.2 contains the rates. From the quotes stated below, a volatility surface can be constructed by using an interpolation technique. For this, a cubic spline interpolation is used.

8.2.1 Market Volatility Surface

In figures 8.1 and 8.2 we show the volatility surface for the EUR/USD market and USD/JPY market respectively, for maturities from December 8, 2006 up to December 8, 2008.

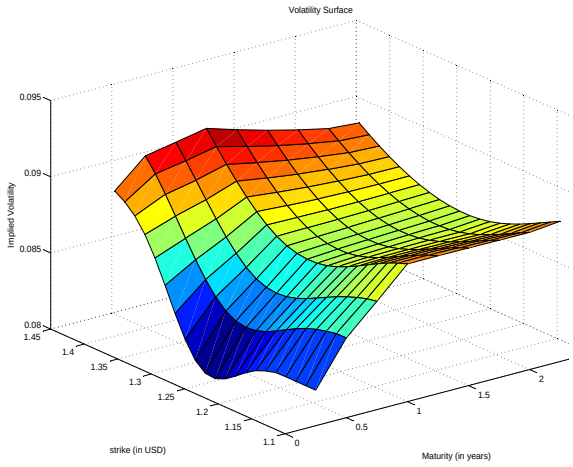

Figure 8.1: EUR/USD Volatility Surface.

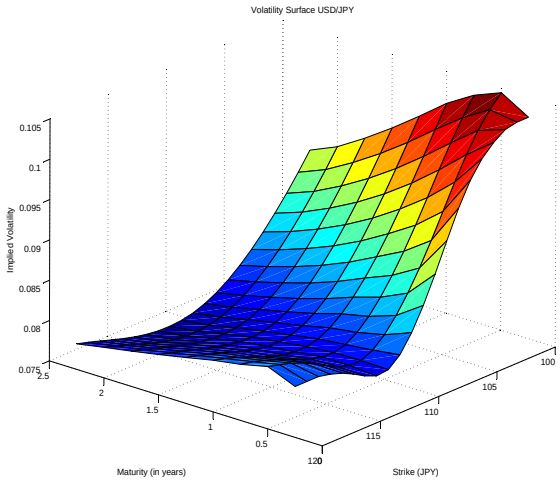

Figure 8.2: USD/JPY Volatility Surface.

8.2.2 Local Volatility Surface

The local volatility surfaces are shown in figures 8.3 and 8.4. We observe that the local volatility surface is indeed very different from the implied volatility surface.

8.3 Base Case

We start our price comparison for a base case. The contracts for the compound option and the forward start option are specified in tables 8.5 and 8.6. The compound option has a maturity

[1] Because we were not able to get real market data, the barrier option market prices are obtained from the ABN Amro program Goldfish. Goldfish also uses an underlying model to compute the option price. However, these prices are checked on a regular basis to see if they match the market prices. It gives a good approximation to the real price.

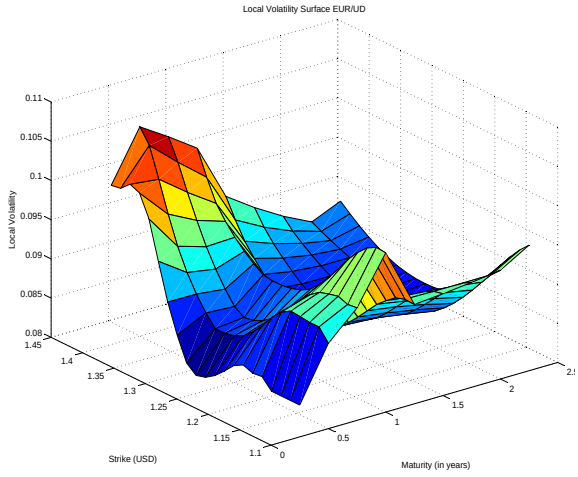

Figure 8.3: EUR/USD Local Volatility Surface.

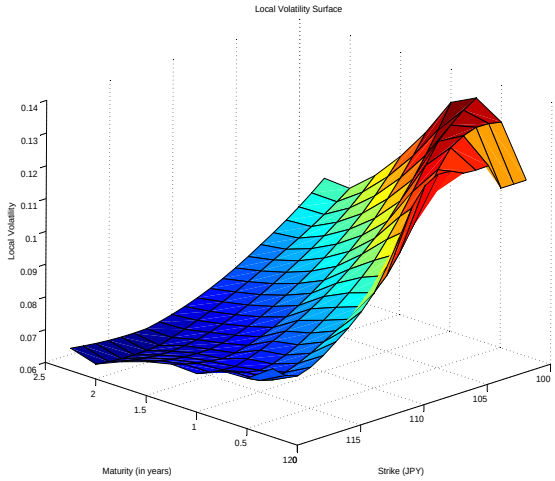

Figure 8.4: USD/JPY Local Volatility Surface.

of six months, the underlying option has a maturity of one year. The strike of the underlying is chosen to be the ATM strike as defined in section 3.6, for the maturity of the underlying. The strike of the compound option is specified as a certain percentage of the spot level. For the forward start option we have the same expiries: the fixing date is at 6 months, the option expiry at one year. We choose a relative strike such that the strike is equal to the spot at the current time, i.e., $\alpha = 1.0$.

Specifications Compound Contract			
	put/call		Call-on-Call
	Maturity	T_1	6 months
	Maturity underlying	T_2	1 year
EUR/USD	Strike	$K_1 = 3\%S_0$	0.038 (USD)
	Strike underlying	$K_2 = K_{ATM,T_2}$	1.29 (USD)
USD/JPY	Strike	$K_1 = 5\%S_0$	5.84 (JPY)
	Strike underlying	$K_2 = K_{ATM,T_2}$	111.1 (JPY)

Table 8.5: Base case for the compound option.

Specifications Forward Start Contract		
put/call		Call
Fixing Date	T_1	6 months
Maturity	T_2	1 year
Strike Type	$K = \alpha S_{T_1}$	Relative
Relative Strike	α	1.0

Table 8.6: Base case for the forward start option.

First we will calculate the price for these contract specifications for all models and analyze the results. We will also compare the values of the greeks for the base case. After that, we will vary certain quantities, keeping the other elements fixed, so that we can see the effect it has on the option price in the different models. We restrict ourselves to the case of T_1 equal to 6 months, T_2 equal to 1 year. For the compound option, we will use different strike values. For the forward start option, we will vary the value of α.

8.4 SVSD Model: Calibration Results

The SVSD Model has to be fitted to the market data to obtain the model parameters. The calibration consists of fitting the market smile, and fitting barrier prices.

Since both the compound and the forward start option depend on two maturities only, it seems enough to calibrate the model to vanilla quotes for the same two maturities, that is, six months and one year. So, the model parameters m, ξ and ρ have the following form:

$$m(t) = \begin{cases} m_1 & t \leq T_1 \\ m_2 & T_1 < t \leq T_2 \end{cases}$$

and similar expressions for the other parameters.

For the barrier calibration we use four barrier options: two down-and-out call options and two up-and-out put options, with the maturities that are used for the vanilla calibration. For the base case, this means that we use the barrier options that can be found in entries 5, 6, 7 and 8 of tables 8.3 and 8.4. The calibration results are given in table 8.7.

Besides the SVSD model, we also include a pure stochastic volatility model in our comparison; this is the SVSD model with α and β set to zero. This models therefore needs to be calibrated to vanilla quotes only. We can do this for the EUR/USD market as well as for the USD/JPY market. The SV-model parameters are also given in table 8.7.

Model Parameters Currency Pair EUR/USD								
	ξ_1	ξ_2	ρ_1	ρ_2	m_1	m_2	α	β
SVSD model	1.2775	1.2974	0.1902	0.3485	0.0805	0.0862	-0.60	5.00
SV model	1.3740	1.7533	0.1153	0.1224	0.0802	0.0816	0.0	0.0

Model Parameters Currency Pair USD/JPY								
	ξ_1	ξ_2	ρ_1	ρ_2	m_1	m_2	α	β
SVSD model	1.5072	1.8993	-0.3875	-0.5847	0.0787	0.0741	0.36	6.78
SV model	1.6115	2.2469	-0.3260	-0.4715	0.0784	0.0714	0.0	0.0

Table 8.7: Calibration results: model parameters for the SVSD model and SV model.

In chapter 5 it has been said that there are two parameters affecting the strangle, ξ and β, and two parameters affecting the risk reversal, ρ and α. We can see this also in the values of the calibrated parameters. In the EUR/USD-SVSD model β is equal to 5.0, in the SV model it is zero. Therefore the value of ξ is lower in the SVSD model than in the SV model. For the risk reversal, the correlation parameter ρ is in this case higher for the SVSD model than for the SV model; this is because the SVSD model calibrated to a negative value for α, which has to be compensated with a higher correlation (compared to the SV model) in order to match the smile. For the USD/JPY market we observe similar behavior.

In the USD/JPY market we find a negative correlation. This negative correlation creates the skew in the USD/JPY smile: decreasing implied volatility as function of strike. The correlation in the USD/JPY market is (in absolute value) larger than in the EUR/USD market, because as said the USD/JPY market is more skewed than the EUR/USD market. The same holds for the strangle: the value of ξ is larger in the USD/JPY market.

As said, a good model should be able to capture the market behavior. The SVSD model is set up to capture both the smile and its dynamics. In chapter 3 empirical market observations have been stated. Two important observations regarding the smile dynamics are repeated:

- **Observation 1**: spot and risk reversal are positively correlated.

- **Observation 2**: spot and ATM are correlated. This correlation may be positive or negative. The sign of the risk reversal is observed to be a good indication of the sign of the correlation between spot and ATM.

The positive value of β implies that $\frac{\partial RR}{\partial S} > 0$, so we have a positive correlation between spot and risk reversal. This is what we would expect, as it is in line with empirical observation 1. We will also see this in the next section.

The shape of the smile is determined by the values of the parameters m, ξ and ρ, and also α and β. The smile dynamics are determined by β for the dynamics of the risk reversal, and α and ρ for the correlation between spot and risk reversal. We can see that these two parameters have different signs: α is negative while ρ is positive. Because the parameters are chosen so that they match the smile, this implies that the negative value of α is compensated by ρ, the net effect of the two matches the market risk reversal. Based on empirical observation 2 we expect spot and ATM to be positively correlated in the EUR/USD market, $\frac{\partial \sigma_{ATM}}{\partial S}$. The negative value of α implies a decrease in ATM when spot rises, the positive value of ρ implies an increase in ATM.

8.5 Market Smiles and Model Smiles

In this section we will take a look at the smiles that are implied by each model. In the first subsection, plots will be presented of the one year smile given by the models. The plots also show what the smile looks like for a higher than initial spot level. In section 8.5.2 we will show a number of plots of the forward smile. In the third subsection we will look at the smile dynamics; in particular, the dynamics that are needed to calculate the compound and forward start option prices for the base case.

8.5.1 Smiles and Smile Dynamics

First it is interesting to see the market smiles for maturities T_1 and T_2. These smiles are plotted in figures 8.5 and 8.6. The figures show that the USD/JPY smile is much more skewed than the EUR/USD smile: the minimum in the USD/JPY market is around 7.5%, the maximum around a value of 10.6%; on the other hand, the EUR/USD market shows a minimum value around 8.3% and a maximum value of 9.3%. This can also be seen from the table 8.1. The 6 months risk reversal for the USD/JPY market is -1.05%, while the 6 months risk reversal for the EUR/USD market is equal to 0.38%. Also the strangles in the USD/JPY market are higher than in the EUR/USD market, 0.18% and 0.13% respectively.

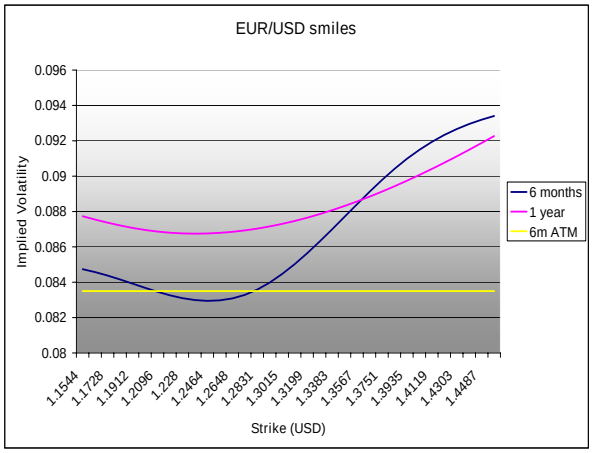

Figure 8.5: EUR/USD market smiles for 6 months and 1 year maturities.

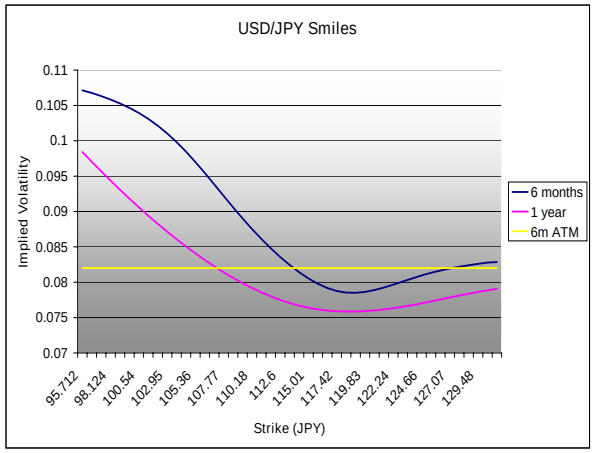

Figure 8.6: USD/JPY market smiles for 6 months and 1 year maturities.

For six months expiry we have also included the at-the-money volatility. Obviously, using a flat volatility would give incorrect results for vanilla options. In the EUR/USD market, high strike options are underpriced with the Black-Scholes model; in the USD/JPY market, low strike options are underpriced with the Black-Scholes model.

In figures 8.7 and 8.8 the model implied smile dynamics are shown, i.e. the smile that the (calibrated) models predict for a higher than initial spot level (keeping all other variables constant). We also plot the initial smile, so that we can see the change compared to the initial smile. The

model implied smile is calculated as follows. For a fixed strike, we can calculate the price of a call option using a specific model. By setting this value equal to the Black-Scholes value of a call option, and solving for the volatility, we obtain the model implied volatility. So, it is the solution σ_{imp} of

$$C_{model} = C_{BS}(S, t; K, T; \sigma_{imp}).$$

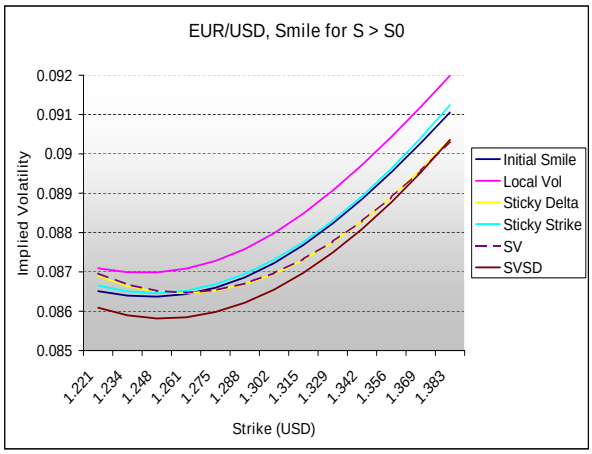

Figure 8.7: EUR/USD Model implied smiles for an increase in spot from $S = 1.267$ to $S = 1.28$.

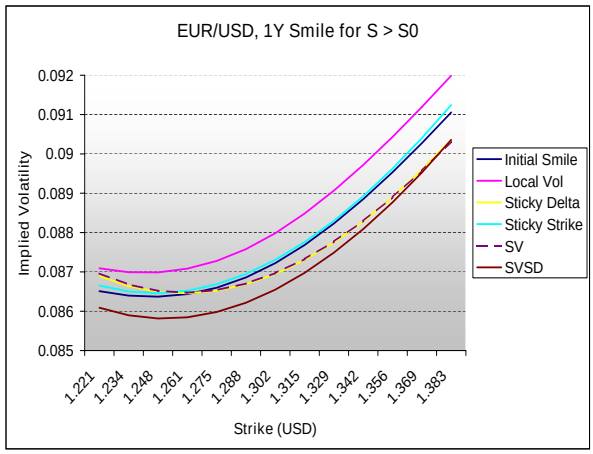

Figure 8.8: USD/JPY Model implied smiles for an increase in spot from $S = 116.7$ to $S = 118$.

From chapter 7 we know that from the Forward Smile Model we can obtain the transition density (or the implied forward volatility). We have obtained the initial smile by setting T_1 equal to one day, and T_2 equal to six months.

For the dVdVdVdS model we have not included a model implied smile, because this does not provide relevant information.

EUR/USD market

Let us first consider the EUR/USD market. The initial spot level is $S = 1.2668$. The ATM strike for a maturity of one year is equal to $K_{ATM} = 1.292$. The plot shows the smiles in case the spot has increased to $S = 1.28$. The new ATM strike is $K_{ATM} = 1.306$.

Pure stochastic volatility models display sticky delta behavior, and we can see that the SV model and sticky delta model have the same dynamics. The SV model also has a correlation parameter, but we do not see the effect of this parameter in this plot (we show the smile for a different spot, but the same calibrated parameter for the volatility, σ_0). For the SV and the sticky delta model, the ATM has not changed in the new situation. (Keep in mind though, that in future realizations this correlation in the SV model does impact the smile; with higher smile levels when spot levels are higher.)

The SVSD model has a lower than initial ATM, which is caused by the negative value of α; this was discussed in the previous subsection (again, in future realizations the smile level will be higher because we have a positive correlation). The smile of the sticky strike model stays the same. Therefore, the ATM does change. For the ATM strike K_{ATM} we find that the ATM in the sticky strike model increases. Finally, for the local volatility model the ATM also increases. The increase in ATM is larger than for the sticky strike model. We can see what was discussed in the literature review in chapter 4: the dynamics of the local volatility model is opposite to the market behavior (the smile shifts to the left), resulting in too extreme dynamics.

To see what happens to the risk reversal it is best to consider each model separately, by plotting the *model implied initial smile* - instead of the initial *market* smile - together with the model implied smile for a higher than initial spot. The 25-delta call and put strikes are given by:

- initial state: $K_{25\Delta-call} = 1.222, \quad K_{25\Delta-put} = 1.370$
- new state: $K_{25\Delta-call} = 1.235, \quad K_{25\Delta-put} = 1.385$

To save space we have included these figures in the Appendix only (see Appendix A).

Then we see that the risk reversal remains unchanged for the sticky delta model and for the SV model, this was already discussed in earlier chapters. When the correlation in the SV model is also taken into account, the smile would be at a higher level, but this has no impact on the risk reversal. For the SVSD model we can see that $\sigma_{25\Delta P}$ decreases, and $\sigma_{25\Delta C}$ increases slightly. Therefore $RR = \sigma_{25\Delta C} - \sigma_{25\Delta P}$ gets higher, and this is exactly what we want. For the local volatility model both $\sigma_{25\Delta P}$ and $\sigma_{25\Delta C}$ increase, but the change is larger for the latter. Therefore, also in the LV model we observe an increase in risk reversal (which is larger than in the SVSD model). Finally we also see an increase in risk reversal for the sticky strike model.

USD/JPY market

Next, consider the USD/JPY market. We have an initial spot level of $S = 116.75$, and the ATM strike is $K_{ATM} = 111.1$. The smiles in figure 8.8 correspond to a spot level equal to $S = 118.0$; the corresponding ATM strike is $K_{ATM} = 112.2$.

The SV and sticky delta model have the same ATM in the new state, which is equal to the ATM value in the initial state: this is the sticky delta behavior. The SV model implied smile is not exactly the same as the sticky delta smile; this is because the models do not have exactly the same fit to the initial smile, see figure 8.9.

We also observe that the SVSD model is almost exactly equal to the SV model. The ATM for this model also remains the same. But since the correlation is higher (in absolute terms) for the SVSD model, including the correlation will expectedly lead to a lower smile than the SV model.

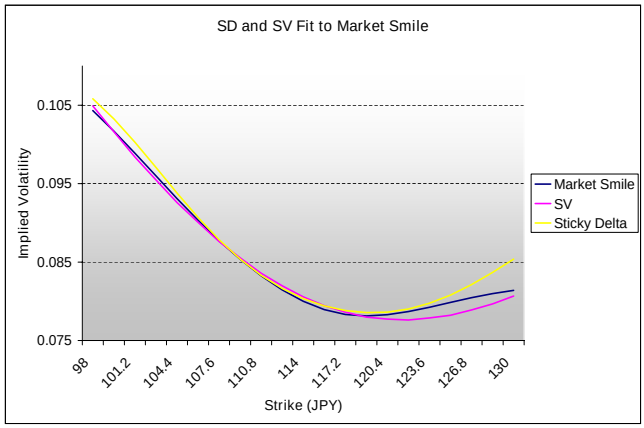

Figure 8.9: Fit of the Sticky Delta model and the SV model to the market smile.

In the sticky strike model and the local volatility model, the ATM decreases; as expected, this decrease is the largest for the local volatility model.

Based on the empirical observations, we would expect the ATM to decrease for increasing spot (empirical observation 2). From these plots we cannot tell which model is the best, since the LV, SS, SV and SVSD model all correspond to this behavior. We do know that the sticky delta model is probably the least suited model as its dynamics does not correspond to what we expect based on empirical observation 2. For increasing spot, the SD model implies the same ATM.

To compare the changes in risk reversal we refer to the plots in Appendix A. The 25-delta call and put strikes are given by:

- initial state: $K_{25\Delta-call} = 117.1, \quad K_{25\Delta-put} = 105.2$
- new state: $K_{25\Delta-call} = 118.3, \quad K_{25\Delta-put} = 106.2$

Obviously, the risk reversals remain unchanged in the sticky delta model and in the SV model. In the SVSD model there is only a very small increase in risk reversal (it becomes slightly less negative). For the sticky strike and LV model the risk reversal increases, the largest increase for the LV model.

8.5.2 Model Implied Forward Smiles

The price of compound and forward start options depend on the forward volatility. With the usual notation, the value CC of a call-on-call compound option is given by

$$CC(S,t) \quad = \quad e^{-r_d T_1} \int_{S^*}^{\infty} \left[C_{BS}(s, T_1; K_2, T_2; \sigma_{12}) - K_1 \right] \rho_{S_{T_1}}(s) ds. \tag{8.1}$$

The value FS of a forward start option is given by

$$FS(S,t) \quad = \quad e^{-r_d T_1} \int_0^\infty C_{BS}(s, T_1; K = \alpha s, T_2; \sigma_{12}) \rho_{S_{T_1}}(s) ds. \tag{8.2}$$

In these expressions σ_{12} denotes the model implied forward volatility. For example, consider the local volatility model. For a fixed strike we can calculate the value of a call option with time to maturity $T_2 - T_1$, conditional on a certain spot level at T_1. The model implied forward volatility is found by setting the calculated value equal to the Black-Scholes value of a call option with time to maturity $T_2 - T_1$, with the same strike and conditional on the same spot. Solving the expression for the volatility gives us the forward implied volatility. So, it is the solution σ_{12} of

$$C_{LV}(S, T_1) \quad = \quad C_{BS}(S, T_1; K, T_2; \sigma_{12}),$$

where C_{LV} is the value of the call option using the local volatility model. Repeating this procedure for a range of strikes enables us to look at the model implied forward smiles.

For the SV and SVSD model we have an extra state variable, the volatility. So, if we want to construct the forward model implied smile for these models, we condition on the spot as well as on the volatility at time T_1. This does make it more difficult to compare the forward smiles of the different models. Conditioning on higher volatilities results in higher smiles, but we have to keep in mind that spot and volatility are correlated. First we show the implied forward smiles for the SV and SVSD model separately, assuming different volatility levels at T_1. This is shown in figures 8.10 and 8.11. Next, figures 8.12 to 8.15 show the model implied forward smiles for the different models, conditional on spot. For the SV and SVSD model, we condition on both spot and volatility. For the SVSD model we also show the impact of assuming a higher volatility level.

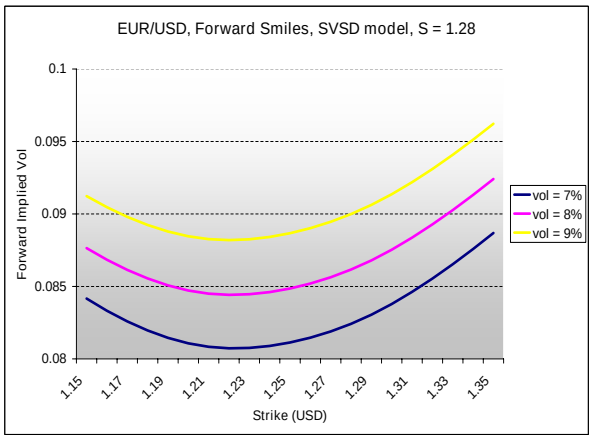

Figure 8.10: EUR/USD Forward Smiles for the SVSD model, conditional on different volatility levels.

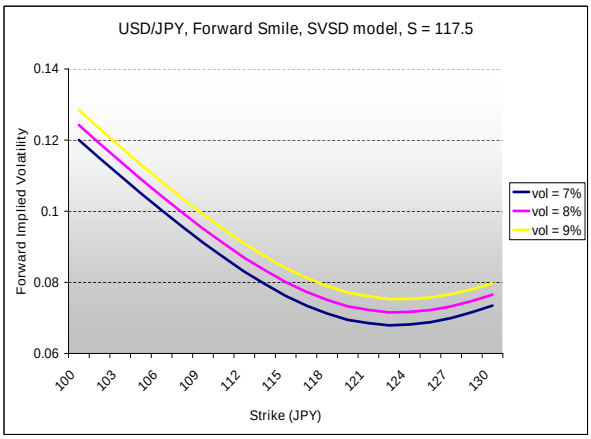

Figure 8.11: USD/JPY Forward Smiles for the SVSD model, conditional on different volatility levels.

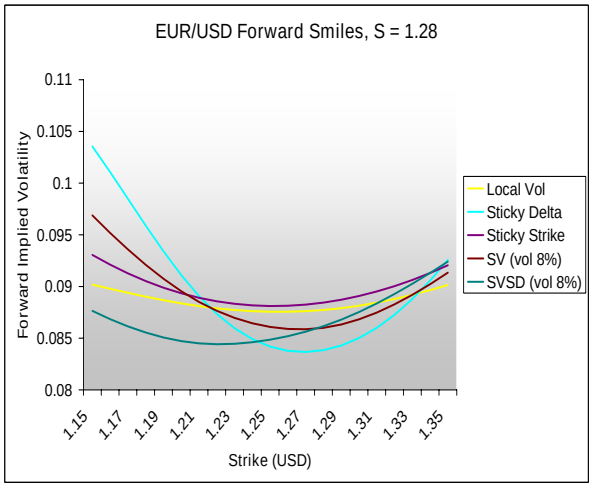

Figure 8.12: EUR/USD Forward Smiles for $S_{T_1} = 1.28$.

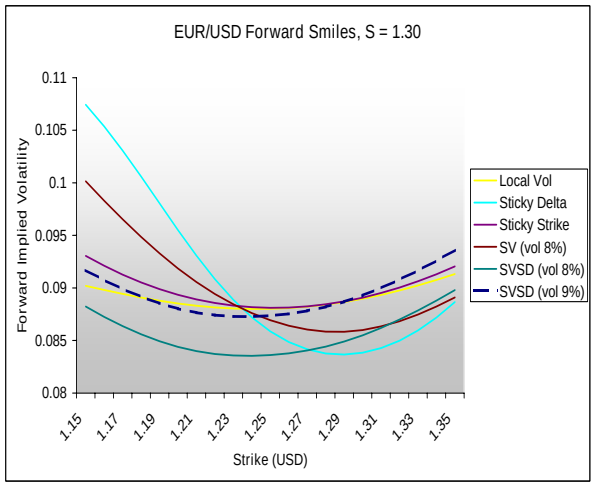

Figure 8.13: EUR/USD Forward Smiles for $S_{T_1} = 1.32$.

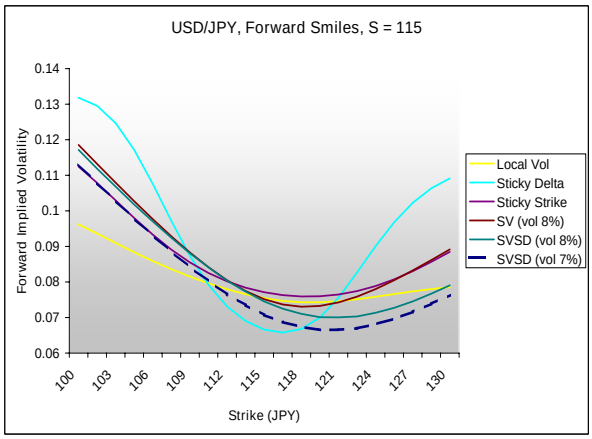

Figure 8.14: USD/JPY Forward Smiles for $S_{T_1} = 115$.

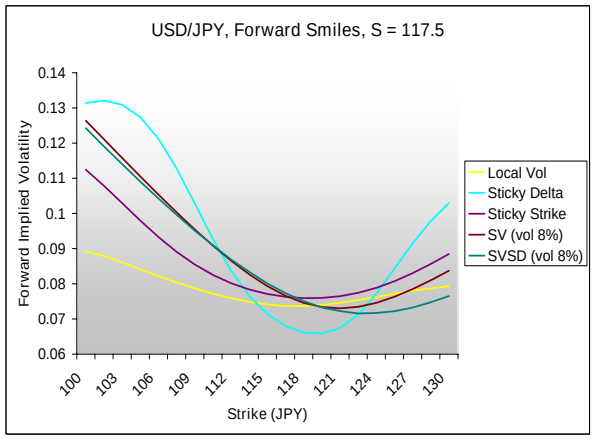

Figure 8.15: USD/JPY Forward Smiles for $S_{T_1} = 117.5$.

We observe that the sticky delta model implies a forward smile that is more extreme (more curved) than the other models, in all cases. By contrast, the local volatility model shows the 'least extreme' smiles, resulting in the flattest smile.

8.5.3 Smile Dynamics

From equations (8.1) and (8.2) we can see that the value of the compound and forward start options are dependent on the smile dynamics. We have to calculate an integral for a range of spot values at T_1. The smile dynamics are implied by the forward volatility that a certain model calculates for different spot values.

We will start with the compound option with its underlying strike K_2. To see what smile dynamics each model implies, we can plot the model implied forward volatility as a function of the spot level at T_1. This is not the smile, since we keep the strike K_2 fixed. So it does not present

the dynamics of the whole smile, but only for one specific strike value. This way we can see the implied forward volatility σ_{12}, for a range of spot values. This is shown in figures 8.16 and 8.17 for the EUR/USD and USD/JPY market respectively. In these figures, we display the smile dynamics for all the models. In this way we can see the difference in smile dynamics that each model implies.

We have not included the dVdS model, because it provides no information. We can calculate the value of a call option at T_1 for a range of spot levels, but this is not used in the calculation of the compound option value (this value is determined by the at-the-money Black-Scholes value of a compound option, plus the smile correction).

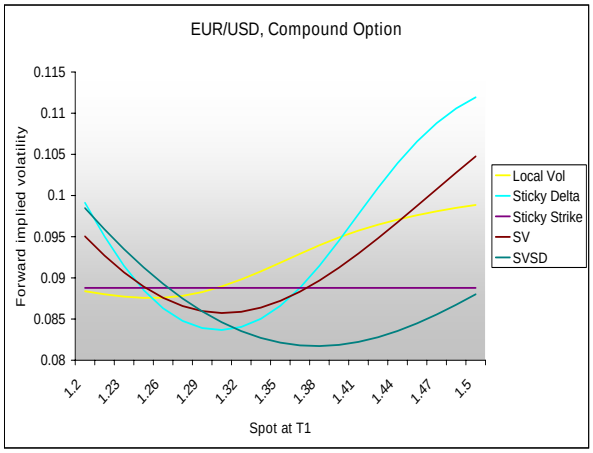

Figure 8.16: EUR/USD 'Compound Option Smile Dynamics': Model implied volatility for a fixed strike, conditional on a range of spot levels.

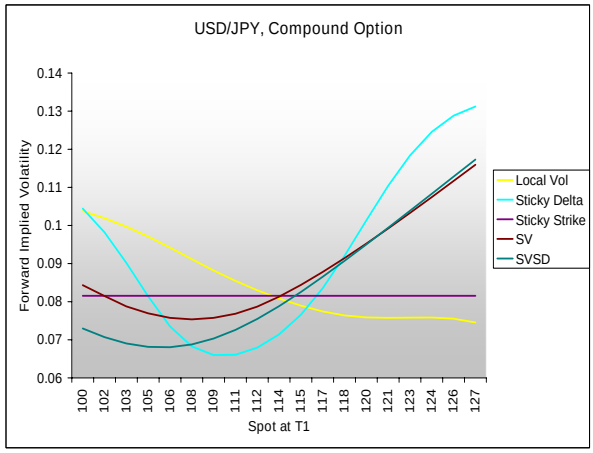

Figure 8.17: USD/JPY 'Compound Option Smile Dynamics': Model implied volatility for a fixed strike, conditional on a range of spot levels.

From these figures we can make a number of expectations with respect to the compound prices. The models match the vanilla smile. Therefore, the models should result in the same probability density function for the spot at T_1. This implies that the difference between the model prices result from the difference in implied smile dynamics, see equations (8.1) and (8.2).

For the compound option, the integral is calculated over the region $[S^*, \infty]$, where S^* is the critical asset value such that the call value of the underlying option is above the strike K_1. The value of S^* also depends on the forward volatility, so it takes on a different value in each model. To get an idea of the value of the critical asset value one can calculate this using the Black-Scholes model. In the EUR/USD market, this value is then given by $S^* = 1.29$, in the USD/JPY market this value is given by $S^* = 118$, so in both cases this critical asset value is just above the current spot level. Therefore, only spot values at T_1 on the right half of the plots in figures 8.16 and 8.17 are important. Besides this, we know that the values close to this critical asset value are most important in determining the price, as the density for large spot values is smaller.

We see that the models imply different dynamics. The difference between the models is larger in the USD/JPY market. Therefore, we expect to see larger difference for the compound prices in this market. In making the plots for the SV and SVSD model, we have assumed the same volatility of 8% for all spot levels. However, the correlation implies a higher volatility for higher spot levels, and lower volatilities for lower spot levels. Therefore, the true shape of the plot may differ from the one showed.

In the EUR/USD market, we can see that the local volatility model and the sticky strike model are close to each other, both being higher than the other models. Therefore, we expect these two models to give the highest compound option price. In the sticky strike model the forward volatility depends only on the strike, not on the spot level, this explains the horizontal line for the model. The SV model and the SVSD model are close to each other. The sticky delta model calculates the lowest volatility close to S^*, so according to this picture we expect this model to give the lowest price.

In the USD/JPY market, we see that for spot levels above 118 the differences between the models are larger than in the EUR/USD market. The sticky delta model is the highest, so it is expected to give the highest price. The lowest price is expected to be from the local volatility model, followed by the sticky strike model.

Note that the smile dynamics displayed so far are not representative for the forward start option, as the strike of the forward start option depends on the spot at T_1. In the base case we have $K = S_{T_1}$. So, to make the same sort of plot for a forward start option, we have to set the strike equal to the spot in every point. The results are shown in figures 8.18 and 8.19 for the EUR/USD and USD/JPY market, respectively.

In this case, the sticky delta model results in a straight line, the sticky strike model does not. Also the SV model displays a straight line. In the EUR/USD market, this should really be an increasing line (correlation included); in the USD/JPY market we expect it to be a decreasing line. In the EUR/USD market, the sticky delta model implies the lowest volatility; we expect this model to give the lowest price. Either the local volatility or the sticky strike model may give the highest price. Again the differences in the USD/JPY market are larger compared to the EUR/USD market. Clearly, the sticky delta model is expected to give the lowest price. As discussed in the previous subsection, we trust this model the least.

We will refer to these plots and our expectations in the next section in analyzing the pricing results for the base case.

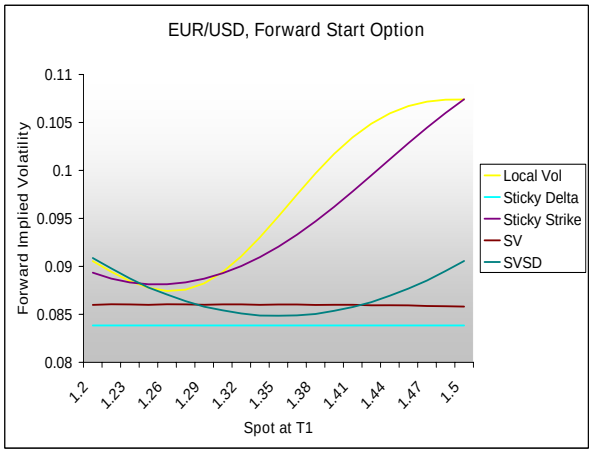

Figure 8.18: EUR/USD 'Forward Start Option Smile Dynamics': Model implied volatility for a fixed strike, conditional on a range of spot levels.

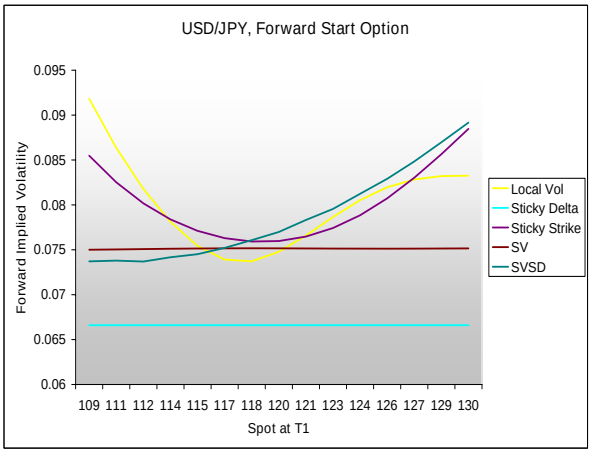

Figure 8.19: USD/JPY 'Forward Start Option Smile Dynamics': Model implied volatility for a fixed strike, conditional on a range of spot levels.

8.6 Price and Greeks

This section discusses the price and greeks for the compound and forward start option in the base case.

8.6.1 Model Prices for the Base Case

The prices of the different models in the base case are given in table 8.6.1. We have included a Black-Scholes value two times: first using the ATM volatility for T_2, and second using the implied volatility for T_2. For the compound option, we use the implied volatility corresponding to K_2, for the forward start option we use the implied volatility corresponding to $K = \alpha S_0$. We calculated the Black-Scholes values using the formulas derived in section 2.7.

OPTION PRICES				
	EUR/USD		USD/JPY	
Model	**Compound**	**Forward Start**	**Compound**	**Forward Start**
BS (ATM)	0.01691	0.03522	0.8277	1.5148
BS (impl)	0.01690	0.03606	0.8254	2.4796
LV	0.01678	0.03467	0.7081	1.3986
dVdS	0.01686	0.02682	0.7823	0.3720
SS	0.01657	0.03567	0.7281	1.5402
SD	0.01635	0.03326	0.8549	1.0834
SV	0.01670	0.03409	0.7951	1.3186
SVSD	0.01637	0.03475	0.7882	1.3552
max abs diff.	5.57 bp	88.5 bp	0.147	2.108
max rel diff.	3.30%	24.82%	17.17%	85.00%

Table 8.8: Price comparison for the base case.

The table shows the prices of the options for the base case in the different models. To see if the models differ from each other a lot, we also show the maximum (absolute[2] and relative) difference between the models. The relative difference is calculated as $\frac{C_{max}-C_{min}}{C_{max}}$. We observe the following:

- In the USD/JPY market, the differences between the models are larger than in the EUR/USD market. We already expected this based on the results of the smile dynamics plots.
- For the forward start option, the dVdS model gives very different pricing results compared to the other models. Especially in the USD/JPY market we see a huge difference.
- In almost all cases the Black-Scholes ATM prices are higher than the model prices, with two exceptions (both exceptions are in the USD/JPY market: for the compound option the SD model gives a higher price, for the forward start option the SS model gives a higher price).

Now we want to see if the smile dynamics plots and the expectations that are based on these plots (discussed in the previous subsection) are in correspondence with the results. We exclude the dVdS values and the Black-Scholes values.

Compound Option

Starting with the EUR/USD compound option, we observe the following:

- The sticky delta model gives the lowest price.
- The highest price is calculated using the local volatility model, after that, the sticky strike model.

Both observations correspond to the expectations stated in the previous section, see figure 8.16.

Next consider the compound option in the USD/JPY market, see figure 8.17. If we put the model prices in order, we get the following result (from highest to lowest price): SD, SV, SVSD, SS, LV. The SV and SVSD values are close to each other. This is in agreement with our expectations. The SV price is a bit higher than the SVSD price; this is probably due to the correlation parameter, which is less negative for the SV model.

Forward Start Option

Now we will analyze the results for the forward start option. In this case, the integral is taken over the full range of spot value at time T_1.

For the forward start option in the EUR/USD market, the price differences are small. The sticky strike model gives the highest price, the sticky delta model the lowest, and the local volatility model, the SV model and the SVSD model are very close to each other. From the smile dynamics plot (figure 8.18) indeed we see that the sticky delta model has the lowest implied volatility. For

[2]In the EUR/USD market, the absolute difference is given in basispoints: 1 bp = 1e-4.

most of the spot values, the local volatility model gives higher volatilities than the sticky strike model. Between S = 1.25 and S = 1.30, the sticky strike model is slightly higher. Since the sticky strike price is higher than the local volatility price, this spot region probably has the highest weights.

The local volatility model does give higher implied volatilities than the SV and the SVSD model, for all spots. However, the local volatility price is approximately the same as the SV and SVSD model prices. This may indicate that the plots for the SV and SVSD model are constructed conditioning on too low volatility values. The lines should probably be higher for both models.

Finally, consider the forward start option dynamics in the USD/JPY market, figure 8.19. The sticky strike model gives the highest price, the sticky delta model the lowest, and the prices of the local volatility model and the SV model result are very close. Looking at the dynamics plots, this again seems reasonable and it is in line with our expected values.

Of course, these results are only for one specific case. In the next section we will present the results for a range of strike prices.

8.6.2 Model Greeks for the Base Case

It is also interesting to look at the greeks that the different models calculate. We concentrate on the delta, gamma and vega. The greeks for both option are presented in tables 8.9 and 8.10 for the compound option and the forward start option respectively.

Compound Option Greeks						
	EUR/USD			**USD/JPY**		
Model	**delta**	**gamma**	**vega**	**delta**	**gamma**	**vega**
BS (ATM)	0.322	4.173	0.194	0.212	0.0405	19.319
BS (impl)	0.321	4.174	0.194	0.212	0.0405	19.301
LV	0.341	5.62	0.377	0.176	0.0499	24.521
dVdS	0.318	5.19	0.371	0.183	0.0554	20.155
SS	0.302	4.36	0.378	0.207	0.0491	25.349
SD	0.304	4.42	0.371	0.231	0.0496	27.079
SV	0.303	4.35	0.116	0.218	0.0482	8.740
SVSD	0.290	4.22	0.115	0.228	0.051	8.856
max diff (abs)	0.051	1.442	0.262	0.057	0.015	18.339
max diff (rel)	15.0%	25.7%	69.4%	24.6%	27.0%	67.7%

Table 8.9: Model greeks for the compound option base case.

Delta

In chapter 3 we have seen that using the correct smile dynamics is important in determining the

Forward Start Option Greeks						
	EUR/USD			USD/JPY		
Model	**delta**	**gamma**	**vega**	**delta**	**gamma**	**vega**
BS (ATM)	0.028	0.0	0.341	0.0130	0.0	29.256
BS (impl)	0.028	0.0	0.341	0.0212	0.0	30.410
LV	0.042	1.161	0.344	-0.0291	0.0234	30.556
dVdS	0.021	-0.152	0.321	0.0031	-0.0006	18.784
SS	0.028	0.000	0.344	0.0132	0.0000	30.159
SD	0.026	0.000	0.340	0.0093	0.0000	28.079
SV	0.027	-0.0134	0.010	0.0124	-0.0001	0.790
SVSD	0.015	0.147	0.015	0.0230	0.0023	1.292
max diff (abs)	92.47 bp	0.0273	1.3129	0.0521	0.0240	29.766
max diff (rel)	25.64%	65.21%	113.08%	226.62%	102.71%	97.41%

Table 8.10: Model greeks for the forward start option base.

right value of the delta. For a call option C:

$$\Delta = \frac{\partial C}{\partial S} + \frac{\partial C}{\partial \sigma_{imp}} \frac{\partial \sigma_{imp}}{\partial S}.$$

In a similar way, the delta of a compound option and of a forward start option also depends on the smile dynamics.

For the EUR/USD market we have the following results, which hold for the compound option as well as the forward start option: the LV model implies opposite dynamic behavior compared to the other models: it calculates a delta value that is higher than the Black-Scholes value, all other models calculate lower values. The lowest delta value is given by the SVSD model.

In the USD/JPY market we observe that the highest delta for the compound option is calculated by the SD model, the lowest delta by the LV model. The LV model, dVdS model and the SS model give lower deltas compared to Black-Scholes, the remaining models higher deltas. For the USD/JPY forward start option, the LV model calculates a negative value for delta. Only the SVSD and dVdS models give delta values that are higher than the Black-Scholes delta.

Gamma

For the compound option in the EUR/USD market, we observe similar model behavior for the gamma values as for the delta values. The lowest gamma value is given by the SVSD model. The LV model and the dVdS model result in gamma values higher than the Black-Scholes gamma. For the compound option in the USD/JPY market, we can see that the Black-Scholes model provides the lowest gamma; the values are higher in all other models.

For the forward start option, the Black-Scholes gamma is equal to zero. In the EUR/USD market, the highest gamma is given by the LV model, the lowest gamma is given by the dVdS model. In the USD/JPY market, the dVdS model results in a negative gamma value, the other

model have positive gamma values. The highest value is given by the LV model.

Vega

It is difficult to compare the vega values of the different models with each other. This is caused by the way these values are calculated. In the SV model and the SVSD model the vegas given by the derivative of the compound price with respect to σ_0, and since both models provide different values for this parameter, we cannot make an exact comparison. In the other models the vega is calculated by shifting the volatility surface:

$$\text{vega} = \frac{CC(S,t;ATM_{up}) - CC(S,t;ATM_{down})}{2\delta ATM}, \tag{8.3}$$

where ATM_{up} means that we shifted the ATM volatility up by an amount of δATM, for all maturities.

Because of these different definitions we see that the SV and SVSD model result in a significant lower vega value than the other models (in both markets and for both options). We have also calculated the vega for the SV model by changing the market values and recalibrating the model, and applying the above relation (8.3). This resulted in a value of vega equal to 0.3778 for the EUR/USD compound option. This indicates that the relation between σ_0 and ATM is not linear.

For the models that calculated the vega in the same way, we see the following. For the compound option the model vega values are higher than the Black-Scholes vegas, both for EUR/USD and USD/JPY. For the forward start option, the vega values resulting from the models are close to the Black-Scholes vega, for EUR/USD and for USD/JPY. In both market, the lowest value is calculated with the dVdS model.

8.7 Strike Influence

In this section we will calculate the model prices for a range of strike prices. For the compound option we vary the underlying strike K_2 as well as the compound strike K_1. For the forward start option we will specify different values for α.

Tables 8.11 and 8.12 show the pricing results for the compound option for varying values of K_1 and K_2, table 8.13 for the forward start option for varying values of α, both in the EUR/USD market. The tables show the prices, and in brackets the rating that we give the model based on its price (1 for the highest price, to 6 for the lowest price). We exclude the Black-Scholes prices from the rating procedure. We do present the prices for these models, so that we can see the impact on the price of using a Black-Scholes model instead of a more 'advanced' model. We repeat this procedure for the USD/JPY market; the results can be found in table 8.14, 8.15 and 8.16.
From the pricing results we can make a few observations. For the EUR/USD market:

Compound Option Value (in bp), EUR/USD						
	Strike K_1 (as percentage of spot)					
Model	1%	2%	3%	4%	5%	6%
BS (ATM)	300.80	225.81	169.11	125.95	93.12	68.25
BS (impl)	300.68	225.70	169.01	125.86	93.04	68.19
LV	299.16 (2)	223.29 (2)	167.78 (2)	126.79 (2)	96.15 (3)	73.02 (4)
dVdS	305.05 (1)	225.60 (1)	168.76 (1)	130.05 (1)	104.0 (1)	86.08 (1)
SS	298.06 (3)	221.52 (3)	165.69 (4)	124.81 (4)	94.69 (5)	72.33 (5)
SD	292.77 (6)	217.15 (6)	163.53 (6)	124.33 (5)	95.18 (4)	73.24 (3)
SV	296.90 (4)	221.48 (4)	166.97 (3)	126.76 (3)	96.79 (2)	74.17 (2)
SVSD	295.47 (5)	218.63 (5)	163.73 (5)	123.77 (6)	94.25 (6)	72.15 (6)
max diff (abs) (bp)	12.28	8.45	5.22	6.29	9.75	13.93
max diff (rel)	4.02 %	3.75 %	3.09 %	4.83 %	9.37 %	16.18 %

Table 8.11: Model prices for varying values of the compound strike K_1 in the EUR/USD market.

Compound Option Value (in bp), EUR/USD							
	Strike K_2						
Model	1.18	1.22	1.26	1.30	1.34	1.38	1.42
BS (ATM)	752.25	484.76	282.41	147.05	67.94	27.75	10.00
BS (impl)	753.12	482.87	280.04	147.77	72.61	34.11	15.55
LV	750.47 (5)	477.93 (3)	275.70 (3)	147.43 (1)	75.33(1)	36.93 (3)	16.93 (5)
dVdS	770.39 (1)	496.75 (1)	284.64 (1)	147.11 (2)	73.90 (3)	39.12 (1)	21.12 (1)
SS	751.21 (4)	477.50 (5)	274.53 (4)	145.13 (4)	73.15(4)	36.31 (5)	17.79 (4)
SD	752.52 (3)	477.92 (4)	273.42 (5)	142.79 (6)	70.45(6)	33.80 (6)	15.66 (6)
SV	752.67 (2)	479.26 (2)	276.09 (2)	146.33 (3)	73.93(2)	37.02 (2)	18.91 (3)
SVSD	749.45 (6)	475.25 (6)	272.14 (6)	143.33 (5)	72.23(5)	36.40 (4)	18.95 (2)
max diff (abs) (bp)	20.94	21.49	12.50	4.63	4.89	5.3	5.46
max diff (rel)	2.72 %	4.33 %	4.39 %	3.14 %	6.48 %	13.59 %	25.84 %

Table 8.12: Model prices for varying values of the underlying strike K_2 of the compound option in the EUR/USD market.

Forward Start Option Value, EUR/USD					
	Value of α				
Model	0.95	0.975	1.0	1.025	1.05
BS (ATM)	770.36	539.37	351.87	212.37	118.01
BS (impl)	775.85	546.93	360.63	221.01	125.35
LV	758.28 (4)	530.33 (3)	346.73 (3)	212.04 (3)	122.24 (5)
dVdS	751.55 (6)	479.70 (6)	268.16 (6)	138.72 (6)	81.890 (6)
SS	766.98 (2)	539.35 (2)	356.70 (1)	222.92 (1)	133.21 (2)
SD	760.16 (3)	520.73 (5)	332.59 (5)	203.71 (4)	126.34 (4)
SV	773.78 (1)	542.32 (1)	340.88 (4)	170.89 (5)	126.75 (3)
SVSD	757.54 (5)	528.30 (4)	347.53 (2)	218.85 (2)	134.76 (1)
max diff (abs) (bp)	22.246	62.626	88.54	84.19	52.87
max diff (rel)	2.87%	11.55%	24.82%	37.77%	39.23%

Table 8.13: Model prices for varying values of α for the forward start option in the EUR/USD market.

Compound Option Value, USD/JPY						
	Strike K_1 (as percentage of spot)					
Model	2%	3%	4%	5%	6%	7%
BS (ATM)	2.106	1.557	1.141	0.828	0.593	0.420
BS (impl)	2.103	1.554	1.138	0.825	0.591	0.418
LV	1.999 (5)	1.421 (5)	1.003 (5)	0.708 (6)	0.501 (6)	0.355 (6)
dVdS	1.933 (6)	1.361 (6)	1.000 (6)	0.782 (4)	0.653 (1)	0.572 (1)
SS	2.049 (4)	1.466 (4)	1.037 (4)	0.728 (5)	0.509 (5)	0.357 (5)
SD	2.170 (1)	1.615 (1)	1.184 (1)	0.855 (1)	0.608 (2)	0.427 (2)
SV	2.129 (2)	1.555 (2)	1.120 (2)	0.795 (2)	0.558 (3)	0.390 (3)
SVSD	2.124 (3)	1.551 (3)	1.114 (3)	0.788 (3)	0.551 (4)	0.384 (4)
max diff (abs) (bp)	0.2368	0.2547	0.1849	0.1468	0.15217	0.2164
max diff (rel)	10.91%	15.77%	15.61%	17.17%	23.23%	37.85%

Table 8.14: Model prices for varying values of the compound strike K_1 in the USD/JPY market.

Compound Option Value, USD/JPY							
	Strike K_2						
Model	105	107.5	110	112.5	115	117.5	120
BS (ATM)	2.963	1.848	1.072	0.577	0.288	0.133	0.0572
BS (impl)	3.287	2.017	1.109	0.541	0.236	0.095	0.0372
LV	2.991 (6)	1.754 (6)	0.942 (6)	0.483 (6)	0.241 (5)	0.115 (6)	0.0515 (5)
dVdS	3.125 (3)	1.824 (4)	1.007 (4)	0.577 (2)	0.375 (1)	0.268 (1)	0.1893 (3)
SS	3.062 (5)	1.807 (5)	0.974 (5)	0.490 (5)	0.241 (6)	0.121 (5)	0.0637 (6)
SD	3.269 (1)	2.006 (1)	1.126 (1)	0.585 (1)	0.292 (2)	0.147 (2)	0.0765 (1)
SV	3.130 (2)	1.894 (2)	1.050 (2)	0.542 (2)	0.269 (3)	0.133 (3)	0.0674 (4)
SVSD	3.117 (4)	1.883 (3)	1.042 (3)	0.537 (4)	0.267 (4)	0.132 (4)	0.0678 (2)
max diff (abs) (bp)	0.2785	0.2520	0.1833	0.1024	0.1342	0.1524	0.1378
max diff (rel)	8.52%	12.56%	16.29%	17.48%	35.77%	56.93%	72.81%

Table 8.15: Model prices for varying values of the compound strike K_2 in the USD/JPY market.

Forward Start Option Value, USD/JPY					
	Value of α				
Model	0.96	0.98	1.0	1.02	1.04
BS (ATM)	3.626	2.416	1.515	0.891	0.491
BS (impl)	4.599	3.427	2.480	1.741	1.185
LV	3.676 (4)	2.360 (4)	1.399 (2)	0.768 (2)	0.396 (3)
dVdS	2.465 (6)	1.013 (6)	0.372 (6)	0.343 (6)	0.579 (1)
SS	3.846 (1)	2.525 (1)	1.540 (1)	0.878 (1)	0.475 (2)
SD	3.602 (5)	2.098 (5)	1.083 (5)	0.528 (5)	0.295 (6)
SV	3.829 (2)	2.395 (2)	1.347 (4)	0.692 (4)	0.343 (5)
SVSD	3.784 (3)	2.386 (3)	1.355 (3)	0.701 (3)	0.344 (4)
max diff (abs)	1.381	1.511	1.168	0.534	0.284
max diff (rel)	35.91%	59.87%	75.85%	60.87%	49.01%

Table 8.16: Model prices for varying values of α for the forward start option in the USD/JPY market.

- The dVdS model calculates the highest compound option price, and the lowest the forward start option price.
- The SVSD model calculates relatively low prices for the compound option. For high values of K_2 however, the model price is increasing compared to the other models.
- The relative error increases as strike increases.

For the USD/JPY market we can do the same:

- The sticky delta model prices compound options high compared to the other models. After the dVdS model, it gives the lowest price for forward start options.
- The LV model results in relatively low compound prices.
- The dVdS model generates unpredictable prices for the compound option, varying from highest to lowest.
- For the forward start option, the lowest prices are given by the dVdS model, except for $\alpha = 1.04$ where it gives the highest price.
- The relative error increases as strike increases.

Besides these observations there seem to be no clear patterns in the pricing results. We can take a look at the difference between the model prices and the Black-Scholes prices. In figures 8.20 to 8.31 plots are presented for the absolute and relative pricing differences. In absolute terms, we see the price differences given by the dVdS model differ a lot from the other models. The other models all show the same pattern. The relative error given by the dVdS model is the highest in all cases.

Further, in the USD/JPY market the sticky delta model gives the largest deviation from the other models (after the dVdS model). In varying K_1, the sticky delta model price is higher than the Black-Scholes model, while the other models all give a lower price than Black-Scholes. In varying K_2 it gives the highest relative error. Finally, for different values of α for the forward start option it gives the largest (negative) relative error.

8.8 SVSD Model characteristics

In this section we will take a closer look at the SVSD model. In the base case we have used two maturities for the vanilla calibration and four barrier options. It is interesting to see if using more

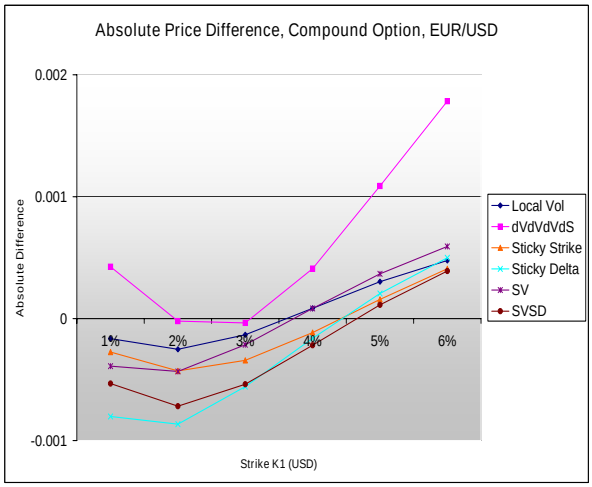

Figure 8.20: EUR/USD Compound option. Absolute price difference with Black-Scholes, for varying values for strike K_1.

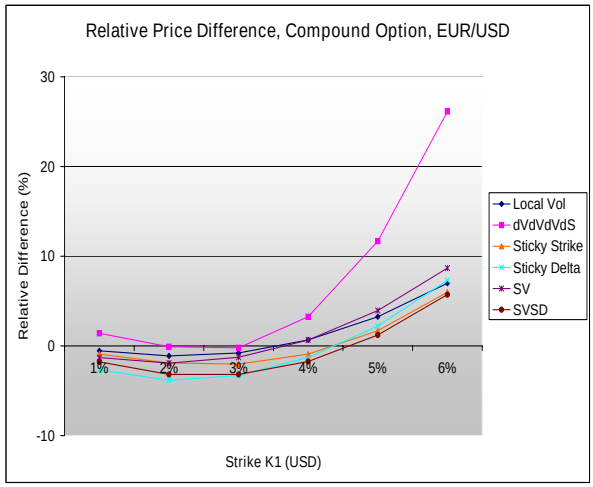

Figure 8.21: EUR/USD Compound option. Relative price difference with Black-Scholes, for varying values for strike K_1.

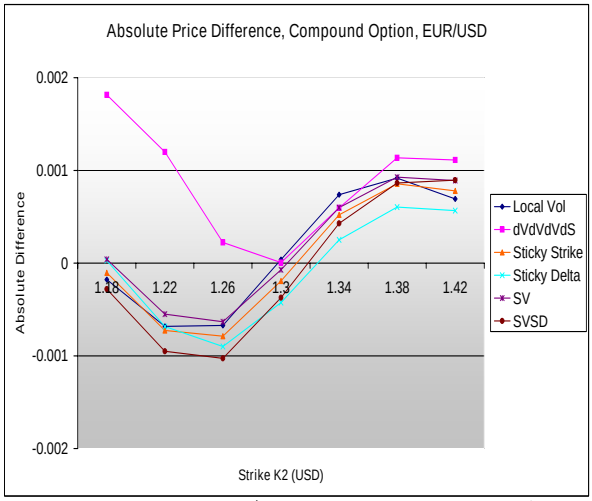

Figure 8.22: EUR/USD Compound option. Absolute price difference with Black-Scholes, for varying values for strike K_2.

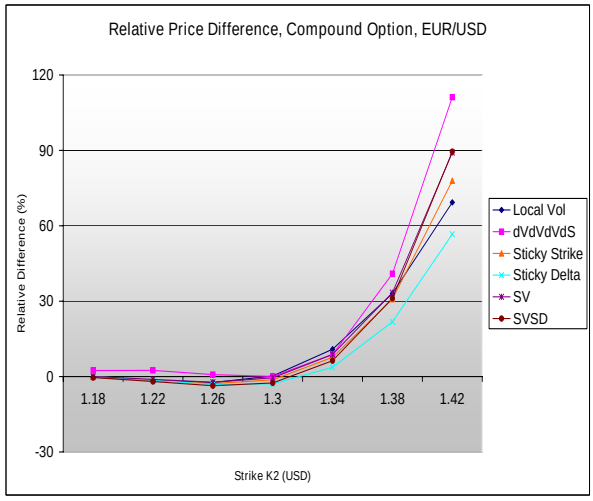

Figure 8.23: EUR/USD Compound option. Relative price difference with Black-Scholes, for varying values for strike K_2.

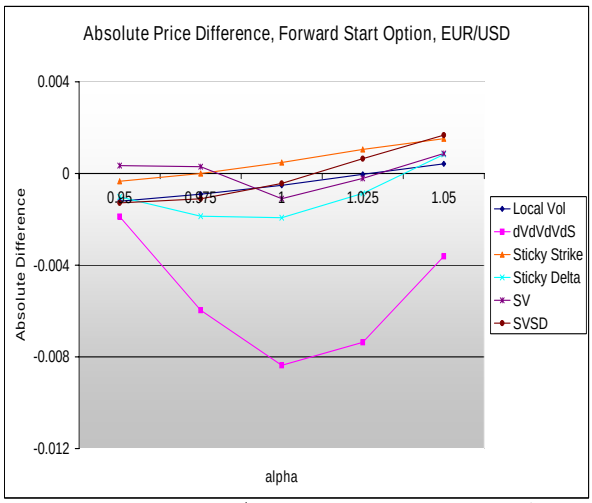

Figure 8.24: EUR/USD Forward start option. Absolute price difference with Black-Scholes, for varying values for strike α.

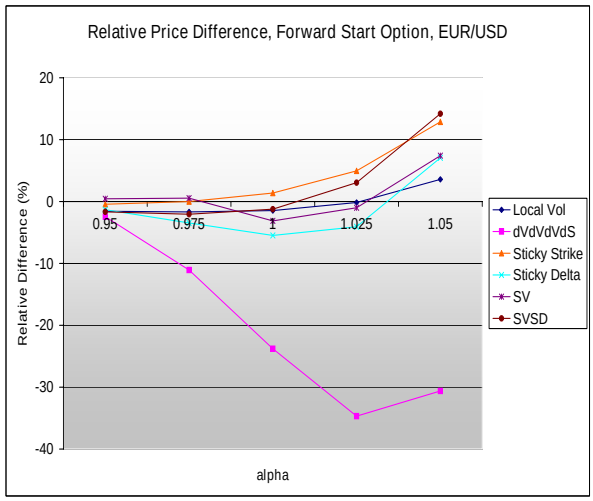

Figure 8.25: EUR/USD Forward start option. Relative price difference with Black-Scholes, for varying values for strike α.

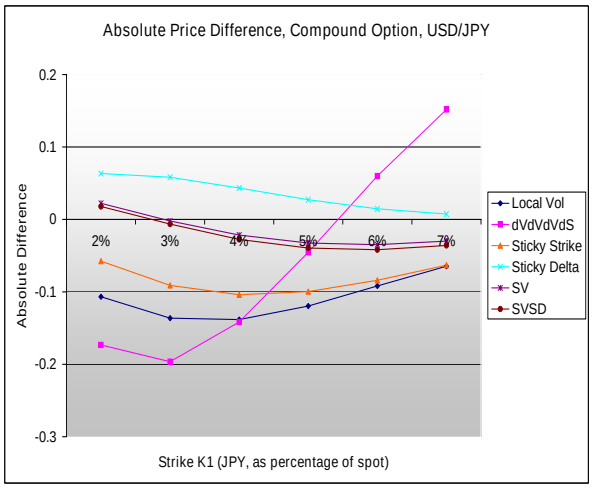

Figure 8.26: USD/JPY Compound option. Absolute price difference with Black-Scholes, for varying values for strike K_1.

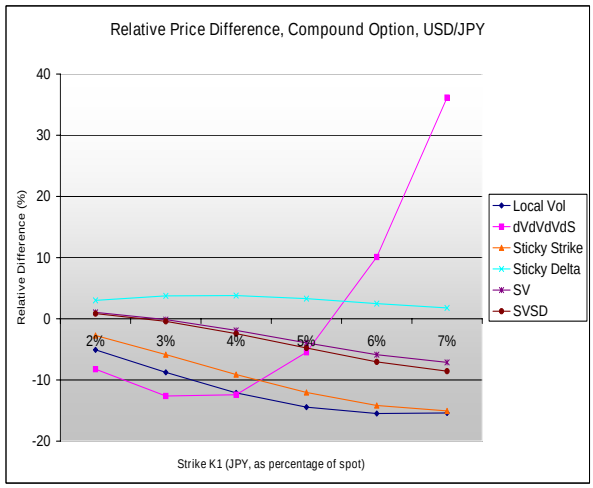

Figure 8.27: USD/JPY Compound option. Relative price difference with Black-Scholes, for varying values for strike K_1.

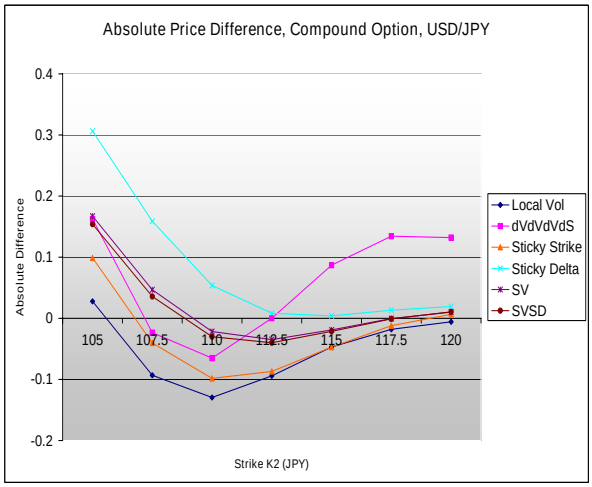

Figure 8.28: USD/JPY Compound option. Absolute price difference with Black-Scholes, for varying values for strike K_2.

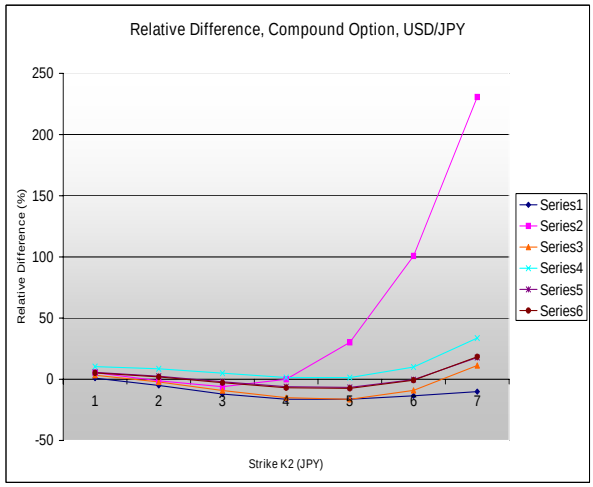

Figure 8.29: USD/JPY Compound option. Relative price difference with Black-Scholes, for varying values for strike K_2.

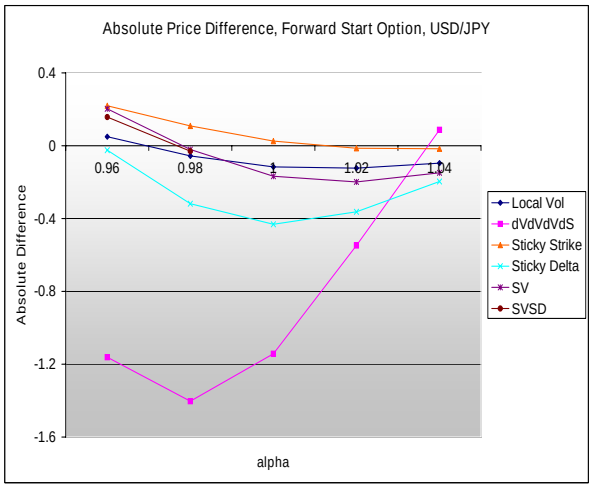

Figure 8.30: USD/JPY Forward start option. Absolute price difference with Black-Scholes, for varying values for strike α.

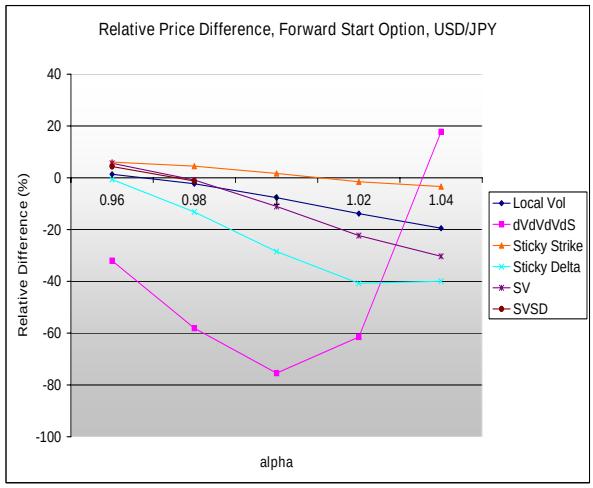

Figure 8.31: USD/JPY Forward start option. Relative price difference with Black-Scholes, for varying values for strike α.

maturities and/or more barrier options has a big impact on the price and greeks of the option. Further, we will vary the value of kappa. Because of the presence of a scale invariance we have used a fixed value of $\kappa = 5$. It can be shown (see Rosien [24]) that the model depends only on $\frac{\xi}{\sqrt{\kappa}}$ and not on both ξ and κ separately. Rosien shows that using a different value for κ does not impact the option price significantly. But we are not sure if the same holds true for the greeks. In this section, we will calculate the compound price and greeks for different values of kappa.

8.8.1 Vanilla and Barrier Influence

We will perform this test for the following cases:

1. Using two barrier options (6 months call, 1 year put: barriers 3 and 6).
2. Using two barrier options(6 months put, 1 year call: barriers 4 and 5).
3. Using six barrier options (3 months, 6 months, 1 year calls and puts: barriers 1 to 6).
4. Using three vanilla maturities (3 months, 6 months, 1 year maturity & barriers of the base case: 2 to 6).
5. Using three vanilla maturities and six barriers (3 months, 6 months, 1 year maturities & barriers 0 to 6).

The barrier numbers refer to the barriers presented in table 8.3 and 8.4. In table 8.17 the results of the calibration for each set are presented.

Model Parameters Currency Pair EUR/USD											
Testcase	ξ_1	ξ_2	ξ_3	ρ_1	ρ_2	ρ_3	m_1	m_2	m_3	α	β
Base case	1.278	1.297	—	0.190	0.349	—	0.0805	0.0862	—	-0.600	5.00
1	0.785	0.234	—	0.162	0.367	—	0.0812	0.0854	—	0.00	20.00
2	1.374	1.753	—	0.115	0.122	—	0.0801	0.0816	—	0.00	0.00
3	1.254	1.210	—	0.189	0.342	—	0.0805	0.0868	—	-0.556	5.688
4	1.254	0.916	0.801	0.161	0.356	0.435	0.0786	0.0896	0.0861	-0.618	9.344
5	1.267	0.885	0.812	0.172	0.339	0.440	0.0786	0.0897	0.0860	-0.618	9.314

Table 8.17: Model parameters for different test cases.

Using two barrier options leads to α and/or β equal to zero. For test case 2 we have zero α and zero β; only the vanilla calibration was needed to get the model barrier prices close enough to the market barrier prices. This suggests that including two barriers is not enough to capture the information that is present in barrier options.

We will only consider a compound option for the EUR/USD market. The price and greeks are shown in table 8.18.

Compound Option Value & Greeks Currency Pair EUR/USD				
Testcase	**Price (bp)**	**delta**	**gamma**	**vega**
Base case	164.37	0.290	4.223	0.1154
1	166.98	0.303	4.346	0.1163
2	163.84	0.314	4.545	0.1158
3	164.07	0.291	4.240	0.1156
4	163.80	0.292	4.246	0.1136
5	163.76	0.292	4.250	0.1136
max diff (abs)	3.25bp	0.0247	0.322	27.36bp
max diff (rel)	1.94%	7.85%	7.09%	2.35%

Table 8.18: EUR/USD Compound option prices for different parameter values.

The prices do not differ from each other much. The maximum price difference is 3.25bp, the maximum relative difference is 1.94%, which is lower than any case of the pricing differences we found in the model comparison of the previous section. The same holds for all the greeks. For the base case we found a relative difference of 15.0% in delta values between the models, 25.7% in gamma values and 69.4% in vega values. From these results we conclude that using a minimum of four barriers is enough to capture the relevant information of barrier options. Further, different combinations of barriers and/or using more maturities for the vanilla calibration lead to different calibration parameters, but the impact on the option prices and greeks is not significant.

8.8.2 Dependence of Price and Greeks on κ

We calibrate the model using values for κ from 3.0 to 7.0. The parameter values that resulted from the calibration are presented in table 8.19.

Model Parameters Currency Pair EUR/USD								
Kappa	ξ_1	ξ_2	ρ_1	ρ_2	m_1	m_2	α	β
3.0	0.992	0.511	0.335	1.000	0.0814	0.0968	-1.618	8.618
4.0	1.149	1.082	0.218	0.387	0.0808	0.0886	-0.755	5.020
5.0 (Base case)	1.278	1.297	0.190	0.348	0.0805	0.0862	-0.60	5.00
6.0	1.307	1.057	0.211	0.424	0.0804	0.0876	-0.618	8.256
7.0	1.416	1.137	0.214	0.436	0.0801	0.0870	-0.618	8.795

Table 8.19: Model parameters for the SVSD model in the EUR/USD market, for different values of the mean reversion speed κ.

For $\kappa = 3.0$ we did not find a satisfactory result, as the correlation is equal to $\rho_2 = 1.00$, which is not a realistic value. Therefore we will not use this test case in pricing the compound option. The pricing results are given in table 8.20.

The prices are decreasing as the value of κ gets higher, but they are very close to each other, the maximum difference being 1.25bp and maximum relative difference of 0.76%. The delta and

Compound Option Value & Greeks Currency Pair EUR/USD				
Kappa	**Price (bp)**	**delta**	**gamma**	**vega**
4.0	164.13	0.2849	4.1568	0.1369
5.0 (Base case)	163.73	0.2897	4.2226	0.1154
6.0	163.24	0.2914	4.2497	0.0992
7.0	162.88	0.2920	4.2614	0.0867
max diff (abs)	1.25bp	70.39bp	0.1047	0.0502
max diff (rel)	0.76%	2.41%	2.46%	36.70%

Table 8.20: SVSD pricing results for the compound option for varying values of κ in the EUR/USD market.

gamma values do also not differ much, and are slightly increasing as function of κ. For the vega values we see a higher relative difference. The higher the value of κ, the lower the value of vega gets. But we cannot compare the vega values exactly as σ_0 is different in each case. However, in the previous subsection we found values for vega that are a lot closer to each other, while the differences in σ_0 for the testcases are of the same amount as in this case. This indicates that varying the value of kappa does impact the value of vega by a significant amount. Using a higher value for κ implies a lower value for vega.

8.9 Hedge Test

We point out that it would be interesting and informative to make a hedge test comparison for the compound and forward start option between the models that were considered in this thesis. In this section we will shortly explain how a hedge test can be performed (see also Rosien[24]) and what information we can get from it.

The idea of a hedge test for the compound and forward start option is to create a portfolio based on the option, the underlying and another option (the 'benchmark option'), and to choose the weights of the portfolio in such a way that the delta and vega of the portfolio are equal to zero. Suppose that on day 1 we sell a certain compound option and we want to hedge it. Then we create a portfolio consisting of this compound option, the underlying asset, and another option. The weights of this portfolio are chosen so that the delta and vega of the portfolio are equal to zero. We make sure that the value of the portfolio is equal to zero, by putting (getting) the money we get (pay) when the portfolio is constructed on (from) a bank account, this is an amount B equal to

$$B_0 \quad = \quad CC(S_0, 0) - w_1 V(S_0, 0) - w_2 S(0),$$

where $CC(S_0, 0)$ is the value of the compound option at time zero and spot S_0, V is the value of the second option, S is the value of the underlying and w_1 and w_2 are the weights. So the portfolio

at the first day is

$$\begin{aligned} P_0 &= -CC(S_0, 0) + w_1 V(S_0, 0) + w_2 S(0) + B_0 \\ &= 0. \end{aligned}$$

After a day, the market has changed. If we had a perfect hedge, the value of the portfolio would still be equal to zero. In practice it is not perfect, and the *Profit or Loss*, in short PnL on day i is equal to the value of the portfolio at day i. At this point the option is rehedged to make it delta and vega neutral again. To this end, the old portfolio is sold and the models are recalibrated to the market. Then the above described procedure is repeated, until the expiry of the option is reached.

When a product is hedged in practice, the main concern is the total profit or loss that is made at the end of the lifetime of the option (the sum of the daily PnL values). Therefore, draw conclusions from the hedge test, we need to perform not only one hedge test, but a whole series of hedge test, each using different market data.

By presenting the end PnL of these tests in a histogram, we can get an idea of the distribution of the end PnL for a specific model. In a perfect hedge, all end PnL value would be zero, leaving only one column in the histogram (for the interval containing the zero value). In a non-perfect hedge the PnL histogram has a similar shape to that of a normal distribution with mean zero (and volatility as small as possible). In this way different models can be compared.

But besides the values of the total end PnL, it is also interesting to see the PnL values in a time series, for each day in the option lifetime. Preferably, the daily PnL values vary around the zero level, with the standard deviation as small as possible. But it may be possible that the results for a model show some sort of pattern in the daily PnL values, for example when we find PnL values that are decreasing in time. This would indicate that there still is some element left unhedged (for example the interest rates should be stochastic). An other possibility is that the total end PnL values are close to zero, but that the variation in the daily values is very large. Or, the other way around, that the daily PnL values do not show large variation but are consistently above or below zero. In the same way, it may also be interesting to make time series plots of the model implied delta and vega values.

So, it should be clear that the result of a hedge test depends on the dynamics implied by the model being used because of the calculation of the greeks. A model that implies the correct dynamics also calculates the correct greeks, and consequently results in a good hedge performance. Therefore such a test can help determining which of the models works best, and to make a rating for the models in both markets (from best to worst).

8.10 Conclusions

In this chapter we have made a comparison of the pricing performance of the different models. This section gives an overview of the conclusions that we derive from the results.

The option prices depend on the forward smile, and also on the density of the underlying at compound expiry / fixing date. Every model that was considered in section 8.5 fits the initial market smile, and therefore this density is correct. As the fit to the market smile is not completely exact there are still differences in the densities implied by the models, but these differences are small and do not affect the option prices significantly. For one specific case we have shown that we can translate the compound and forward start option prices into the dynamic behavior of the models (excluding the dVdS model), that is, into the model implied forward volatilities for a range of spot values.

Our main conclusion is that the dynamics of the model implied forward smile is the most important factor in determining the price of compound and forward start options. Obviously, it is therefore important to use a model that results in *correct* dynamics.

We now continue by reviewing all models separately, giving a short overview of the results for each model. We treat the models in the same order that they were presented in part II of the thesis.

Local Volatility Model

The first model that was presented, in chapter 4, was the local volatility model. The model is able to match the complete vanilla market, but it is well known that the implied dynamics of the model do not match empirical observations. When spot increases, the model implies an increase in ATM for the EUR/USD market, and a decrease for the USD/JPY market. For the RR we find an increase of the RR for an increase in spot in both markets. This is in line with empirical observation, although the dynamics of the forward smile are seen to move in opposite direction compared to the other models. For example for increasing spot in the EUR/USD market, the smile shifts to the left, while the smiles of the other models shift to the right. This may lead to too extreme behavior, which may have its effect on the pricing (and hedging) results. In Hagan[13] an example is given (for a call option) where this behavior leads to a situation in which the Black-Scholes delta is more accurate than the delta resulting from the local volatility model. For the base case we have also calculated the value of delta. In the EUR/USD market we see that for the compound as well as the forward start option the LV delta is higher than the Black-Scholes delta, while the other models calculate lower delta values. A hedge test could give more information about this point.

Hull et al.[18] pricing and hedging tests for compound options and barrier options are pre-

sented, in which the local volatility model is compared to a stochastic volatility model. The results show that the LV model works well for compound options and is an improvement over the Black-Scholes model, but it shows a poor performance for barrier options, while the stochastic volatility model shows good results for both options.

Stochastic Volatility Smile Dynamics Model

We have used the SVSD model that was presented in chapter 5, and the SV model with zero α and β. The SVSD model is set up with a specific goal, which is to extract information about the smile dynamics from the market, by calibrating the model to barrier prices. The parameters α and β serve to meet this objective. However, the results showed that the effect of α is - at least in part - compensated by the opposite effect of the correlation ρ. We have seen this both for the EUR/USD as for the USD/JPY market. From these results it is not clear if the SVSD model results in substantially different dynamic behavior compared to the SV model, viewed in terms of correlation between spot and ATM. The SVSD model does incorporate the correlation between spot and risk reversal, in that sense it is preferred over the SV model.

Further, we have investigated if using more or less barriers, and/or using more maturities has a big impact on the SVSD model prices and greeks. We conclude that, although we do find different calibration parameters, this does not affect the price and greeks significantly, especially compared to the pricing differences between the models. However, a minimum of four barriers is needed to recover the dynamics from the barrier options.

We also calibrated the model using different values for the mean reversion speed κ. From these results we may conclude that the effect of using a different value for kappa is covered by adjusted values of the other model parameters, so that the pricing differences are small. This also holds for the delta and gamma values. The value of κ does seem to have a significant impact on the vega values. To make an exact comparison this should be tested by shifting the volatility surface and recalibrating the model.

Results of pricing and hedge tests for the SVSD model can be found in Rosien[24]. A comparison is made of pricing results and hedge test results of the SVSD model, the SV model and the Black-Scholes model, in pricing barrier options. Pricing and hedge test results for call options for the SV model may be found, for example, in Bakshi et al.[3]. Rosien shows that the pricing results of the SVSD model are an improvement of the SV model. Furthermore, in both papers it is shown that the hedging results for the SV and SVSD model are a clear improvement on the Black-Scholes model. However, the hedge performance of the SVSD model does not show a significant improvement over the SV model.

dVdVdVdS Model

The dVdS model was presented in chapter 6. Contrary to the other models, the dVdS model is not based on an assumption for the process of the underlying, but instead it is a rule of thumb that is used in practice. We can therefore not compare the dynamics implied by this model with the other models, as was done in section 8.5.3. We have compared the pricing results of the different models by varying the option strikes. The results for the dVdS model are most striking. In the EUR/USD market the model seems to overprice the compound option in all cases. Further, the model seems to underprice the forward start option in both the EUR/USD and the USD/JPY market. The pricing results for this model seem to be the most extreme of all models. This is also supported by the results of the price differences with the Black-Scholes model. While the other models all have a similar pattern, the dVdS model does not follow this pattern. It also shows the largest absolute and relative pricing differences with Black-Scholes.

To our knowledge there are no hedge test results that can be found in the literature. In Hoogerwerf[16] dVdS model prices for a number of barrier options are tested against Black-Scholes model prices and LV model prices. The overall conclusion is that the dVdS model always calculates pricer that are closer to the market prices than Black-Scholes. Further, it is also concluded that the dVdS model outperforms the local volatility model. But this result is for barrier options only (and as said, in Hull et al.[18] it is shown that the LV model does perform well for compound options).

Forward Smile Model

In chapter 7 we have derived expressions for the forward smile models. The smile dynamics implied by the models are those of the well known sticky strike and sticky delta rule. These models both give a good fit to the initial smile.

In the sticky delta model, both the ATM and RR remain unchanged for a change in spot. As said, this is not what is observed in practice. The sticky strike smile shape remains the same for a change in spot, meaning that the ATM and the RR do change. While it is not guaranteed that the change in ATM and/or RR corresponds to what is observed in practice, our results show that for an increasing spot, both the ATM and the RR show changes that cope with empirical observations. This means that the ATM increases in the EUR/USD market, decreases in the USD/JPY market, and the RR increases in both markets.

The pricing results show that in all cases the sticky delta model tends to overprice compound options, and underprice forward start options. We also note that this model is more extreme than the other models (more curved forward smiles in section 8.5.2. Further, for the compound option it predicts the most 'extreme' dynamics (figures 8.16 and 8.17); for the forward start option it

predicts forward volatilities that are lower than all other models.)

For this model there are no pricing or hedge test results available.

Chapter 9

Conclusion

9.1 Outline

In this thesis a comparison is made for two types of exotic options, the compound option and the forward start option. In this comparison we have included the Black-Scholes model, the local volatility model, the stochastic volatility smile dynamics model and a pure stochastic volatility model, the dVdS model and the forward smile models. This chapter gives a short summary of the thesis. It reviews the project objective and why there is a need to develop new models. Further it describes the approach we took and the methods we used, the results that were obtained and finally the conclusions that we can extract from the results. We conclude by giving some suggestions for further research.

9.2 Project, Results and Conclusions

We have started by introducing the well-known Black-Scholes model, and deriving the partial differential equation that an option should satisfy in the Black-Scholes model. Empirical evidence has shown that options with different strikes and maturities have different implied volatilities. This observation is not in agreement with the Black-Scholes model, because it assumes that the volatility is constant. Using the Black-Scholes model with its constant volatility therefore leads to incorrect vanilla option prices.

Many models have been developed to overcome this problem. Most of these new model are able to match the complete volatility surface. This implies that these models are able to calculate the correct prices for European option, i.e., options in which the payoff is only dependent on the value of the underlying asset at one point in time, the maturity.

However, it turns out that this feature is not sufficient for the pricing of path-dependent options, and for hedging. Both path-dependent options and hedging requires the knowledge of the smile *dynamics*: the change in the smile for a (small) change in spot. In this thesis we have

concentrated on the pricing of exotic option only, and not on the hedging performance. Just as the smile can be related to the density of the underlying at maturity, the smile dynamics can be related to the transition density from a future state to a further future state. The marginal densities do not provide information about the transition densities. Therefore, while models may agree on European call and put option prices, they may give very different prices of path dependent option.

In this thesis we considered two types of exotic options, the compound option and the forward start option. Both types depend on the smile dynamics in a relative simple way, because the prices of these options depend only on the joint density of the underlying at two points in time. Therefore, compound and forward start option prices depend on the forward volatility σ_{12}, and more importantly on the dynamics of the forward volatility. As said, different models may imply very different dynamics.

We have compared the pricing performance of a number of models: the local volatility model, the stochastic volatility smile dynamics model, the dVdS model, the sticky strike model and finally the sticky delta model. Each model is based on a different approach. We have compared the forward volatilities of these models for a range of spot values and a fixed strike - excluding the dVdS model. This gives a clear representation of the smile dynamics implied by the different models. We have also shortly looked at (some of) the greeks. Further we have compared the prices implied by the models for a range of strike prices.

We have shown that the prices of compound and forward start options depend crucially on the model used, and more specifically on the dynamics that are implied by the model. We have shown that the option price can be linked to the model implied forward volatility for a range of spot values, i.e., the smile dynamics for a fixed strike. For this reason, we conclude that it is important for a model to incorporate the right smile dynamics in order to obtain correct pricing results.

However, while we have shown that different models lead to different prices, from our results we cannot conclude which model gives the 'correct' price. At this point it does seem likely that the SVSD model is the best model because it seems to recover smile dynamics that are closest to what can be observed in the market. The (few) results that are present in the literature also show that this model performs well in pricing and hedging barrier options.

We cannot give a suggestion about the model we believe performs the worst. We have seen that the pricing results for the dVdS model deviate the most from the other models. The model tends to overprice compound options, and underprice forward start options, compared to the other models. Further, when comparing the prices with the Black-Scholes price, we have seen that all

but the dVdS model show a a similar pattern. However, we do not have enough information to conclude that this model is incorrect. Pricing results from the literature also show that the model performs better than the Black-Scholes model and, at least for barrier options, also outperforms the LV model.

Considering the other models, we know that the sticky delta model does not recover dynamic behavior that is observed in practice. On the other hand, the LV model does show this dynamic behavior, but it may be too extreme.

9.3 Suggestions for Further Research

Our pricing test only showed that the models resulted in different prices, but we cannot conclude which model is the 'right' model. The quality of the models can be further investigated by performing a hedge test and comparing the results of the different models. Because of time restrictions we were not able to do this, but we do suggest to do this in a future research project. The result of a hedge test depends on the dynamics implied by the model being used because of the calculation of the greeks, and therefore such a test can help determining which of the models works best, and to make a rating for the models in both markets (from best to worst). In this hedge test, it is important to calculate the greeks in a similar manner for all models (by shifting the volatility surface).

Further, for the SVSD model we have seen that using different values of the mean reversion speed does not have a significant impact on the option price, but our results showed that it is likely that is does impact the vega by a significant amount. We suggest to investigate this further, specifically by shifting the volatility surface, and by performing the hedge test for different values of κ.

Appendix A

Smile Dynamics: Risk Reversal

The figures show the initial model implied smile and the model implied smile for a higher than initial spot level. The plots give information about the change in risk reversal for a positive change in spot. This is discussed in section 8.5.1.

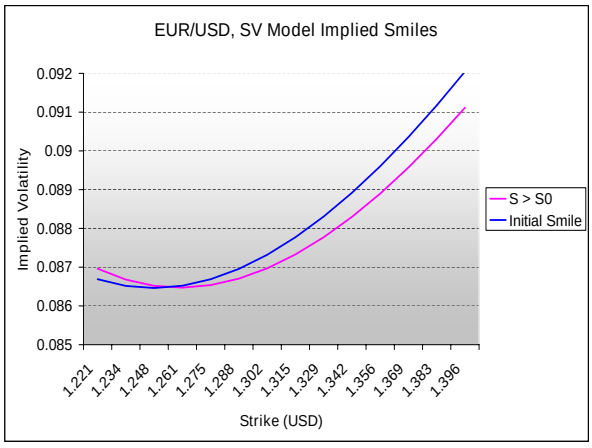

Figure A.1: EUR/USD SV model implied smiles.

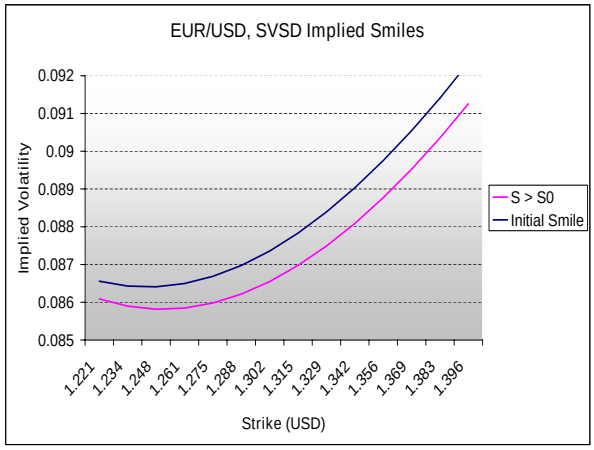

Figure A.2: EUR/USD SVSD model implied smiles.

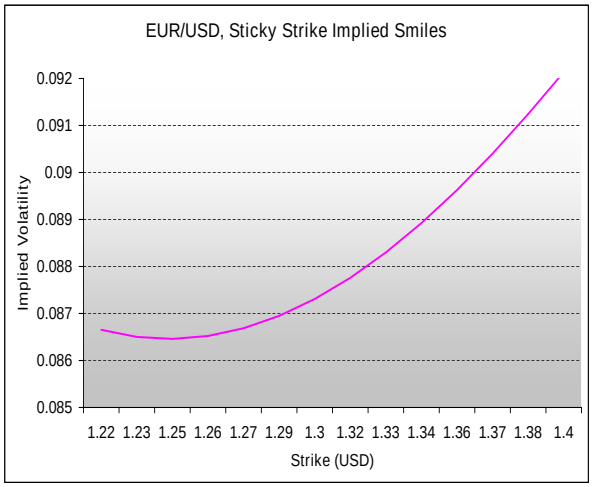

Figure A.3: EUR/USD Sticky Strike model implied smiles.

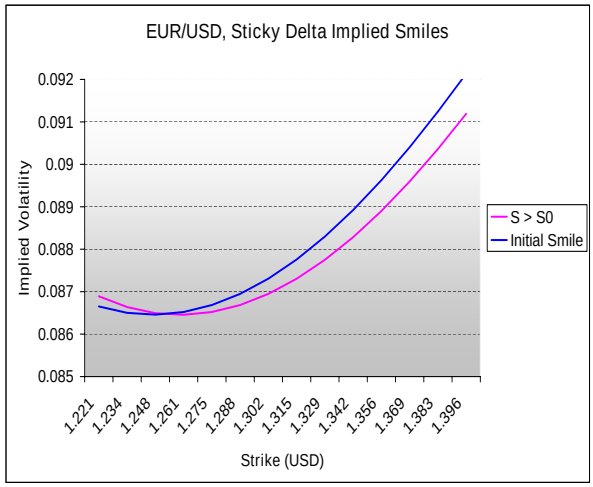

Figure A.4: EUR/USD Sticky Delta model implied smiles.

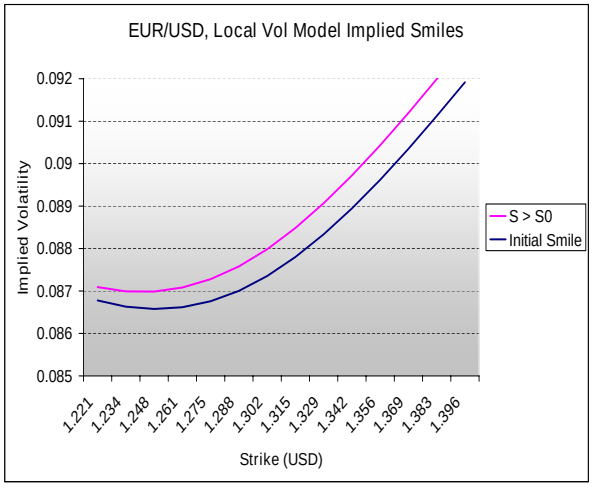

Figure A.5: EUR/USD Local Vol model implied smiles.

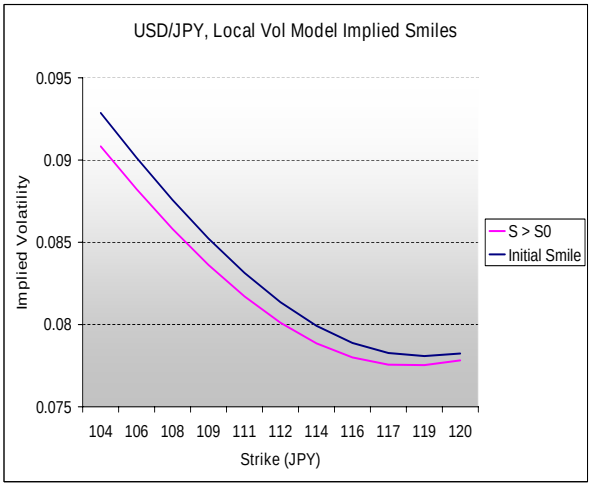

Figure A.6: USD/JPY Local Vol model implied smiles.

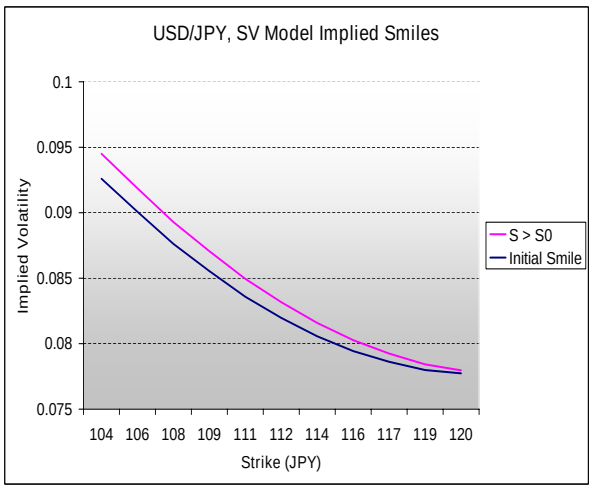

Figure A.7: USD/JPY SV model implied smiles.

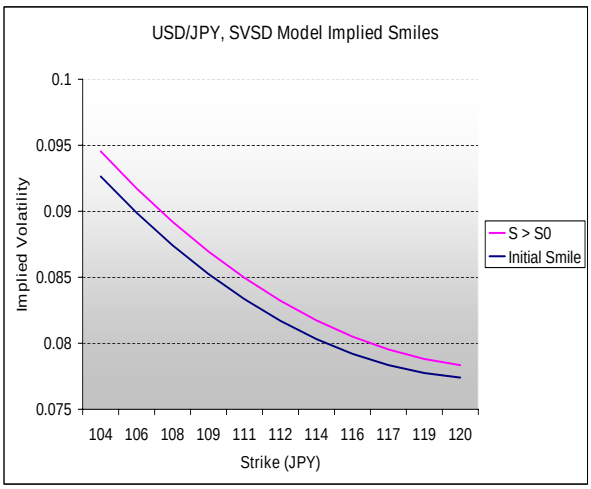

Figure A.8: USD/JPY SVSD model implied smiles.

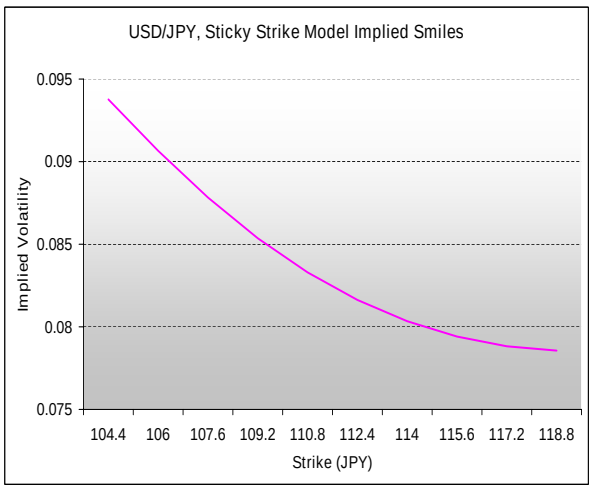

Figure A.9: USD/JPY Sticky Strike model implied smiles.

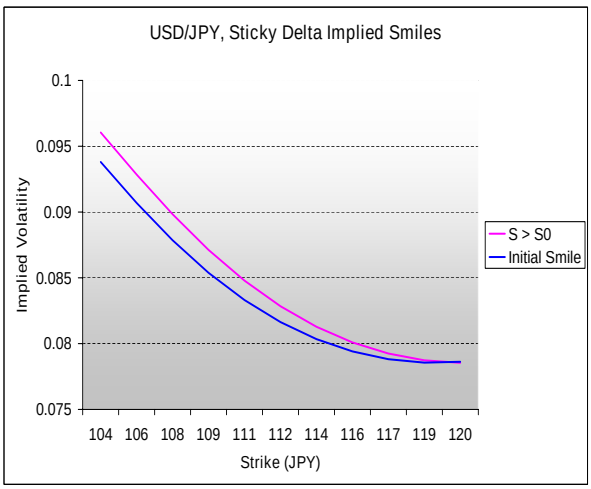

Figure A.10: USD/JPY Sticky Delta model implied smiles.

Bibliography

[1] E. Ayache, P. Henrotte, S. Nassar, and X. Wang. *Can anyone solve the smile problem?* Wilmott magazine, January 2004.

[2] G. Baker, R. Beneder, and A. Zilber. *FX Barriers with Smile Dynamics.* Working paper ABN AMRO, 2004.

[3] G. Bakshi, C. Cao, and Z. Chen. *Empirical Performance of Alternative Option Pricing Models.* Journal of Finance, Vol.52 (5), p.2003-2049, December 1997.

[4] R. Beneder. *Validation of the Skew Adjustment for USD/BRL Barrier Options.* Working Paper, ABN AMRO, February, 2003.

[5] T. Bjork. *Arbitrage Theory in Continuous Time.* Oxford University Press, 1998.

[6] G. Blacher. *A new Approach for designing and calibrating stochastic volatility models for optimal delta-vega hedging of exotics.* Presentation Global Derivatives, 2001.

[7] F. Black and M. Scholes. *The Pricing of Options and Corporate Liabilities.* Journal of Political Economy, Vol. 81 (3), p.637-654, 1973.

[8] P. Carr and L. Wu. *Stochastic Skew in Currency Options.* http://129.3.20.41/eps/fin/papers/0409/0409014.pdf, May 2004.

[9] I. Craig and A. Sneyd. *An Alternating Direction Implicit scheme for Parabolic Equations with Mixed Derivatives.* Computational Mathematics and Applications, Vol. 16 (4), p.341-350, 1988.

[10] E. Derman. *Laughter in the Dark - The Problem of the Volatility Smile.* May 2003.

[11] B. Dumas, J. Fleming, and R.E. Whaley. *Implied Volatility Functions: Empirical Tests.* Journal of Finance, Vol 53 (6), p.2059-2106, December 1998.

[12] B. Dupire. *Pricing with a Smile.* Risk Magazine, p.18-20, January 1994.

[13] P.S. Hagan, D. Kumar, A.S. Lesniewski, and D.E. Woodward. *Managing Smile Risk.* Wilmott Magazine, 2002.

[14] J. Hakala and U. Wystup. *Foreign Exchange Risk - Models, Instruments and Strategies.*

[15] S. Heston. *A Closed-Form Solution for Options with Stochastic Volatility with Applications to Bond and Currency Options.* The Review of Financial Studies, Vol 6 (2), p.327-343, 1993.

[16] R. Hoogerwerf. *GFXO dVdVdVdS method.* Working paper, ABN AMRO, 2001.

[17] J.C. Hull. *Options, Futures and Other Derivatives.* Prentice Hall, fifth edition, 2003.

[18] J.C. Hull and W. Suo. *A Methodology for Assessing Model Risk and its Application to the Implied Volatility Function Model.* Journal of Financial and Quantitative Analysis.

[19] K.J. in 't Hout and B.D. Welfert. *Stability of ADI schemes applied to convection-diffusion equations with mixed derivative terms.* Accepted for publication in Applied Numerical Mathematics, October 2005.

[20] N. Jackson. *The NCS implied volatility model with application to FX markets.* Working paper, ABN AMRO, October 2004.

[21] Zilber A. Nauta, B.J. *An approach to the Forward Smile.* Working Paper, ABN AMRO, June 2005.

[22] W.H. Press, S.A. Teukolsky, W.T. Vetterling, and B.P. Flannery. *Numerical Recipes in C++ - the Art of Scientific Computing.* Second edition, Cambridge University Press, 2002.

[23] M.A.H. Rosien. *Recent Developments in Stochastic Volatiliy Modelling.* Literature Study, executed at ABN AMRO, January 2004.

[24] M.A.H. Rosien. *Smile Dynamics Extracted From Barrier Options - an FX spot-inhomogeneous stochastic volatility model, calibrated to barrier options to extract the smile dynamics from the market.* Master's Thesis, executed at ABN AMRO, June 2004.

[25] P. Wilmott. *Paul Wilmott on Quantitative Finance, Volume 2.* John Wiley & Sons, Chichester, 2000.

[26] A. Zilber. *Stochastic Volatility Model.* Master's Thesis, executed at ABN AMRO, 2002.

[27] A. Zilber. *dVdV dVdS method per bucket vs. the Smile Calculator implementation of the smile adjustment.* Working Paper, ABN AMRO, March 2004.